ABSTRACT

Title of Document: PROBING THE INTERNALIZATION MECHANISM OF A BACTERIOPHAGE-ENCODED ENDOLYSIN THAT CAN LYSE EXTRACELLULAR AND INTRACELLULAR STREPTOCOCCI

Yang Shen, Doctor of Philosophy, 2013

Directed By: Assistant Professor Daniel C Nelson, Department of Veterinary Medicine

Bacteriophage-encoded peptidoglycan hydrolases, or endolysins, have been investigated as an alternative to antimicrobials due to their ability to lyse the bacterial cell wall upon contact. However, pathogens are often able to invade epithelial cells where they can repopulate the mucosal surface after antibiotic or endolysin prophylaxis. Thus, there is growing interest in endolysins that can be engineered, or inherently possess, a capacity to internalize in eukaryotic cells such that they can target extracellular and intracellular pathogens. Previously, one streptococcal specific endolysin, PlyC, was shown to control group A Streptococcus localized on mucosal surfaces as well as infected tissues. To further evaluate the therapeutic potential of PlyC, a streptococci/human epithelial cell co-culture model was established to differentiate extracellular vs. intracellular bacteriolytic activity. We found that a

single dose (50 μg/ml) of PlyC was able to decrease intracellular streptococci by 96% compared to controls, as well as prevented the host epithelial cells death. In addition, the internalization and co-localization of PlyC with intracellular streptococci was captured by confocal laser scanning microscopy. Further studies revealed the PlyC binding domain alone, termed PlyCB, with a highly positive-charged surface, was responsible for entry into epithelial cells. By applying site-directed mutagenesis, several positive residues (Lys-23, Lys-59, Arg-66 and Lys-70&71) of PlyCB were shown to mediate internalization. We then biochemically demonstrated that PlyCB directly and specifically bound to phosphatidic acid, phosphatidylserine and phosphatidylinositol through a phospholipid screening assay. Computational modeling suggests that two cationic residues, Lys-59 and Arg-66, form a pocket to help secure the interaction between PlyC and specific phospholipids. Internalization of PlyC was found to be via caveolae-mediated endocytosis in an energy-dependent process with the subsequent intracellular trafficking of PlyC regulated by the PI3K pathway. To the best of our knowledge, PlyC is the first endolysin reported that can penetrate through the eukaryotic lipid membrane and retain biological binding and lytic activity against streptococci in the intracellular niche.

PROBING THE INTERNALIZATION MECHANISM OF A BACTERIOPHAGE-ENCODED ENDOLYSIN THAT CAN LYSE EXTRACELLULAR AND INTRACELLULAR STREPTOCOCCI

By

Yang Shen

Dissertation submitted to the Faculty of the Graduate School of the
University of Maryland, College Park, in partial fulfillment
of the requirements of the degree of
Doctor of Philosophy
2013

Advisory Committee:
Professor Daniel C Nelson, Chair
Professor Vincent Lee
Professor Siba Samal
Professor Kevin McIver
Dr. David Donovan

© Copyright by
Yang Shen
2013

Dedication

I dedicate this dissertation to my parents,

Ping Shen and Jiannian Tan,

for their unconditional love and support.

Acknowledgements

I want to express my gratitude to the people who were there during my graduate training for their continuous support that make this thesis possible.

My deepest gratitude goes to my advisor Dr. Daniel Nelson for four years of support and guidance, particularly for the opportunity that he offered me the cutting edge research environment, and his support to afford me exposure in several international conferences. For the past five years, Dr. Nelson has not only trained me to be the scientist I am today, but has been an incredible mentor to my career development. He supervised me with great patience and freedom, inspired me with resources and ideas, and taught me how to collaborate with other experts in multiple disciplines. He certainly has a positive impact on me in many ways, such as his wisdom, creativity, humor, and generosity, all that I greatly appreciate.

I would like to thank my advisory committee, Drs. David Donovan, Kevin McIver, Vincent Lee, and Siba Samal for their support and valuable advice that has helped me in the progress of my research.

I would also like to thank Dr. Silvia Muro for providing me with the endocytic inhibitors that helped me to accomplish some key experiments to elucidate the endocytic pathway upon PlyC internalization.

I would also like to thank Dr. Travis Gallagher for his input on solving the crystal structure of PlyC mutants and Mr. Yizhou Yin for his help on the molecular docking of PlyCB with phosphatidylinositol and phosphatidylserine.

I would also like to thank Professor Vincent Fischetti and Dr. Dennis Spencer from Rockefeller University, for the collaboration on human primary epithelial cell

model, Professor Shuwei Li for his support on our joint research project, Professor Shunyuan Xiao for his ideas and guidance on phospholipid screening assay, Dr. Yiyuan Yin for her help on characterizing PlyC mutants by mass spectrometry, Dr. Joseph Kotarek for his help on characterizing PlyCB mutants by Infrared spectroscopy, and Mr. Kenneth Jensen for his help on western blot of phospholipids screening assay.

I would also like to thank Mr. Daniel Serrano and Dr. James Hoopes for their valuable suggestions on my dissertation.

Last, but not the least, I certainly want to thank my lab mates, Ryan Heselpoth, Sarah Highfill, Mike Mitchell, Mariel Escatte, Patrick Bales, Sara Liden, Steve Swift, Emilija Renke, for all their assistance and the fellows and friends in the IBBR institution/MOCB department for being there for me.

Table of Contents

Dedication ii

Acknowledgements iii

Table of Contents v

List of Tables vii

List of Figures viii

List of Abbreviations x

Chapter 1: Introduction and literature review 1

Pathogenesis of Group A streptococcal infections 1
Types of infection and significance 1
Virulence factors 2
Vaccine development 6
Treatment strategy and current challenge 7
Alternative antimicrobials: bacteriophage and its encoded endolysin 8
Bacteriophage: 8
Bacteriophage-encoded endolysin: 9
A unique streptococcal endolysin: PlyC 28

Chapter 2: Identification of intracellular bacteriolytic activity of PlyC against internalized GAS 33

Background 33
Failure of antibiotic treatment to eradicate GAS 33
Intracellular delivery of endolysin by fusing a cell-penetrating peptide 34
Results 35
Establishment of a GAS/human epithelial cell co-culture model and validation of internalized GAS 35
Wild-type PlyC possesses an inherent activity against internalized GAS 37
Intracellular bacteriolytic activity of PlyC is dose-dependent and relies on its enzymatic activity 38
Fate of internalized GAS and host epithelial cells with antibiotic or PlyC treatment for additional 24 hours 40
PlyC shows a similar efficacy against internalized GAS in a model of primary human tonsil epithelium 42
Confocal microscopy shows that fluorescently-labeled PlyC internalizes and co-localizes with intracellular GAS 43
Conclusion 44

Chapter 3: Elucidating the interaction between PlyC and the plasma membrane upon internalization 48

Background 48
Results 50
PlyCB domain is responsible for internalization of PlyC 50
Site-directed mutagenesis and characterization of various PlyCB mutants 51
Benchmark extracellular and intracellular bacteriolytic activity of mutants against wild-type PlyC 55
Fluorescence microscopic characterization of PlyCB mutants 56
Neither heparan sulfate nor chondroitin sulfate serve as cell surface receptor that mediates the internalization of PlyCB 58
Phospholipid-PlyCB interaction screening assay 60
Predicted molecular docking of PlyCB with specific phospholipids 61
Structural effects of the $PlyCB_{R66E}$ 63
Conclusion 64

Chapter 4: Probing the uptake and trafficking mechanisms of PlyC 68

Background 68
Results 68
Internalization of PlyC does not compromise membrane integrity 68
Internalization of PlyCB is dependent on temperature and interaction with lipid raft domains 69
Internalized PlyCB is associated with endocytic pathway 72
Intracellular trafficking of PlyCB is regulated by PI3K pathway. 75
Conclusion 77

Chapter 5: Thesis discussion and future perspectives 79

Comparison of the internalization mechanism of GAS and other bacteria 79
Comparing internalization and intracellular trafficking of GAS and PlyC 80
Comparing internalization mechanisms of TAT (cell-penetrating peptide) and PlyC 80
Fusion to cell-penetrating peptide enable endolysin to kill intracellular bacteria 82
Structure-function relationship 83
Future directions 86
Therapeutic perspective 87
Concluding remarks. 89

Appendices 90

Materials, methods , and protocols 90

Non-Dissertation Publications 116

Bibliography 117

List of Tables

Table 1.1 Summary of *in vitro* studies with Gram-positive phage endolysins.....15

Table 1.2 Summary of *in vivo* studies with phage endolysins.....20

List of Figures

Figure 1-1. GAS virulence factors interact with the host at various levels 3
Figure 1-2. Attachment and internalization of streptococci by epithelial cell 5
Figure 1-3. Modular structure of the endolysin 10
Figure 1-4. Structure of the peptidoglycan and cleavage sites by the endolysins 14
Figure 1-5. Electron micrograph of bacteria treated by the endolysins 18
Figure 1-6. Biochemical characterization of the PlyC endolysin 29
Figure 1-7. *In vitro* and *in vivo* efficacy of PlyC against GAS 30
Figure 1-8. Crystal structure of PlyC 32
Figure 2-1. Schematic illustration, CFU results and confocal microscopy of co-culture assay 36
Figure 2-2. CFU result of recovered internalized streptococci post-endolysin treatment 38
Figure 2-3. Intracellular killing activity of PlyC is dose-dependent 39
Figure 2-4. Fate of internalized GAS and host epithelial cells with antibiotic or PlyC treatment for additional 24 hours 41
Figure 2-5. CFU count from co-culture model with human primary tonsil cells 42
Figure 2-6. Confocal microscopy of internalization of PlyC targeting intracellular GAS 44
Figure 3-1. Structure and electrostatic surface potential of PlyC 49
Figure 3-2. Characterization of internalization ability of PlyC, PlyCA and PlyCB 51
Figure 3-3. Biochemical and biophysical characteristics of PlyC and its mutants ..... 53 & 54
Figure 3-4. Extracellular and intracellular bacteriolytic activity of PlyC 56
Figure 3-5. Fluorescent microscopic characterization of PlyCB and its mutants 57

Figure 3-6. Effects of the presence of soluble GAGs or GAG lyase on internalization of PlyCB 59
Figure 3-7. Biochemical characterization of PlyCB and PlyCB mutants by phospholipids screening assay 61
Figure 3-8. Molecular docking of PlyCB with specific phospholipids 62
Figure 3-9. Structural effects of the R66E mutation in PlyCB 64
Figure 4-1. Membrane integrity test after incubation with PlyC 69
Figure 4-2. Internalization of PlyCB is dependent on temperature and interaction with lipid raft domains 71
Figure 4-3. Internalized PlyCB is associated with endocytic pathway 74
Figure 4-4. Intracellular trafficking of PlyCB is regulated by PI3K pathway 76
Figure 5-1. Structural view of B domain of the anthrax toxin and PlyCB subunit of the PlyC endolysin 85

List of Abbreviations

In alphabetical order

BLAST	Basic Local Alignment Search Tool
CBD	Cell-wall binding domain
CFU	Colony forming units
CS	Chondroitin sulfate
CS-B	Chondroitin sulfate-B
CSPG	Chondroitin sulfate proteoglycan
CPP	Cell-penetrating peptide
CytD	Cytochalasin D
DAPI	4',6-diamidino-2-phenylindole
Fn	Fibronectin
GAG	Glycosaminoglycan
GAS	Group A Streptococcus
GlcNAc	N-acetylglucosamine
GM1	Monosialotetrahexosylganglioside
HS	Heparan sulfate
HSPG	Heparan sulfate proteoglycan
IgG	Immunoglobulin G
LTA	Lipoteichoic acid
mDAP	meso-diaminopimelic acid
MDC	Monodansylcadaverine
MRSA	Methicillin-resistant *Staphylococcus aureus*
MurNAc	N-acetylmuramic acid
PA	Phosphatidic Acid
PDB	Protein data bank
PEG	Polyethylene glycol
PG	Peptidoglycan
PI	Propidium iodide

PI3K	Phosphoinositide 3-kinase
PIP	Phospholipid
PlyC	Endolysin from the streptococcal bacteriophage C1
PlyCA	Catalytic domain of PlyC
PlyCB	Cell wall binding domain of PlyC
PtdIn	Phosphatidylinositol
PtdSer	Phosphatidylserine
PtdEtn	Phosphatidylethanolamine
PtdCho	Phosphatidylcholine
STSS	Streptococcal toxic shock syndrome
TAT	Transactivator of transcription from HIV
THY	Todd-Hewitt broth supplemented with 1% [wt/vol] yeast extract
WHO	World Health Organization

Chapter 1: Introduction and literature review

Pathogenesis of Group A streptococcal infections

Types of infection and significance

Streptococcus pyogenes (group A Streptococcus or GAS) is a Gram-positive human pathogen that typically colonizes the skin and mucosal surface, capable of causing an exceptionally broad spectrum of diseases that range from mild superficial conditions, such as pharyngitis ('strep throat'), tonsillitis, and impetigo, to cellulitis in the deeper tissues. However, GAS may also elicit severe life-threatening complications, including pneumonia, bacteremia, necrotizing fasciitis (‘flesh-eating disease’), and streptococcal toxic shock syndrome (STSS). In addition, some GAS infections can lead to post infectious autoimmune sequelae such as acute rheumatic fever, streptococcal arthritis, and post-secondary glomerulonephritis [for an extensive review, see (Cunningham 2000)]. One of most common childhood illnesses in the United States is streptococcal pharyngitis, which accounts for an estimated 15 million outpatient physician visits each year (Hing, Hall et al. 2008). In the United States, the economic burden of streptococcal pharyngitis among children has been estimated between $224 million to $539 million per year (Pfoh, Wessels et al. 2008). Furthermore, 9,000-11,500 cases of invasive GAS disease occur annually, resulting in 1,000-1,800 deaths. STSS and necrotizing fasciitis each comprise an average of about 6%-7% of these invasive cases (CDC 2008). Overall, group A streptococcal disease remains a major worldwide health concern, and the World Health Organization has

estimated that severe GAS infections causes more than 500,000 deaths globally each year (Carapetis, Steer et al. 2005).

Virulence factors

Group A Streptococcus ensures itself a successful pathogen by adapting to the diverse physiological environment on/in the human host. For pathogenicity, GAS produces various virulence factors that interact with the host at many cellular and tissue levels. The cell surface of GAS accounts for many of the bacterium's determinants of virulence, especially those associated with colonization, internalization, and evasion of phagocytosis and the host immune responses. Antigenic components on the surface include the group specific carbohydrate, which is the basis for the Lancefield stereotyping method (Facklam 2002), cell wall peptidoglycan, lipoteichoic acid (LTA), and a variety of surface proteins, such as M protein, C5a peptidase, fimbrial proteins and fibronectin-binding proteins (protein F). Moreover, several extracellular products from GAS have been elucidated as virulence factors, including proteases, DNases, streptokinase, hyaluronidase, super antigens, and hemolysin (Cunningham 2000). The function of the virulence factors and their roles in the regulatory pathogenic network is summarized below (**Figure 1-1**). In addition, *Mga* is a key transcription factor in the regulatory network upon expression of GAS virulence genes, has been characterized as a multiple gene regulator for virulence in group A streptococci. Its major role is to activate the transcription of several virulence genes that including those for M protein (*emm*), C5a peptidase (*scpA*), M-like proteins (*mrp, enn,* and *fcR*), serum opacity factor (*sof*), and secreted inhibitor of complement (*sic*) (McIver 2009).

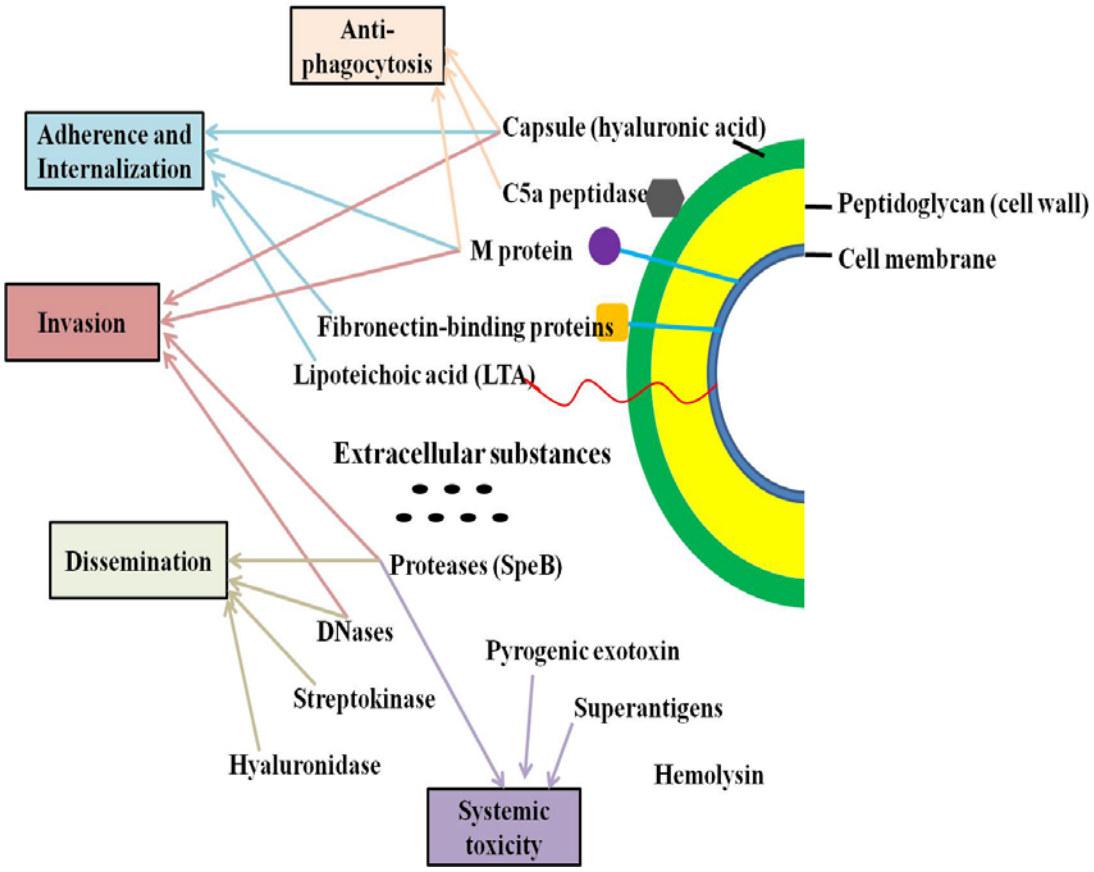

Figure 1-1. GAS virulence factors interact with the host at various levels

Importantly, many of the known streptococcal virulence factors play a role in different stages of infection. At the organism level, these virulence factors are involved in facilitating dissemination throughout the body circulation and can induce systemic toxicity. At the cell or tissue level, these factors contribute to the pathogenicity of GAS by mediating adherence to host cells, promoting internalization and invasion, and then evading phagocytosis. Modified from (Cunningham 2000; Tart, Walker et al. 2007).

Interaction of bacterial surface proteins with host proteins of extracellular matrix as well as cell surface receptors are crucial during the host-pathogen interaction process. It is now realized that GAS utilizes whole sets of adhesins such as lipoteichoic acids (LTA), M protein, serum opacity factor, and multiple fibronectin-binding proteins to establish direct contact with the host tissue (Nitsche-Schmitz, Rohde et al. 2007; Nobbs, Lamont et al. 2009). Both the M proteins (Ellen and

Gibbons 1972) and LTA (Beachey and Simpson 1982) are attached externally to the cell surface and mediate bacterial adherence to host cells. The key mediator on GAS surface is the streptococcal fibronectin (Fn)-binding protein, that can be detected in about 80% of all GAS isolates (Goodfellow, Hibble et al. 2000). Fn-binding protein has been shown to promote streptococcal adherence to the amino terminus of fibronectin, which acts as bridging molecule between streptococci and the $\alpha_5\beta_1$ integrin on the eukaryotic cells (Hanski, Horwitz et al. 1992; Ozeri, Rosenshine et al. 1998). Once adhered, GAS possess the ability to internalize and survive in an intracellular environment (**Figure 1-2**) (Fluckiger, Jones et al. 1998). The capability of GAS to promote internalization by human non-phagocytic cells was observed at mid 1990s (LaPenta, Rubens et al. 1994). Although the intracellular fate of GAS after internalization is not well understood, studies have been suggested that internalization of GAS is associated with recurrent streptococcal infection (Ogawa, Terao et al. 2011), because GAS, in a rare event, can circuvent host defence by escaping from fusion with the lysosomes, externalize by inducing apoptosis of host cell and sebsequently repopulate the mucosal surface after antibiotic prophylaxis (Marouni and Sela 2004; Kwinn and Nizet 2007).

In addition, GAS can use various virulence factors to avoid phagocyte engagement, inhibit complement and opsonization, block phagocytotic uptake, promote host cell apoptosis, and resist specific effectors or phagocyte killing by antimicrobial peptides and reactive oxygen species (Kwinn and Nizet 2007).. In summary, internalization by host cells has important implications in the pathogenesis of streptococcal infections.

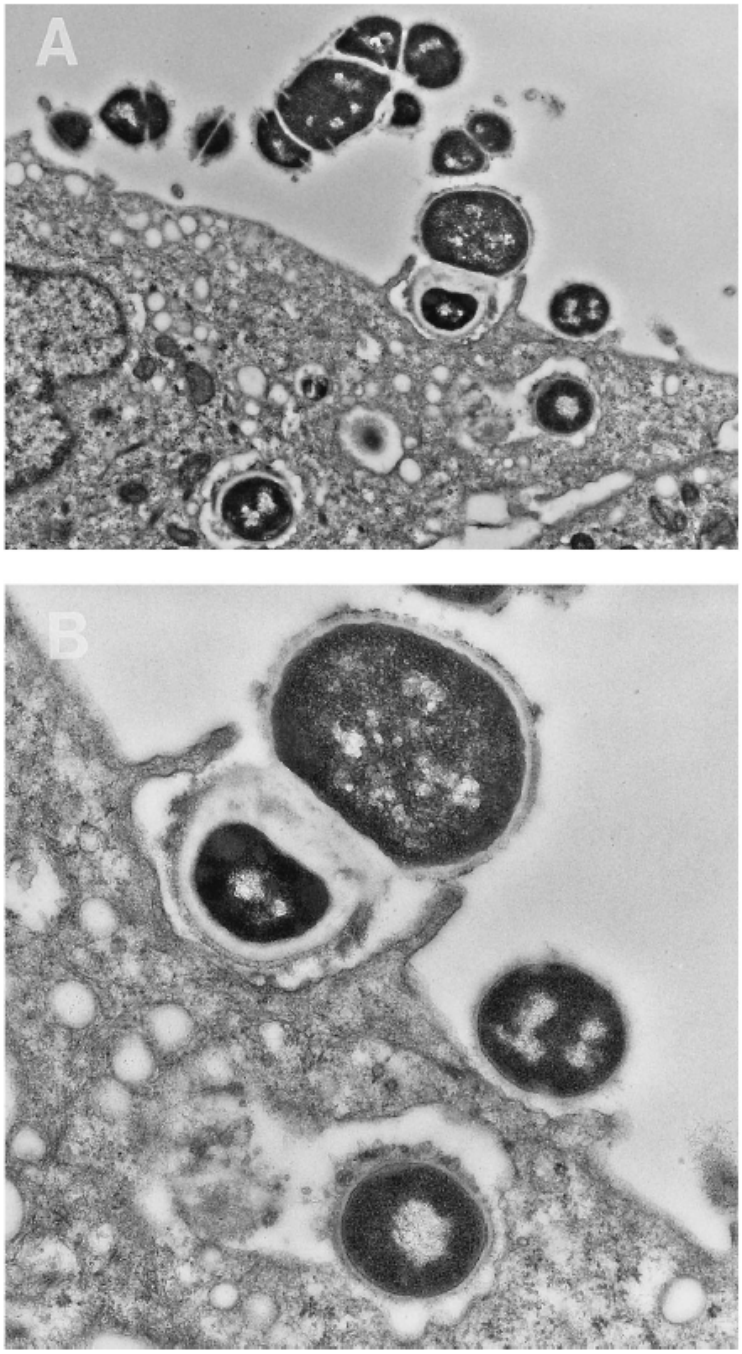

Figure 1-2. Attachment and internalization of streptococci by epithelial cell

Streptococci were observed being engulfed by membrane extension upon internalization into epithelial cell. Intracellular streptococci are found enclosed in cytoplasmic vacuoles. Magnification, 12,700 X (A) and 24,300 X (B) (Fluckiger, Jones et al. 1998).

Vaccine development

To date, no effective vaccine for GAS is commercially available. However, GAS vaccine development has been primarily focused on the highly variable N-terminus (determining serotype) of the M protein, which led to successful phase I/II clinical trials of a 26-valent recombinant M protein vaccine in 2005 (McNeil, Halperin et al. 2005). However, epidemiological surveys show that the 26-valent vaccine would provide good coverage of circulating strains of GAS in developed countries (over 72%) but low coverage in many developing countries (as low as 24% in the Pacific region) (Steer, Law et al. 2009). Most recently, the 26-valent vaccine was reformulated into a 30-valent vaccine to increase the coverage of circulating *emm* types in the United States, Canada and Europe as well as developing countries (Dale, Penfound et al. 2011). In preclinical studies, the 30-valent vaccine has been shown to induce functional opsonic antibodies against all *emm* types of GAS represented in the vaccine. And a phase I clinical evaluation of the 30-valent vaccine in adult volunteers is expected in 2013.

Alternatively, interest in using the conserved region at the carboxyl C-terminus of M protein for vaccine development has increased (Zaman, Abdel-Aal et al. 2012). In addition, other candidates, including streptococcal C5a peptidase, streptococcal carbohydrate, fibronectin-binding proteins, cysteine protease and streptococcal pili, have been recently reported in several vaccine studies (Shet, Kaplan et al. 2003; Sabharwal, Michon et al. 2006; Steer, Batzloff et al. 2009), supporting further investigation of novel GAS vaccine development.

Despite considerable progress having been made with several vaccine candidates, as mentioned above, there remain significant hurdles to GAS vaccine development. These include safety concerns, lack of understanding of immune sequelae, insufficient epidemiological data and minimal development of combination antigen vaccines (Steer, Dale et al. 2013). As such, more investment and collaboration is required to develop a safe and effective GAS vaccine.

Treatment strategy and current challenge

Even though most antibiotics are still effective against GAS, antibiotic treatment failure in cases of streptococcal infection have been frequently reported (Conley, Olson et al. 2003; Baldassarri, Creti et al. 2006; Passali, Lauriello et al. 2007).

GAS are traditionally considered as extracellular pathogens. However, many of them have a remarkable capability to internalize into human eukaryotic cells (Nitsche-Schmitz, Rohde et al. 2007; Nobbs, Lamont et al. 2009). This has a crucial influence not only on bacterial persistence, but also on the progression of infection into deeper tissues. Evidence that intracellular habitation of GAS has *in vivo* relevance comes from an examination of tonsils that were excised from patients with recurrent tonsillitis. The presence of viable intracellular streptococci in these tonsils suggested that the internalization by host cells created a bacterial reservoir by avoiding direct contact with antibiotics, which is responsible for the recurrence of the infection (Osterlund and Engstrand 1997; Osterlund, Popa et al. 1997). Significant efforts have been taken to investigate this unique pathogenic niche as well as new

ways to control intracellular pathogens, including the need for alternative antimicrobials that can work in both extracellular and intracellular environments.

Alternative antimicrobials: bacteriophage and its encoded endolysin

Bacteriophage:

Bacteriophage are viruses that target and replicate within bacteria in a species-specific manner (Clokie, Millard et al. 2011). They were first discovered in 1915 by Frederick Twort (Twort 1915) , and in 1917 Felix d'Herelle realized that they had the potential to kill bacteria (d'Herelle 1917). As a natural killer, the idea of developing bacteria-fighting viruses as an antimicrobial agent against infections was first established in the 1930s. (Larckum 1932), only to be abandoned because the discovery of antibiotics against bacterial disease. However, in an era when traditional antibiotics are rapidly losing their effectiveness, the interest to develop bacteriophage for therapeutic use is being revisited (Alisky, Iczkowski et al. 1998; Merril, Scholl et al. 2003; Kutter, De Vos et al. 2010). For the past few decades, many studies have demonstrated the therapeutic potential of bacteriophage against Gram-positive or-negative pathogens *in vivo* [for an extensive review, see (O'Flaherty, Ross et al. 2009)]. One advantage of using whole phage as therapeutic agents is the ‘amplification mode’; that is, the lytic cycle in which one phage enters a bacterium and replicates, releasing hundreds of phage progenies after lysis, which then go on and infect adjacent bacteria and so on. On the other hand, an inevitable concern with phage therapy is the rapid development of resistance to phage infection, since bacteria have evolved strategies to survive in the phage-infested environment. Scientists have developed a cocktails of phages designed to circumvent resistance. This approach has

proven successful in limited clinical settings (Merabishvili, Pirnay et al. 2009) with a Phase II clinical trial currently being carried by 'Ampliphi Biosciences Corporation'. However, development of a consistent composite mixture of phage that is acceptable to the FDA is unlikely to be straightforward due to concerns of potential transfer of toxin genes or foreign DNA (Sulakvelidze, Alavidze et al. 2001).

Bacteriophage-encoded endolysin:

Although bacteriophage continue to generate interest as an alternative to antibiotics, focus is shifting to the use of purified phage components as an alternative protein-based antibacterial agents due to their bacteriolytic activity. Bacteriophage encode endolysins (peptidoglycan hydrolyses) that function to lyse the bacterial cell wall for release of phage progeny during the latter stage of the phage lytic cycle (Fischetti 2008). Timing of lysis is initiated by holins, which perforate the bacterial membrane and allow the cytoplasmically accumulated endolysins access to the highly cross-linked peptidoglycan (Wang, Smith et al. 2000). Significantly, in the absence of holins or parental bacteriophage, exogenous addition of these purified endolysins can also lyse the peptidoglycan of susceptible Gram-positive organisms. Once the structural peptidoglycan is compromised, internal turgor pressure, measured at 20-50 atmospheres for Gram-positive organisms (Arnoldi, Fritz et al. 2000), causes a rapid osmotic lysis of the bacterial membrane resulting in cell death. With few exceptions, this enzyme-mediated “lysis from without” phenomenon – a term which has been used to describe a variety of phenomena in which an extracellular agent destroys a bacterial cell envelope (Abedon 2011) – is restricted to Gram-positive species as the Gram-negative peptidoglycan is protected by an outer membrane that is not

permeable to an exogenous enzyme under normal conditions. Nonetheless, peptidoglycan hydrolases encoded by Gram-positive phage represent an attractive therapeutic option (Loessner 2005; Borysowski, Weber-Dabrowska et al. 2006; Donovan 2007; Hermoso, Garcia et al. 2007; Fischetti 2010).

- **Basic modular structure of endolysin**

Endolysins from Gram-positive infecting bacteriophage typically display a modular structure with one or more catalytic domains and a cell wall binding domain (Garcia, Garcia et al. 1988; Garcia, Garcia et al. 1990) depicted in **Figure 1-3**.

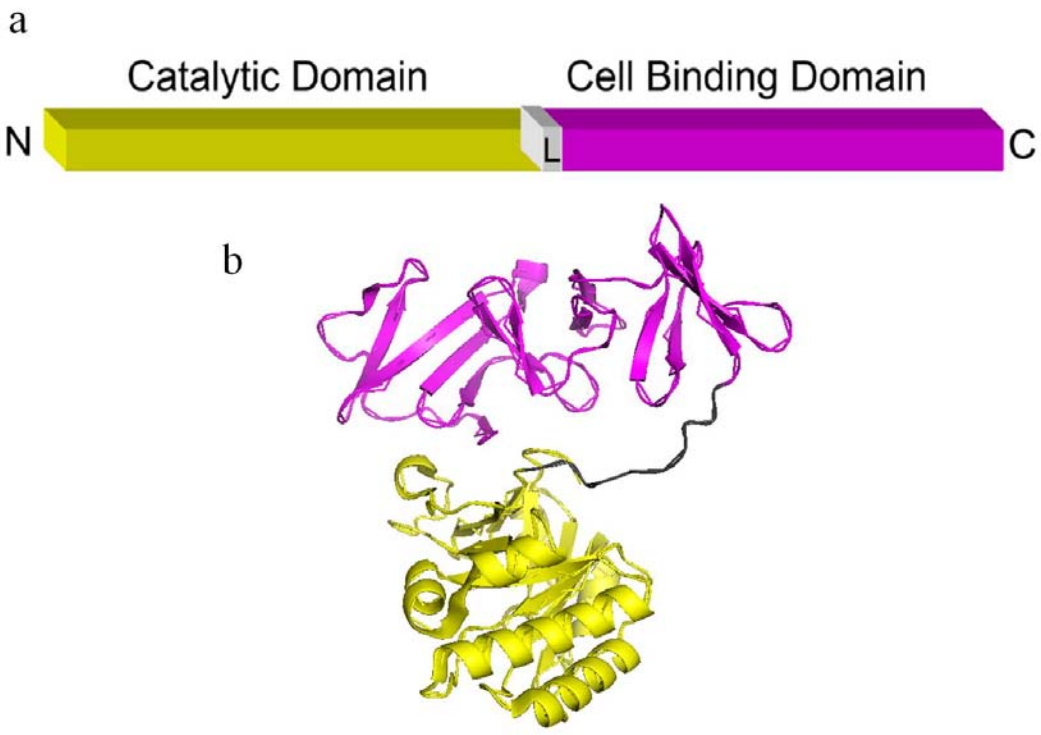

Figure 1-3 Modular structure of endolysin

(a) Basic architecture of endolysin (Fischetti 2008). (b) Crystal structure of Cpl-1 endolysin from phage Cp-1 (Hermoso, Monterroso et al. 2003). Note that the catalytic domain is in yellow, the linker region (L) that connects the catalytic domain to the cell wall binding domain (in magenta) is colored by dark gray.

For the catalytic domain, one of the best characterized endolysin activities is the cysteine, histidine-dependent amidohydrolases/peptidases (CHAP) endopeptidase (Bateman and Rawlings 2003; Rigden, Jedrzejas et al. 2003) with active site residues that are conserved across many species and have been shown to be essential for activity by site-directed mutagenesis (Pritchard, Dong et al. 2004; Nelson, Schuch et al. 2006). Other catalytic domains exist and have been described in more detail by Nelson *et al.* (Nelson, Rodriguez et al. 2012). Meanwhile, bacteriophage derived endolysin also possess a cell-wall binding domain (CBD) that recognizes epitopes on the cell wall surface. These epitopes can be carbohydrates, teichoic acids, or peptide moieties of the peptidoglycan in a species- or even strain-specific manner (Schmelcher, Tchang et al. 2011). Frequently the CBD has been found to be required for 'lysis from without' activity of the endolysin as the catalytic domain alone has highly diminished activity against the host organism, presumably as a consequence of catalysis occurring after only random encounters between the catalytic domain and the sessile bond of the peptidoglycan, or the enzyme is completely inactive (Porter, Schuch et al. 2007). In contrast, however, there are other reports where deleting the CBD does not affect the lytic activity (Low, Yang et al. 2005) or even results in increased lysis from without (Cheng and Fischetti 2007; Horgan, O'Flynn et al. 2009; Gerova, Halgasova et al.). In addition to a catalytic domain and a CBD, Gram-positive phage endolysins often have a flexible linker sequence of 10-20 amino acids that connect two globular (catalytic and cell wall binding) domains. However, little information is known about the function of this linker region.

In contrast to Gram-positive bacteria, the Gram-negative peptidoglycan is contained within the periplasmic space between the inner and outer bacterial membranes. It is relatively thin (5-10 layers) compared to the Gram-positive peptidoglycan (up to 40 layers) and lysis “from within” is via a holin and endolysin during the phage lytic cycle. Accordingly, endolysins from phages that infect Gram-negative hosts are typically comprised of a single globular catalytic domain, which in most case supplies one of the two glycosidase activities. The catalytic domains do not appear to require any specific binding domain to recognize and digest the Gram-negative peptidoglycan.

The two notable exceptions include the *Pseudomonas* phage endolysins KZ144 and EL188, which harbor a distinct N-terminal cell wall binding domain in addition to a catalytic domain (Briers, Volckaert et al. 2007). Moreover, the binding domains alone were shown to be sufficient to directly bind to purified *Pseudomonas aeruginosa* cell walls (Briers, Schmelcher et al. 2009).

Although the modular nature of phage endolysins was initially described in the early 1990’s (Diaz, Lopez et al. 1990; Garcia, Garcia et al. 1990; Diaz, Lopez et al. 1991; Croux, Ronda et al. 1993), it has not been until recently that exploiting the modular nature of endolysins has become a major biotechnological focus for the development of endolysin.

- **Cell wall architecture and catalytic activities of endolysins**

In order to preserve bacterial cell structural integrity, the peptidoglycan is an essential scaffold/polymer found on the outside of the cytoplasmic membrane of most bacteria. As its name implies, the main structural features of peptidoglycan are linear

glycan strands cross-linked by short peptide stems, which in turn are cross-linked either directly together or through a peptide "bridge" (**Figure 1-4**). The hetero-polymer glycan strand is conserved in both Gram-positive and -negative bacteria and composed of alternating N-acetylmuramic acid (MurNAc) and N-acetylglucosamine (GlcNAc) residues coupled by β(1→4) linkages. The peptide stem is covalently attached to the glycan polymer by an amide bond between each MurNAc and an L-alanine residue, which is the first amino acid of the "peptide" part. The rest of the peptide stem contains alternating L- and D-form amino acids that are conserved in Gram-negative organisms, but is diverse for Gram-positive ones. For many Gram-positive organisms, the third residue of the stem peptide is L-lysine, which is cross-linked to an opposing stem peptide on a separate glycan polymer through an interpeptide bridge, the composition of which varies between species. For instance, the interpeptide bridge of *S. aureus* is pentaglycine whereas di-alanine is present in *S. pyogenes* (depicted in **Figure 1-4***)*. In Gram-negative organisms and some genera of Gram-positive bacteria (i.e., *Bacillus* and *Listeria*), a meso-diaminopimelic acid (mDAP) residue is present at position number three of the stem peptide instead of L-lysine. In these organisms, mDAP directly crosslinks to the terminal D-alanine of the opposite stem peptide (i.e. no interpeptide bridge). Whether an interpeptide bridge is present or not, the joining of opposing stem peptides gives rise to the three dimensional lattice that is a defining characteristic of the bacterial peptidoglycan.

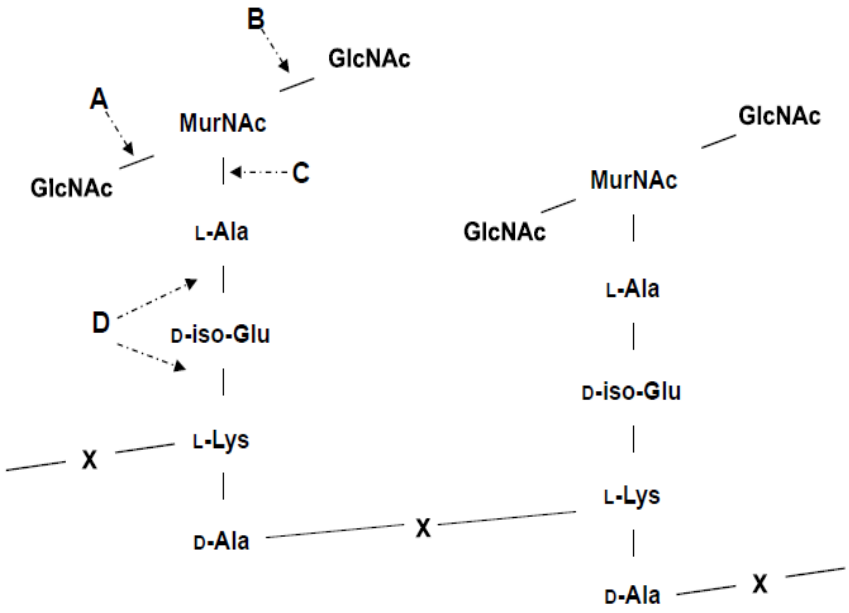

Figure 1-4. Structure of the peptidoglycan and cleavage sites by the endolysins

Glycosidase cleave the carbohydrate backbone. (A) *N*-acetylglucosaminidase cleaves on the reducing side of GlcNAc. (B) Lysozymes or muramidases are N-acetylmuramidases that cleave on the reducing side of MurNAc. Another glycosidase-like enzyme that cleaves this same bond but does not require hydrolysis of water is the lytic transglycosylase. (C) The N-acetylmuramoyl-L-alanine amidase cleaves the first amide bond between the peptide moiety (L-alanine) and the glycan moiety (MurNAc). (D) Numerous endopeptidase cleavage sites are present on the pepdidoglycan. Note, X is the transpeptide bridge, the length and composition of which varies depending on species. (Shen 2012).

Due to a moderately conserved overall structure of the PG, there are only a limited number of covalent bonds that are available for cleavage by endolysins. Generally, endolysins (as well as autolysins and exolysins) can be classified into three different groups depending on their cleavage specificity: those that cleave between two sugar residues (i.e., glycosidases and lytic transglycosylases), those that cleave between a sugar residue and an amino acid (i.e. N-acetylmuramoyl-L-alanine amidases), and those that cleave between two amino acids (i.e. endopeptidases), each

of which is summarized (**Figure 1-4.**) and select examples are presented in **Table 1-1**.

Table 1-1. Summary of *in vitro* studies with Gram-positive phage endolysins (Shen 2012).

Endolysin	Target	Catalytic activities by homology	In vitro activity	Reference
λSa2	*Streptococcus agalactiae*	Glycosidase + endopeptidase	Activity on purified peptidoglycan as analyzed by mass spec	(Pritchard, Dong et al. 2007)
Cpl-1	*Streptococcus pneumoniae*	N-acetylmuramidase	5 log decrease of cfu in 30 sec with 100 µg	(Garcia, Garcia et al. 1987)
PAL	*Streptococcus pneumoniae*	N-acetylmuramoyl-L-alanine amidase	4 log decrease of cfu in 30 sec with 100 U/ml	(Loeffler, Nelson et al. 2001)
PlyGBS (B30)	*Streptococcus agalactiae*	N-acetylmuramidase + endopeptidase	2 log decrease of cfu in 60 min with 40 U	(Pritchard, Dong et al. 2004; Cheng, Nelson et al. 2005)
PlyC	*Streptococcus pyogenes*	N-acetylmuramoyl-L-alanine amidase	7 log decrease of cfu in 5 sec with 10 ng	(Nelson, Loomis et al. 2001)
Ply700	*Streptococcus uberis*	N-acetylmuramoyl-L-alanine amidase	0.5 log decrease of cfu in milk in 15 min with 50 µg/ml	(Celia, Nelson et al. 2008)
PlyG	*Bacillus anthracis/cereus*	N-acetylmuramoyl-L-alanine amidase	6 log decrease of cfu in 15 min with 20 U	(Schuch, Nelson et al. 2002)
PlyB	*Bacillus cereus*	N-acetylmuramidase	OD_{600} decrease from 0.45 to 0.05 with 2.5 µM. PlyG also had similar results	(Porter, Schuch et al. 2007)
Φ11	*Staphylococcus aureus*	N-acetylmuramoyl-L-alanine amidase + endopeptidase	OD_{600} decrease from 0.3 to 0.15 in 20 minutes with 20 µg/ml	(Navarre, Ton-That et al. 1999)

LysK	*Staphylococcus aureus*	N-acetylmuramoyl-L-alanine amidases + endopeptidase	3 log decrease of cfu in 1 hour with crude lysate	(O'Flaherty, Coffey et al. 2005)
ClyS	*Staphylococcus aureus*	N-acetylmuramoyl-L-alanine amidase	3 log decrease of cfu in 30 min with 250 µg	(Daniel, Euler et al. 2010)
Ply511	*Listeria monocytogenes*	N-acetylmuramoyl-L-alanine amidase	OD_{600} decrease from 1.6 to 0.25 in 20 minutes with 180 U/ml	(Gaeng, Scherer et al. 2000)
PlyPSA	*Listeria monocytogenes*	N-acetylmuramoyl-L-alanine amidase	OD_{600} decrease from 1.0 to 0.2 in 10 min with 2.8 nmol	(Korndorfer, Danzer et al. 2006)
Ply500	*Listeria monocytogenes*	L-alanyl-D-glutamate endopeptidase	OD_{600} decrease from 1.0 to 0.2 in 1 min at 4.8 µg/ml or 3 min at 1.6 µg/ml	(Schmelcher, Tchang et al. 2011)
Ply118	*Listeria monocytogenes*	L-alanyl-D-glutamate endopeptidase	OD_{600} decrease from 1.6 to 0.5 in 20 minutes with 60 U/ml	(Gaeng, Scherer et al. 2000)

- **Summary of *in vitro* studies of endolysin**

Upon direct contact with Gram-positive bacteria, endolysin actively digests the cell wall peptidoglycan that results in bacterial cell osmotic lysis (**Figure 1-5**). During the past decades, numerous citations have reported in vitro activity (i.e. lysis from without) of endolysins against Gram-positive pathogens. The "substrate" for these enzymes is complex (often the three dimensional superstructure of the peptidoglycan as well as secondary binding sites for the CBDs). Thus, synthetic small molecular weight chromogenic or fluorogenic compound are rarely adequate as substrates for these enzymes. Instead, isolated cell walls or even whole cells remain the substrates of choice. As such, the most common assay involves the use of a

spectrophotometer to measure the loss of turbidity of a suspension of live cells due to lysis from without (i.e. drop of OD_{600nm} per unit time). This method has been used to describe a "unit" of enzyme activity based on the dilution of an endolysin solution needed to reduce the optical density by half in a defined amount of time (Fischetti, Gotschlich et al. 1971; Loeffler, Nelson et al. 2001). While approaches that rely on turbidometric analysis are simplistic and easy to use, they are an indirect measure of lysis (and cell death) and subject to numerous biological factors. First, the phase of growth affects the thickness of the peptidoglycan, which in turn can affect the apparent rate of lysis. An enzyme tested on mid-log cells may have several orders of magnitude greater activity than the same enzyme assayed on stationary phase cells. Likewise, the turgor pressure of the cell is important as is the osmolarity of the solution. Similarly, cells in media lyse much more slowly than cells resuspended in distilled water.

Also, as cells lyse, they release DNA and other cellular components, causing the viscosity of the reaction tube to rise, altering condition for further lysis less efficient. Finally, because endolysins are often species specific, it is difficult to compare the activity of one enzyme against another when the substrate is a different bacterial species. Despite these caveats, Mitchell and colleagues have developed a mathematical approach to estimate kinetic constants based on a turbidometric reduction assay (Mitchell, Nelson et al. 2010).

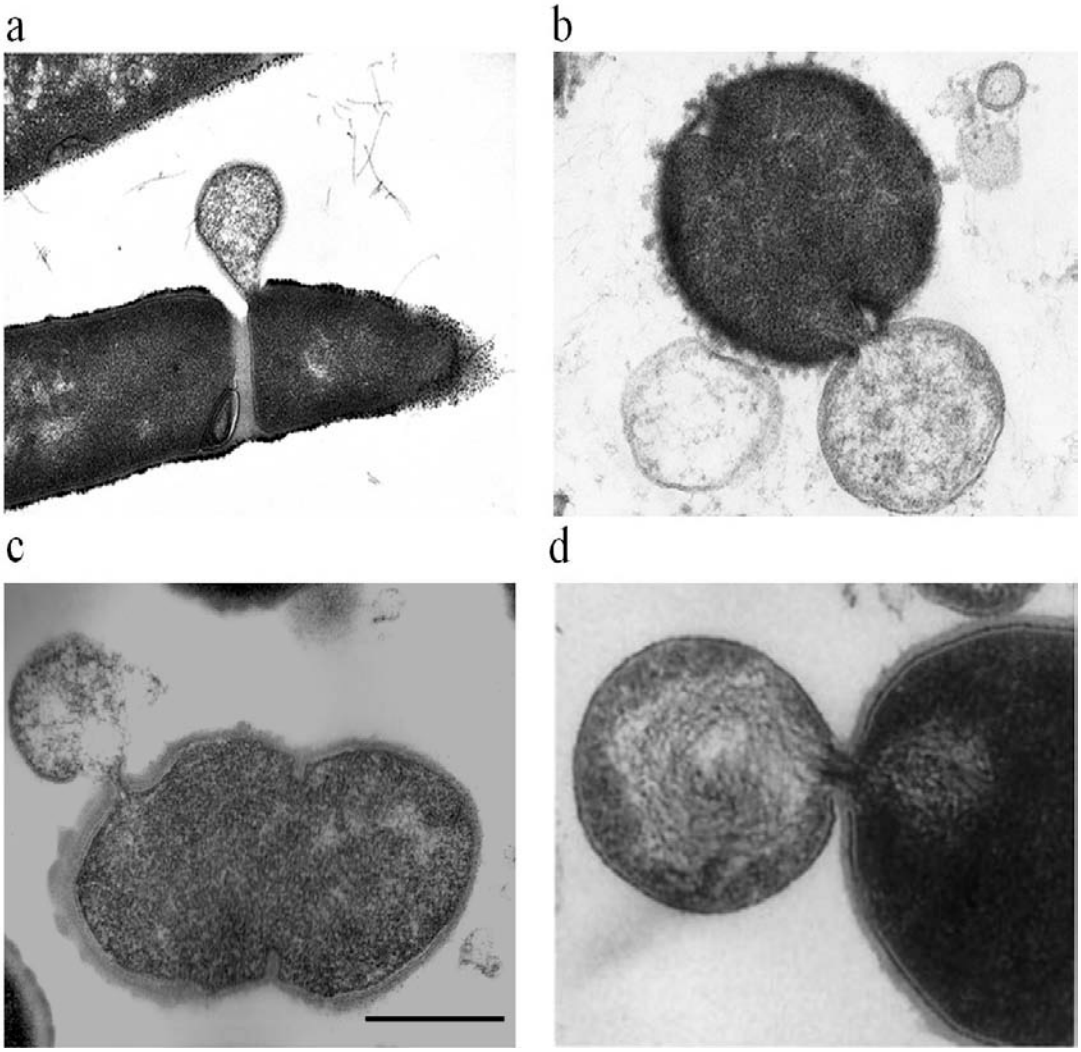

Figure 1-5. Electron micrograph of bacteria treated by the endolysins

(a) *Bacillus anthracis* is treated with PlyG endolysin (Schuch, Nelson et al. 2002). (b) *Staphylococcus aureus* is treated with ClyS endolysin (Daniel, Euler et al. 2010). (c) *Streptococcus pneumoniae* is treated with PAL endolysin (Loeffler, Nelson et al. 2001). (d) *Streptococcus pyogenes* is treated with PlyC endolysin (Nelson, Loomis et al. 2001). Note that in each image, the endolysin is weakened the cell wall causing the cytoplasmic membrane to externalize. Total magnification is x50,000, scale bar is 0.5 μm.

Another common type of *in vitro* endolysin assay is based on colony counts whereby a known amount of bacteria is exposed to an endolysin for a given amount of time, serially diluted, and then plated on growth media. Activity is then reported as

a log-fold decrease in colony forming units (cfu) over a defined interval. While this method is often used to quantify cell death, the high affinity of the CBDs for the bacterial surface can allow for a situation where the reported activity (i.e. rate of cell death) is overestimated. For example, an endolysin may bind the bacterial surface via the CBD in seconds, but catalytic lysis may not immediately occur. If the endolysin remains bound during the serial dilution step, actual lysis and cell death may take place on the agar plate at a later time point. As such, reported activity especially for short incubations times can be overestimated.

Table 1-1 contains a list of *in vitro* results for many endolysins that produce lysis from without on Gram-positive organisms. This list is not intended to be comprehensive. Instead, its purpose is to provide activity data for many of the endolysins mentioned in this chapter including in terms of the diversity of activity displayed by these enzymes in different assays. A thorough inspection of this table will reveal something already obvious to those in the field, namely that not all endolysins are created equal. Some kill/lyse very efficiently in seconds at microgram or even nanogram quantities whereas others need much higher doses and longer incubation times to show any lytic activity.

- **Summary of *in vivo* studies of endolysin**

Although endolysins have been studied extensively for their role in the bacteriophage replication cycle for over half a century, particularly the T-even phage that infect Gram-negative hosts. It has only been in the past twenty years that scientists have begun evaluating the use of endolysins in animal infection models of

human disease. **Table 1-2** shows a complete list to date of all reported *in vivo* therapeutic trials that utilize endolysins which are further summarized below.

Table 1-2. Summary of *in vivo* studies with endolysins, adapted from (Shen 2012)

Bacteria	**Endolysin**	**Reference**
Streptococcus pyogenes	C1*	(Nelson, Loomis et al. 2001)
Streptococcus agalactiae	PlyGBS	(Cheng, Nelson et al. 2005)
Bacillus anthracis	PlyG	(Schuch, Nelson et al. 2002)
	PlyPH	(Yoong, Schuch et al. 2006)
Streptococcus pneumoniae	Cpl-1	(Loeffler, Nelson et al. 2001)
	Cpl-1	(Loeffler, Djurkovic et al. 2003)
	Cpl-1	(Loeffler and Fischetti 2003)
	Cpl-1	(Jado, Lopez et al. 2003)
	Cpl-1	(Entenza, Loeffler et al. 2005)
	Cpl-1	(McCullers, Karlstrom et al. 2007)
	Cpl-1	(Grandgirard, Loeffler et al. 2008)
	Cpl-1	(Witzenrath, Schmeck et al. 2009)
	PAL	(Loeffler and Fischetti 2003)
	PAL	(Jado, Lopez et al. 2003)
Staphylococcus aureus	MV-L	(Rashel, Uchiyama et al. 2007)
	$CHAP_k$	(Fenton, Casey et al. 2010)
	LysGH15	(Gu, Xu et al. 2011)
	ClyS**	(Daniel, Euler et al. 2010)
	P-27/HP	(Gupta and Prasad 2011)
	ClyS**	(Pastagia, Euler et al. 2011)
	Chimeras	(Schmelcher, Powell et al. 2012)
	PlySs2	(Gilmer, Schmitz et al. 2013)

*Renamed PlyC according to (Nelson, Schuch et al. 2006)
**Chimeric construct from the bacteriophage Twort and ΦNM3 endolysins

Fischetti and co-workers were the first to use a purified endolysin therapeutically in an *in vivo* model of streptococcal infection (Nelson, Loomis et al. 2001). It was found that oral administration of an endolysin (250 U) from the streptococcal C1 bacteriophage, named PlyC in a subsequent publication (Nelson, Schuch et al. 2006), provided protection from colonization in mice challenged with 10^7 GAS. Furthermore, when 500 U of this enzyme was administered orally to 9 heavily colonized mice, no detectable streptococci were observed 2 hours post-

endolysin treatment and only one mouse had any measurable streptococcal counts 24 and 48 hours later.

PlyGBS, which is 97% identical to B30 endolysin (Pritchard, Dong et al. 2004), is another phage endolysin that is active against GAS as well as groups B, C, G, and L streptococci. This enzyme was tested in a murine vaginal model of *Streptococcus agalactiae* (i.e. group B streptococci) colonization to see if PlyGBS could be a potential therapeutic for pregnant women to prevent transmission of neonatal meningitis-causing streptococci to newborns (Cheng, Nelson et al. 2005). A single vaginal dose of 10 U was shown to decrease colonization of pathogenic group B streptococci by ~3 logs. Significantly, PlyGBS was found to have a pH optimum ~5.0, which is similar to the range normally found within the human vaginal tract. Furthermore, this enzyme did not possess bacteriolytic activity against common vaginal microflora such as *Lactobacillus acidophilus*, suggesting a pathogen-specific therapeutic that, unlike broad range antibiotics, would likely reduce the concern of resistance development in exposed commensal bacteria.

Several phage endolysins have also been used against germinating spores and vegetative cells of *Bacillus* species. 50 U of PlyG, an endolysin isolated from the *B. anthracis* γ phage, was shown to rescue 13 out of 19 mice in an intraperitoneal mouse model of septicemia and extended the life of the remaining mice several fold over controls (Schuch, Nelson et al. 2002). Notably, this enzyme displayed a favorable temperature profile and was able to remain fully active after heating to 60°C for an hour. Moreover, the extreme lytic specificity of this enzyme toward *B. anthracis* and not other *Bacillus* species was exploited for diagnostic purposes in a luminescent-

based ATP assay of *B. anthracis* cell lysis. A second *Bacillus* endolysin, PlyPH, also active against *B. anthracis*, is unique in that it has high activity over a broad pH range, from pH 4.0 to 10.5. This enzyme also protected 40% of mice in an intraperitoneal *Bacillus* infection model compared to 100% death in control mice (Yoong, Schuch et al. 2006). Taken together, the robust and specific properties of the *Bacillus* endolysins make them amenable to therapeutic treatment and diagnostics of *B. anthracis*.

The most extensively studied endolysins in animal models are Cpl-1, an N-acetylmuramidase from the Cp-1 pneumococcal phage, and PAL, an N-acetylmuramoyl-L-alanine amidase from the Dp-1 pneumococcal phage. 100 U/ml PAL was shown to need only 30 seconds to cause an ~4 log drop in viability of 15 different *S. pneumoniae* serotypes representing multi-drug resistant isolates as well as those that contain a thick polysaccharide capsule (Loeffler, Nelson et al. 2001). In a mouse model of nasopharyngeal carriage, 1,400 U of PAL was shown to eliminate all pneumococci. In another study, Cpl-1 was shown to be effective in both a mucosal colonization model and in blood via a pneumococcal bacteremia model (Loeffler, Djurkovic et al. 2003). Because the catalytic domains of PAL and Cpl-1 hydrolyze different bonds in the pneumococcal peptidoglycan, these two enzymes were shown to be synergistic in a mouse intraperitoneal infection model (Jado, Lopez et al. 2003). (See the next section for more information about synergy) In a study on the effectiveness of endolysins against *in vivo* biofilms, Cpl-1 was shown to work on established pneumococcal biofilms in a rat endocarditis model (Entenza, Loeffler et al. 2005). Infusion of 250 mg/kg was able to sterilize 10^5 cfu/ml pneumococci in

blood within 30 minutes and reduce bacterial titers on heart valve vegetations by >4 log cfu/g in 2 hours. In an infant rat model of pneumococcal meningitis, an intracisternal injection (20 mg/kg) of Cpl-1 resulted in a 3 log decrease of pneumococci in the cerebrospinal fluid and an intraperitoneal injection led to a decrease of 2 orders of magnitude (Grandgirard, Loeffler et al. 2008). Additionally, Cp-1 was shown to save 100% of mice from fatal pneumonia when administered 24 hours after infection and 42% of mice when administered 48 hours after infection, a time point at which bacteremia was fully established (Witzenrath, Schmeck et al. 2009). Finally, Cpl-1 treatment of mice colonized with *S. pneumoniae* in an otitis media model was shown to significantly reduce co-colonization by challenge with influenza virus (McCullers, Karlstrom et al. 2007). Given that pneumococci are early colonizers to which additional pathogens and viruses might adhere, eliminating this population could have a multiplier effect on controlling infectious diseases.

The prevalence of methicillin-resistant *Staphylococcus aureus* (MRSA) as a primary source of nosocomial infection and community-acquired MRSA as an emerging public health threat has generated a considerable amount of interest in identifying and evaluating highly active staphylococcal endolysins. The first staphylococcal-specific endolysin investigated *in vivo* was MV-L, which was cloned from the ΦMR11 bacteriophage (Rashel, Uchiyama et al. 2007). This enzyme rapidly lysed all tested staphylococcal strains *in vitro*, including MRSA and vancomycin-intermediate/resistant clones. *In vivo*, this enzyme reduced MRSA nasal colonization ~3 logs and provided complete protection in an intraperitoneal model of staphylococcal infection when administered 30 minutes post-infection. At 60 minutes

post-infection, the same amount of MV-L provided protection in 60% of mice vs. controls. More recently, an endolysin from the GH15 phage, LysGH15, showed 100% protection in a mouse intraperitoneal model of septicemia (Gu, Xu et al. 2011). Likewise, CHAPk, a truncated version of the endolysin LysK, effected a 2 log drop in nasal colonization of mice when given 1 hour post challenge (Fenton, Casey et al. 2010). Lastly, ClyS is the first engineered endolysin to be tested in an animal model (Daniel, Euler et al. 2010). This enzyme is a chimera between the N-terminal catalytic domain of the Twort phage endolysin (Loessner, Gaeng et al. 1998) and the C-terminal cell wall-binding domain of the ΦNM3 phage endolysin. Like MV-L, ClyS displayed potent bacteriolytic properties against multi-drug resistant staphylococci *in vitro*. In a mouse MRSA decolonization model, 2-log reductions in viability were observed 1 hour following a single treatment of 960 μg of ClyS. Similarly, a single dose (1 mg) of ClyS provided protection when administered 3 hours post-staphylococcal challenge in an intraperitoneal septicemia model. Additionally, ClyS was shown to be effective and synergistic with oxacillin when treating topical infections of *S. aureus* (Pastagia, Euler et al. 2011).

- **Synergy studies**

Studies have shown that some endolysins can synergistically work with other endolysins or with some antibiotics both *in vitro* and *in vivo*. Synergy studies typically use a checkerboard broth microdilution method that allows for the concurrent determination of the minimal inhibitory concentration (MIC) of each (endolysin or antibiotic).The fractional MIC values of each agent are then put on an X/Y plot, which is called an isobologram. A linear relationship corresponds to an

"additive" effect. For example, if 0.5 MIC of agent A + 0.5 MIC of agent B displays the same efficacy as 1.0 MIC of either agent A or B, the two agents are additive. However, if the relationship has an inverse, non-linear curve, the effect is said to be "synergistic" (i.e., if 0.25 MIC each of agents A and B were equal to 1.0 MIC of either agent alone).

Using this method, the pneumococcal Cpl-1 endolysin, a muramidase, was shown to be synergistic with the PAL, an L-alanine amidase, and the bacteremic titer was reduced to a greater extent than by either endolysin alone (Jado, Lopez et al. 2003; Loeffler and Fischetti 2003). Since these enzymes hydrolyze different bonds, synergy is believed to be due to a greater destabilization of the three-dimensional peptidoglycan matrix. Cpl-1 was also found to be synergistic with penicillin as well as gentamicin (Djurkovic, Loeffler et al. 2005). In a similar fashion, the staphylococcal endolysin LysH5 was found to be synergistic with nisin, an antimicrobial peptide (Garcia, Martinez et al. 2010), and LysK was shown to be synergistic with lysostaphin, a staphylococcal exolysin in another recent *in vitro* study (Becker, Foster-Frey et al. 2008). Finally, ClyS, a fusion endolysin described above, was shown to be synergistic with oxacillin and vancomycin *in vitro* and with oxacillin *in vivo* in a mouse model of *S. aureus* septicemia (Daniel, Euler et al. 2010). The approach of combining lysins with antibiotics generally gives rise to increased antibacterial efficacy.

- **Immunogenicity**

As endolysins are globular proteins, they would be expected to elicit antibodies which may render them inactive and could hinder their therapeutic

development when administrated systemically. Toward this end, two decisive papers use *in vivo* models to address this issue. The first study from Loeffler and colleagues showed that intravenous injection of Cpl-1, a pneumococcal endolysin, into mice three times a week for four weeks resulted in positive IgG antibodies against the endolysin in 5 out of 6 mice (Loeffler, Djurkovic et al. 2003). Next, these "immunized" mice and naïve control mice were challenged with intravenous pneumococci followed by a 200 µg dose of Cpl-1 10 hours post challenge. Surprisingly, pneumococcal titers were reduced to the same level in both groups of mice at 15 minutes. *In vivo* analysis showed that in five out of six cases, mice that received three intravenous doses of Cpl-1 tested positive for immunoglobulin G (IgG) against the enzyme but this only had a moderate inhibitory effect on activity. Moreover, when rabbit hyperimmune serum was raised against the pneumococcal endolysin Cpl-1, it was found that lytic activity *in vitro* was slowed but not blocked. Similar *in vitro* results were seen with *B. anthracis* and *S. pyogenes* endolysins summarized in (Fischetti 2005).

In the second study, Jado and colleagues challenged mice with pneumococci followed by treatment with either of the pneumococcal endolysins, Cpl-1 or PAL (Jado, Lopez et al. 2003). Ten days later they confirmed the recovered mice had high IgG antibody titers to both enzymes, re-challenged the mice with pneumococci, and retreated with the endolysin. Significantly, pneumococcal titers fell 2-3 logs upon administration of the enzymes and all mice survived with no signs of anaphylaxis or adverse side events. These studies suggest that while antibodies can readily be raised to endolysins due to their proteinaceous nature, the antibodies do not effectively

neutralize the bacteriolytic actions of these enzymes *in vitro* or *in vivo*. Another potential use of endolysins can also be envisioned to apply topically, to mucous membranes (oral, nasal, or vaginal cavities) in order to minimize the effects of immune response .

- **Resistance development**

Resistance development is another obvious concern about the therapeutic use of endolysins. To date, there are no reports of strains sensitive to an endolysin developing resistance to the same endolysin. However, in fact, there have been a few reports where researchers have actively tried, but failed, to develop resistance to endolysins. In one study, *S. pneumonia, S. pyogenes,* and *B. anthracis* were exposed to sublethal doses of Cpl-1, PlyC, and PlyG, respectively summarized in (Fischetti 2005). Surviving colonies were grown and once again exposed to sublethal doses of the corresponding endolysin. In some cases, over 100 rounds of screening took place. At different cycles, surviving colonies were tested with lethal doses and resistance was never observed.

In a separate study, resistance to an endolysin was investigated more formally (Schuch, Nelson et al. 2002). Here, *Bacillus* species were screened for spontaneous resistance to PlyG, a *Bacillus*-specific endolysin, as well as two antibiotics, streptomycin and novobiocin. Resistant colonies were readily isolated for both antibiotics at a frequency of ~1×10^{-9}, but no resistance was found for PlyG at the same screening frequency. Next, bacilli were exposed to a chemical mutagen known to induce random mutations and the screening was repeated. This time, spontaneous resistance to the antibiotics occurred at frequencies of ~1×10^{-6} but no resistance was

observed for PlyG (0.5-50 U) even at a frequency >5 × 10^{-9}. Therefore, even under conditions that promote spontaneous resistance to antibiotics by ~3 logs, no resistance could be detected for this endolysin.

An explanation for the lack of observed resistance to endolysins has been put forth by Fischetti (Fischetti 2005). In brief, he postulates that phage and their bacterial hosts have co-evolved over the millennia such that phages have evolved to target conserved bonds in the peptidoglycan in order to guarantee survival of the progeny phage. As such, resistance, if present, would be a rare event. Nonetheless, resistance to these enzymes will always be a real concern. Most famously, resistance has been well documented for lysostaphin, an exolysin secreted by *Staphylococcus simulans* (Thumm and Gotz 1997). While this enzyme is not a phage endolysin, it is a peptidoglycan hydrolase with a similar catalytic and binding domain to many known phage endolysins (Schindler and Schuhardt 1964).

A unique streptococcal endolysin: PlyC

Endolysins from bacteriophage that infect Gram-positive bacteria are generally between 25–40 kDa in size, composed of two or more domains, and are the product of a single coding gene (Fischetti 2008). The notable exception is an endolysin from the streptococcal bacteriophage C1, termed PlyC, which is uniquely composed of two separate gene products, PlyCA and PlyCB (**Figure 1-6a**). Further biochemical and biophysical characterization of this enzyme uncovered that the PlyC holoenzyme (114 kDa) contains one PlyCA subunit and eight identical PlyCB subunits (**Figure 1-6b and e**). A putative cysteine, hisidine-dependent

amidohydrolase/peptidase (CHAP) domain within PlyCA was confirmed to contain

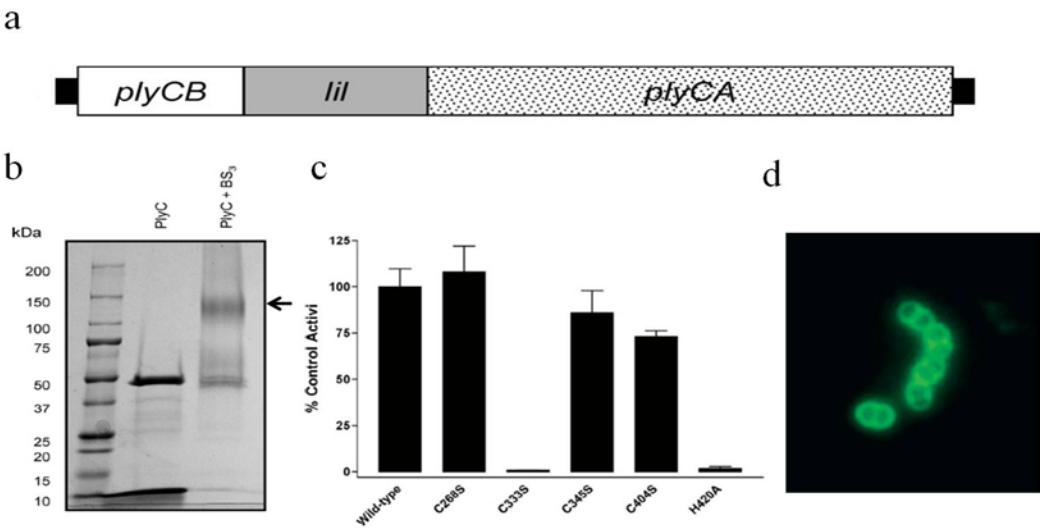

e

Protein	ε_p, ml/(mg·cm)	Experimental UV/RI	Computed UV/RI	Residual²	Correct assumption?
PlyC (8:1 model)	1.218	1.600	1.509	0.008	Yes
PlyC (2:2 model)	2.011	1.600	2.491	0.794	No

Figure 1-6. Biochemical characterization of the PlyC endolysin

(a) Gene structure of *plyC* gene. (b) SDS/PAGE of PlyC shows the presence of the 50-kDa PlyCA and 8-kDa PlyCB subunits. However, cross-linking of PlyC by BS^3 shows a strong band at around ~120 kDa (arrow), suggesting that PlyC is a multimeric endolysin. (c) Putative active-site mutants of PlyCA (C333S and H420A) displays no lytic activity, whereas non-active-site mutants (C268S, C345S, and C404S) shows near wild-type activity. (d) PlyCB labeled with Alexa Fluor 488 specifically labels *S. pyogenes*. Total magnification is 1000X. (e) Extinction-coefficient analysis for two stoichiometric models of PlyC. Images are adapted from (Nelson, Schuch et al. 2006).

the catalytic activity and point mutagenesis established Cys-333 and His-420 as the active-site residues (**Figure 1-6c**). Furthermore, PlyCB was found to self-assemble into an octamer. This complex alone was able to direct streptococcal cell-wall-specific binding (**Figure 1-6d**). Finally, extinction-coefficient analysis suggested that

the stoichiometry of the 8 PlyCB:1 PlyCA model does fit the linear regression of the standard proteins (Nelson, Schuch et al. 2006).

The therapeutic potential of this lytic enzyme was also described *in vitro* (**Figure 1-7a**) and in an *in vivo* model of upper respiratory streptococcal colonization (Nelson, Loomis et al. 2001). This study showed that 1,000 units (~10 ng) of enzyme is sufficient to sterilize a culture of 10^7 group A streptococci within 5 seconds. 5 ng of PlyC was given orally to 9 heavily colonized mice (10^7 per mouse), no detectable streptococci were observed 2 h after endolysin treatment (**Figure 1-7b**), suggesting that this approach could be used to either eliminate or reduce streptococci from the upper respiratory mucosal epithelium of either carriers or infected individuals, thus reducing group A streptococci associated disease.

a

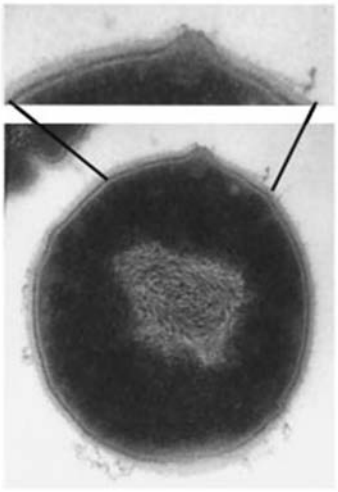

b

Mouse	Day 1	Day 2	Day 3	Day 7
Lysin treated				
1	0	0	0	0
2	0	0	0	0
3	0	0	0	0
4	0	0	0	0
5	0	0	1	0
Total	0/5	0/5	1/5	0/5
Buffer treated				
1	26	14	7	0
2	>300	17	100	83
3	9	0	15	0
4	>300	>300	>300	220
5	2	2	30	0
Total	5/5	4/5	5/5	2/5

Indicated numbers are cfus.

Figure 1-7. *In vitro* and *in vivo* efficacy of PlyC against GAS

(a) a thin-section electron micrograph of GAS treated for 15 seconds with PlyC. The cell wall is weakened, allowing the membrane to subsequently extrude through the hole. 50,000X. (b) Mouse colonization by GAS treated with PlyC (1000 units) or buffer. Images are adapted from (Nelson, Loomis et al. 2001).

Last year, the crystal structure of PlyC was solved (McGowan, Buckle et al. 2012), which confirmed the 8PlyCB:1PlyCA stoichiometry of the holoenzyme (**Figure 1-8**). Surprisingly, the structural and biochemical studies identified two distinct catalytic domains in PlyCA: The aforementioned C-terminal CHAP domain as well as an N-terminal glycosidase (GyH) domain, both of which contribute to cell lysis. Synergy or cooperation between the CHAP and GyH domains may, in part, explain the extreme lytic activity displayed by PlyC compared with traditional endolysins. Another unique feature of PlyC that stands out in comparison with other endolysins (with a single CBD domains) is the presence of the octameric cell wall binding subunit, PlyCB, which forms a symmetrical ring. Structure-guided mutagenesis revealed several key residues contributing to 8 identical binding grooves in the outer aspect of the PlyCB octameric ring (McGowan, Buckle et al. 2012). In summary, this novel structure might explain why PlyC is at least 1,000x more active than any other known endolysin.

Most recently, we successfully demonstrated that PlyC retained its bacteriolytic properties against group A streptococcal biofilm bacteria, destroying the biofilm in a layer by layer process (Shen, Koller et al. 2013). Taken together, the significant amount of information known about this unique endolysin, encouraged me to exploit the feasibility of engineering PlyC to target and control intracellular streptococci that are usually associated with refractory streptococcal infection.

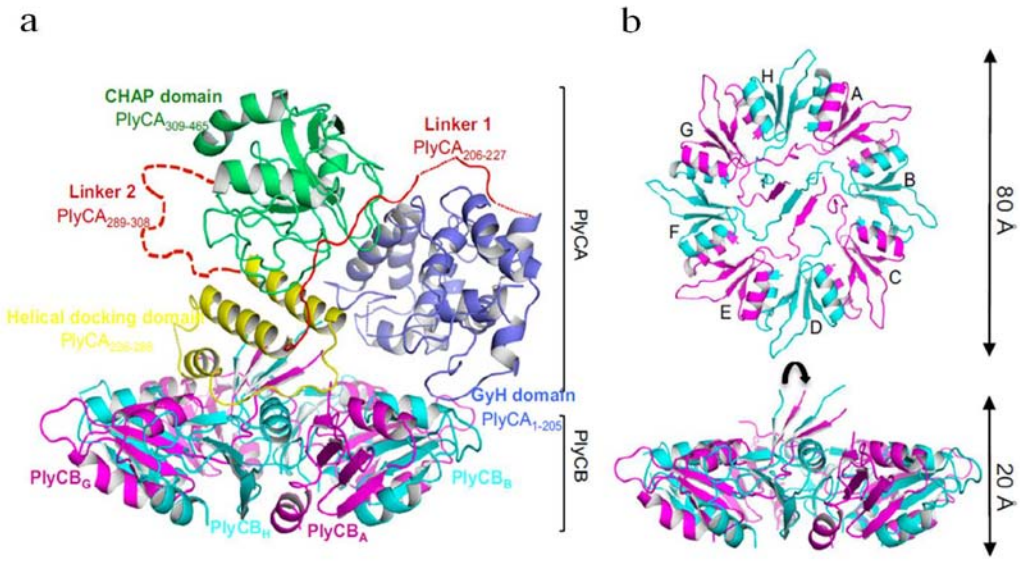

Figure 1-8. Crystal structure of PlyC

(a) The 3.3-Å X-ray crystal structure of PlyC whereby PlyCB monomers are colored alternately in magenta/cyan and labeled monomers A–H. The PlyCA molecule is colored by domain as indicated. The model show the N-terminal residues 1–205 in light blue, the linker 1 (residues 206–227) in red, the helical structure (residues 226–288) that docks PlyCA to PlyCB in yellow, the second disordered linker 2 (residues 289–308) in a dashed red line, and the CHAP domain (residues 309–465) in green. Regions of disordered/absent density are depicted by dashed lines. (b) The PlyCB CBD alone colored alternately in magenta/cyan and labeled A–H. (McGowan, Buckle et al. 2012).

Chapter 2: Identification of intracellular bacteriolytic activity of PlyC against internalized GAS

Background

Failure of antibiotic treatment to eradicate GAS

Traditional antibiotic treatment has been demonstrated to be unable to eradicate group A streptococci in up to 30% of patients with pharyngotonsillitis (Neeman, Keller et al. 1998). Several hypotheses have been proposed to explain the treatment failure, such as coexistence of oropharyngeal beta-lactamase-producing bacteria, interference by aerobic and anaerobic commensals, and penicillin tolerance by biofilm formation (Ellen and Gibbons 1972; Beachey and Simpson 1982; Goodfellow, Hibble et al. 2000; Lembke, Podbielski et al. 2006; Ogawa, Terao et al. 2011). Yet at present, more studies support the hypothesis that adoption of an intracellular niche may protect group A streptococcus from antibiotic treatment. Adherence to and internalization into host cells not only significantly contribute to the pathogenesis of group A streptococcal infections, but also cause eradication failure and persistent throat carriage. Given the fact that traditional antibiotics are unable to penetrate the host cell membrane (Darouiche and Hamill 1994; Thulin, Johansson et al. 2006), internalized GAS can repopulate on the mucosal surface after antibiotic prophylaxis. Therefore, there is growing interest to develop a novel antimicrobial that can target intracellular streptococci responsible for persistence.

Intracellular delivery of endolysin by fusing a cell-penetrating peptide

Intracellular delivery using cell-penetrating peptides (CPPs; also known as protein transduction domains) has been recognized as a novel method of efficiently introducing exogenous proteins into eukaryotic cells. These CPPs are a group of small cationic peptides that have a remarkable ability to drive proteins and cargos across the membrane by direct diffusion or fluid phase endocytosis (Fonseca, Pereira et al. 2009). The presence of cationic residues, such as lysine and arginine, are the key elements that mediate binding and interact by forming bidentate hydrogen bonds with sulfate, phosphate or carboxylate anions on the plasma membrane (Rothbard, Jessop et al. 2004). One of the most well-characterized cell-penetrating peptides, termed 'TAT', is a transduction domain derived from the HIV Tat (transactivator of transcription) protein. This short peptide, with an amino acid sequence of RKKRRQRRR, can be genetically fused to various nanoparticulate pharmaceutical carriers, such as proteins, liposomes, nanoparticles, and then transport those macromolecular cargoes into cells *in vitro* and *in vivo* (Wadia, Stan et al. 2004; Gump and Dowdy 2007; Torchilin 2008). Although bacteriophage-encoded endolysins have shown their therapeutic potential against bacteria pathogens *in vitro* and *in vivo* (Loeffler, Nelson et al. 2001; Cheng, Nelson et al. 2005; Celia, Nelson et al. 2008). No efforts have been reported to test or engineer these endolysins to target pathogens in intracellular niches. Therefore, the hypothesis we wanted to test is that whether or not TAT fusions to endolysins can facilitate the intracellular delivery and subsequent elimination of internalized GAS.

Results

Establishment of a GAS/human epithelial cell co-culture model and validation of internalized GAS

In order to determine the intracellular bacteriolytic efficacy of TAT-labeled and wild-type endolysins against internalized GAS, we first established a GAS/human epithelial cell co-culture assay (**Figure 2-1a**) to evaluate the rate of GAS adherence and invasion. In this model, epithelial cells were grown to 80% confluent monolayers in 24-well tissue culture plates (approximately 2 x 10^5 cells/well). Overnight pathogenic GAS strain D471 was washed in sterile phosphate-buffered saline (PBS), resuspended in serum-free media, and the concentration was adjusted to ~2 x 10^7 colony forming units (CFU) and incubated with epithelial cells at a multiplicity of infection (MOI) = 100 bacterial cells/ one epithelial cell for 1 hour. Then, the epithelial cells were lysed and lysis solution was serially diluted and plated on THY agar plates for enumeration of viable CFUs (for details, see method section See **J**). As depicted in **Figure 2-1b**, both A549 and Hep-2 cell lines showed similar percentage of adhered (~3% for Hep-2, 8% for A549) and internalized (0.01% for Hep-2, 0.08% for A549) GAS compared to the initial inoculums of bacteria. These results are consistent with previous reports from other groups (Jadoun, Ozeri et al. 1998; Ryan, Pancholi et al. 2001). Furthermore, the adherent and internalized GAS (stained by fluorescence-labeled wheat germ agglutinin) were visualized and validated in a z-stack analysis by confocal microscopy (**Figure 2-1c)**.

a

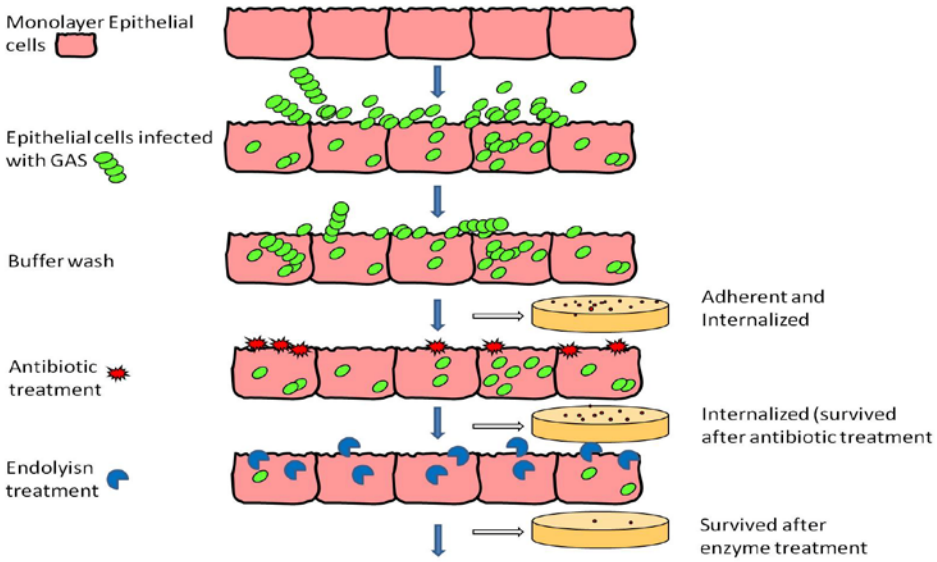
Monolayer Epithelial cells
Epithelial cells infected with GAS
Buffer wash
Antibiotic treatment
Endolyisn treatment
Adherent and Internalized
Internalized (survived after antibiotic treatment
Survived after enzyme treatment

b

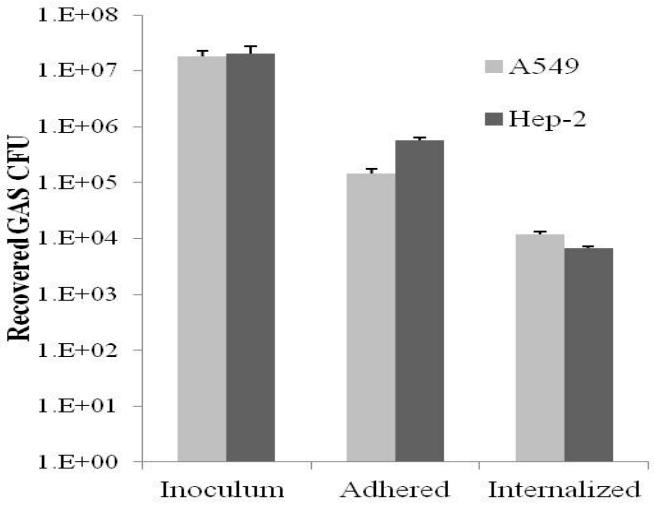
1.E+08
1.E+07
1.E+06
1.E+05
1.E+04
1.E+03
1.E+02
1.E+01
1.E+00
Recovered GAS CFU
A549
Hep-2
Inoculum
Adhered
Internalized

c

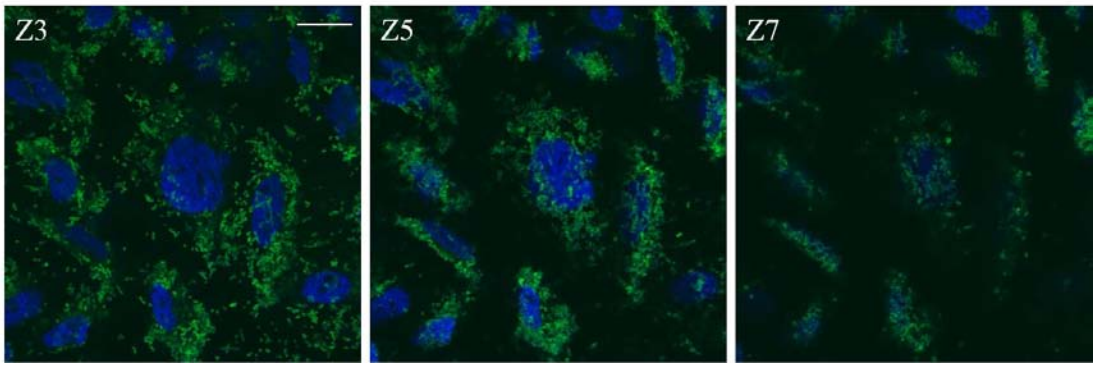
Z3
Z5
Z7

Figure 2-1. Schematic illustration, CFU count and confocal microsocopy of co-culture assay

(a) Schematic flow chart illustrating the co-culture model. (b) Determination of rate of adherent and internalized GAS colonies in the co-culture model with A549 cells (light gray bars) or Hep-2 cells (dark gray bars). (c) Visulization of adherent and internalized GAS into Hep-2 cells by confocal microsocpy. Nucleus (blue) is highlighted by DAPI staining, GAS (green) is pre-stained with wheat germ agglutinin-Alexa Fluor 488 conjugates. Note that the interval between each slice is 2 μm, in a total of 6 μms in the Z-axis. Z3 is the closest focal plane to coverslip. Scale bar is 20 μm.

Wild-type PlyC possesses an inherent activity against internalized GAS

Next, three recombinant TAT-labeled streptococcal specific endolysins B30 (Donovan, Foster-Frey et al. 2006), Ply700 (Celia, Nelson et al. 2008) and PlyC were constructed by using a Quick-change Site-Directed Mutagenesis Kit, over-expressed in *E.coli*, purified by the method previously described (Donovan, Foster-Frey et al. 2006; Nelson, Schuch et al. 2006; Celia, Nelson et al. 2008). Wild-type and TAT-labeled endolysins displayed similar *in vitro* bacteriolytic activity by the turbidity reduction assay (data not shown). The intracellular bacteriolytic activity was then evaluated in the co-culture model as previously described (**Figure 2-1a**). Neither wild-type or TAT-labeled Ply700 or B30 showed any efficacy against internalized GAS (**Figure 2-2**). In contrast, TAT-labeled PlyC possessed an ability to eliminate intracellular GAS. Much to our surprise, wild-type PlyC contained the same intracellular killing activity as TAT-labeled PlyC. Thus, the rest of this dissertation is focused on elucidating how wild-type PlyC is able to translocate the plasma membrane and kill intracellular streptococci when other endolysins cannot.

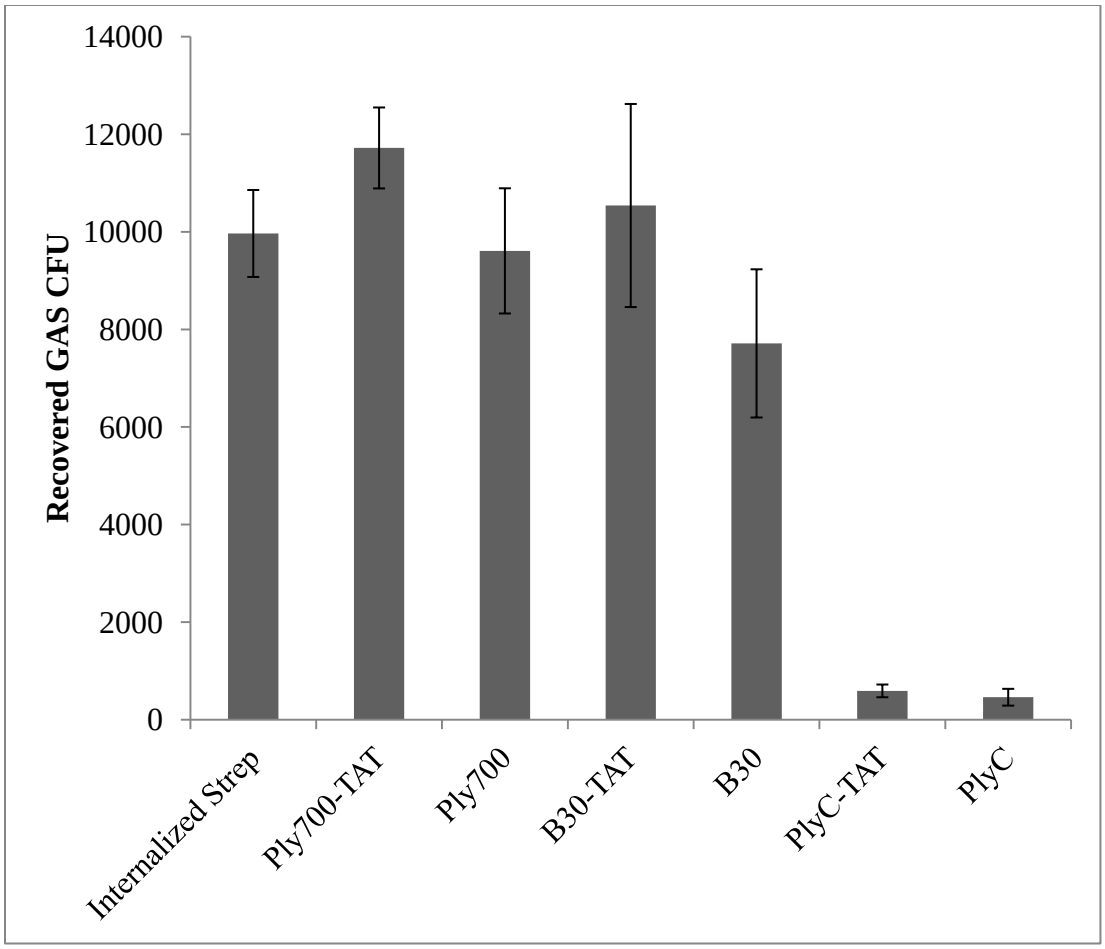

Figure 2-2. CFU count of recovered internalized GAS post-endolysin treatment

The co-culture was first treated with 10 μg/ml penicillin and 200 μg/ml gentamicin for 1 hour, the antibiotic was then removed and incubated with growth medium in the presence of wild-type or TAT-labeled endolysin (50 μg/ml) for another hour before lysis and enumerate recovered GAS colonies.

Intracellular bacteriolytic activity of PlyC is dose-dependent and relies on its enzymatic activity

To investigate whether PlyC killing of internalized GAS is dose-dependent, various concentrations of PlyC were added to the co-culture as previously described (**Figure 2-1a**). **Figure 2-3** illustrates a dose-dependent response with half of the internalized streptococci killed by as little as 0.08 μg/ml of PlyC, 90% eliminated

with 10 μg/ml and 2 logs of killing with 50 μg/ml. In addition, heat-denaturing PlyC prior to addition to the co-culture completely abolished PlyC's intracellular activity, suggesting that this intracellular killing phenomenon requires PlyC enzymatic activity.

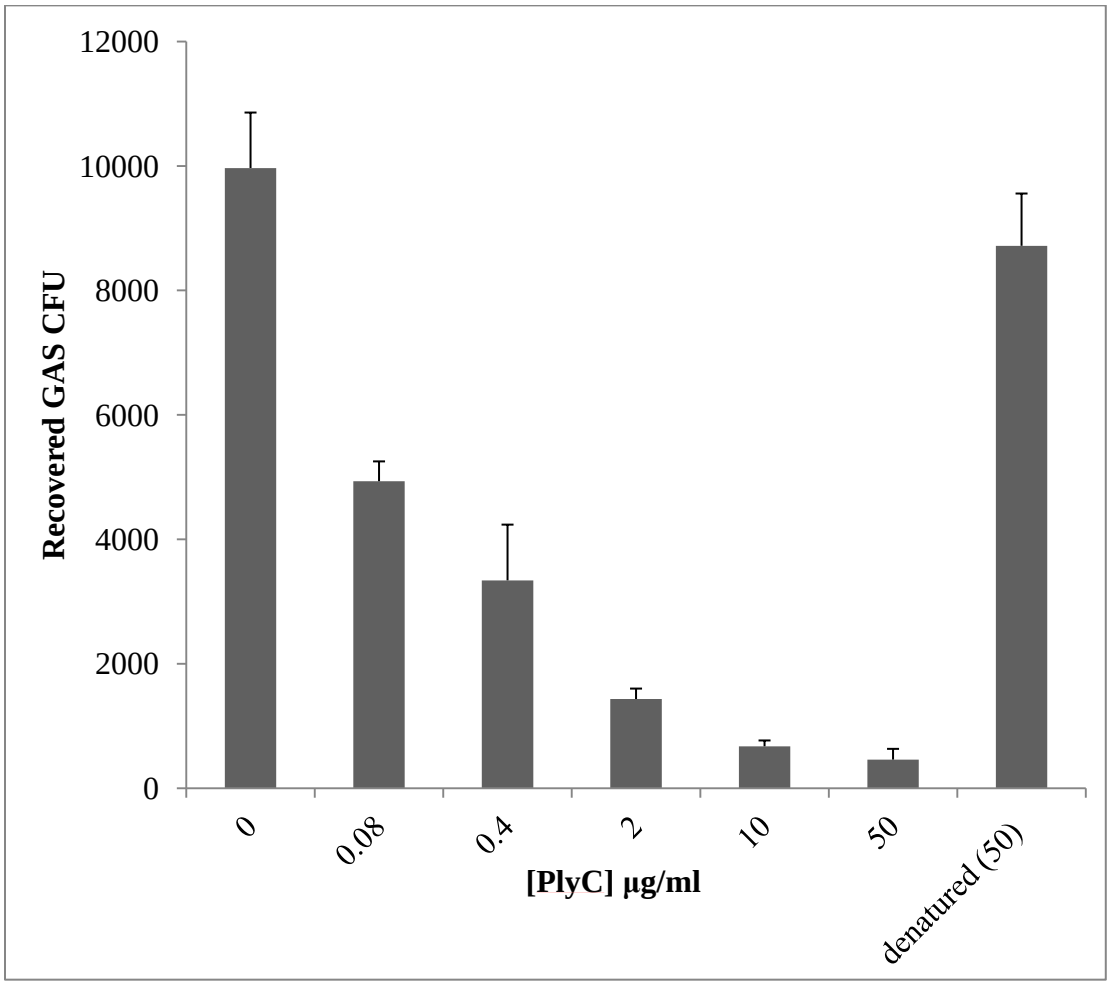

Figure 2-3. Intracellular killing activity of PlyC is dose-dependent

The co-culture was first treated with 10 μg/ml penicillin and 200 μg/ml gentamicin for 1 hour, afterwhich the antibiotic was then removed and the co-culture wasincubated with growth medium in the presence of various concentration of PlyC for another hour before lysis and enumeration of recovered GAS colonies. The denatured PlyC was performed by heating the PlyC in medium at 70ºC for 30 min before the experiment.

Fate of internalized GAS and host epithelial cells with antibiotic or PlyC treatment for additional 24 hours

Figure 2-1b demonstrated that ~ 1% of adherent GAS became internalized in epithelial cells. We therefore wanted to determine the fate not only of the intracellular GAS, but also of the infected epithelial cells under various treatments in the co-culture system (**Figure 2-4.**) When antibiotics are removed from the co-culture and epithelial cells harboring intracellular GAS are incubated for an additional 24 hours, massive bacterial growth is visible in the growth medium, accompanied by significant epithelial cell death (99.4%) as determined by a trypan blue dye exclusion assay, suggesting that internalized GAS are able to repopulate the mucosa after antibiotic prophylaxis (Marouni and Sela 2004). When we repeat the same experiment but supplement with media in the presence of antibiotic (10 μg/ml penicillin and 200 μg/ml gentamicin) during additional 24 hour incubation, no GAS can be detected in the supernatant (data not shown) and only 4.7 % of internalized GAS were recovered from host cells after lysis. However, a significant amount of epithelial cell death (88.5%) was observed, indicating that antibiotic prophylaxis does not protect epithelial cells from GAS-mediated autolysis and furthermore, intracellular GAS persist even in the presence of extracellular antibiotics. Alternatively, when the media was supplemented with 50 μg/ml PlyC for the 24 hour incubation, no intra- or extracellular GAS were recovered. Moreover, ~70% of the epithelial cells remained viable demonstrating that internalized GAS were completely eliminated by the PlyC endolysin.

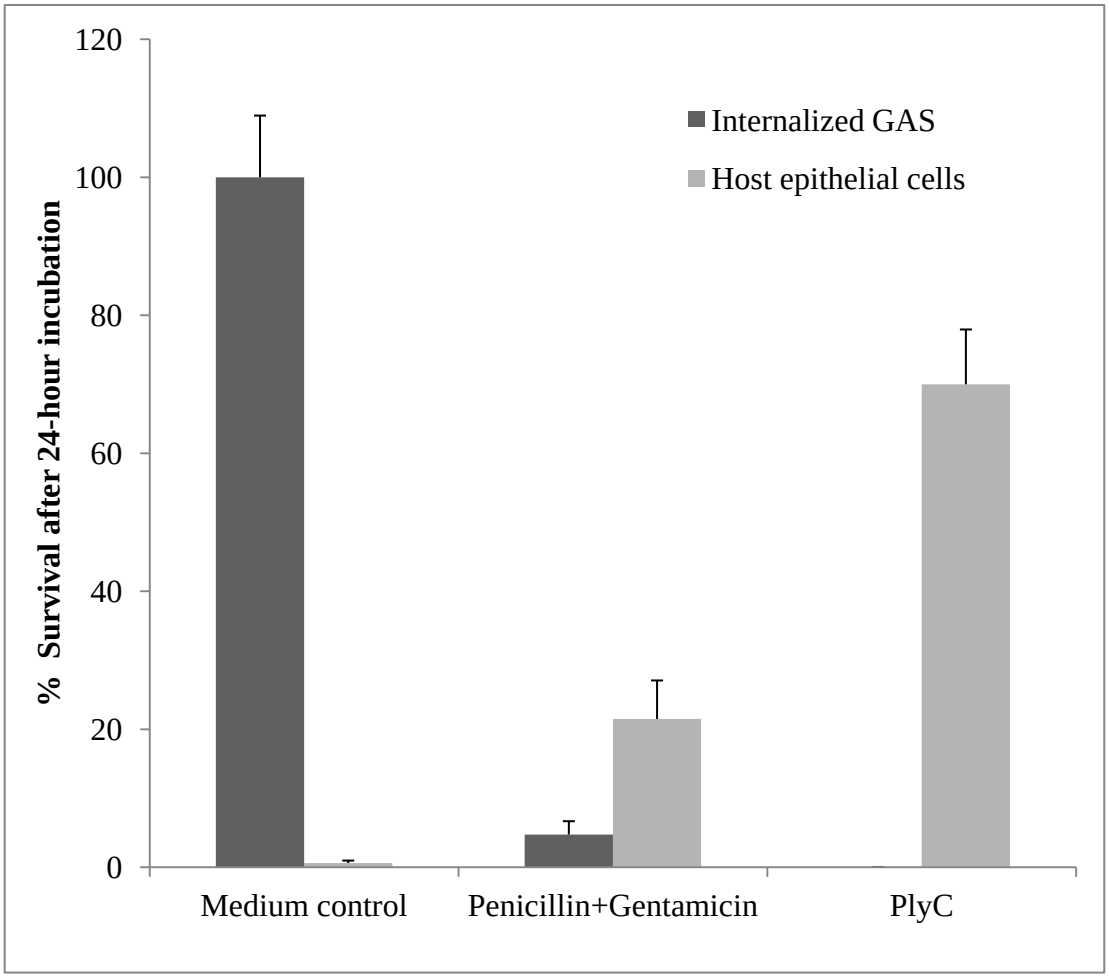

Figure 2-4. Fate of internalized GAS and host epithelial cells with antibiotic or PlyC treatment for additional 24 hours

The co-culture was first treated with 10 μg/ml penicillin and 200 μg/ml gentamicin for 1 hour. The antibiotic were then removed and replaced with fresh growth medium "Medium control", or fresh medium supplemented with antibiotics "Penicillin+Gentamicin" for additional 24 hour incubation. For the PlyC group, the co-culture was first treated with PlyC 50 μg/ml for 1 hour, the endolysin was then removed and supplemented with normal growth medium in the presence of 50 μg/ml PlyC for additional 24 hour incubation. The internalized GAS (dark gray bars) was plated onto THY agar plate after host cell lysis for numeration. The recovered host epithelial cells (light gray bars) were detached by trypsinization and then stained with Trypan Blue and counted by haemocytometer.

PlyC shows a similar efficacy against internalized GAS in a model of primary human tonsil epithelium

We realize that our co-culture model relies on cancer epithelial cell lines, which does not represent a clinically relevant cell type. As such, we also tested PlyC in a co-culture model with human primary tonsil epithelial cells isolated and cultured (see material and method for details) at The Rockefeller University. Although we did not see any effect with a low concentration of PlyC (1 or 10 μg/ml), ~ 90% of internalized GAS were eliminated when treated with a higher concentration of PlyC (50 μg/ml) (**Figure 2-5**) .

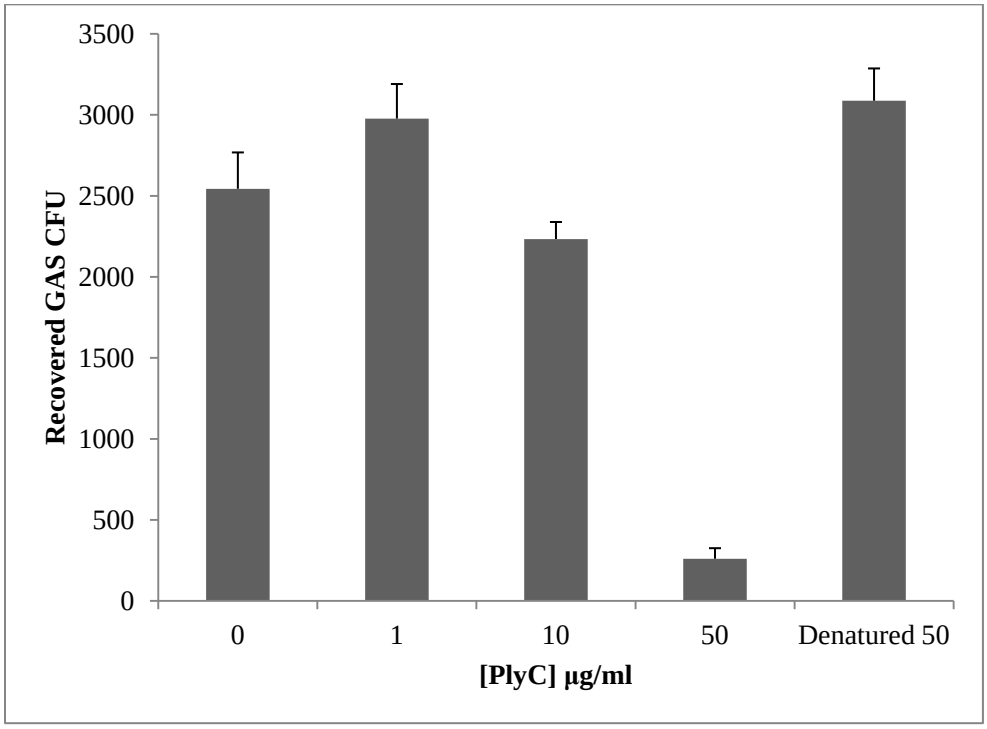

Figure 2-5. CFU count from co-culture model with human primary tonsil cells

The co-culture was first treated with 10 μg/ml penicillin and 200 μg/ml gentamicin for 1 hour after which the antibiotic was removed and the cell were incubated in the presence of various concentration of PlyC for 1h before lysis and enumeration of GAS.

Confocal microscopy shows that fluorescently-labeled PlyC internalizes and co-localizes with intracellular GAS

Endolysin are capable of killing only extracellular bacteria by digesting the cell wall upon contact, while their access to intracellular Gram-positive pathogens is restricted by the plasma membrane of the infected host epithelial cells. Previously, we have demonstrated that PlyC directs itself to the binding ligands on the bacterial cell wall with high affinity because of its cell wall binding domain. Thus, the decoration with fluorescently-labeled PlyC primarily occurs at the all over the surface of chain-like streptococcal cell (**Figure 1-6 d**). To test our hypothesis that PlyC possesses an inherent ability to internalize and eliminate intracellular GAS, we employed confocal laser scanning microscopy to capture the event of fluorescence-labeled PlyC entering epithelial cells and co-localizing with intracellular GAS. As **Figure 2-6** depicts in a single focal plane at peri-nucleus, fluorescence labeled PlyC (red) co-localizes with GAS bacteria (green) at a peri-nuclear location in the merged image. Note that wild-type PlyC was used in the experiment, the cell wall of GAS were ruptured and no visible intact chain-like streptococci were observed through the Z-stack compared to **Figure 2-1c**. These evidence suggests that internalized PlyC retains its bioglocial function (enzymatic activity and affinity to bacterial cell wall) after internalization in the intracellular environment. Furthermore, the maxium projection constructed by the entire Z-stack images shows that all intracellular GAS were targeted and ruptured by internalized PlyC, and no extracellular GAS was detected outside or between the host cell boundary indicated by the actin filaments statining.

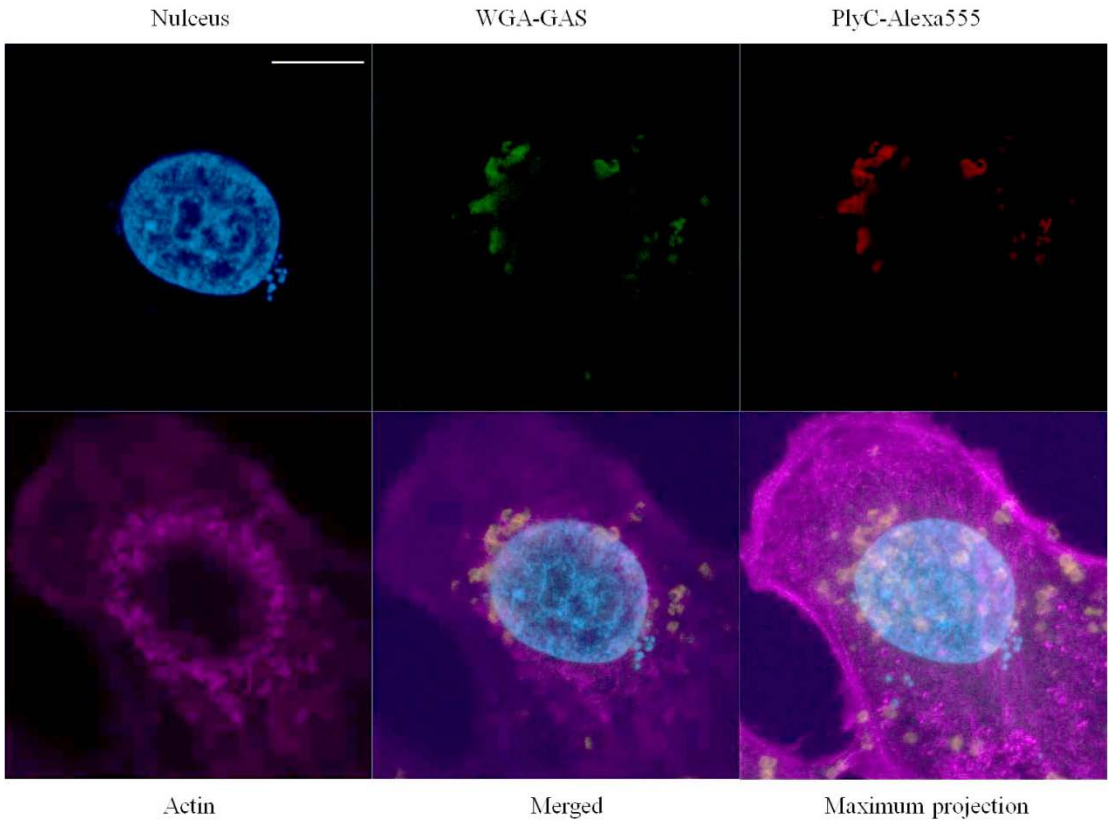

Figure 2-6. Confocal microscopy of internalization of PlyC targeting intracellular GAS

A single focal plane at the nucelus (Cyan, DAPI stained), GAS bacteria (green, wheat germ agglutinin-Alex488 stained phalloidin), the PlyC endolysin (red, Alexa fluor 555 conjugated), and actin structure (Magenta, Alexa fluor 647 conjugated) are shown in the same focal plane. Note the fluorescence labeled PlyC (red) was co-localized with GAS bacteria (green) at a peri-nuclei localization in the merged image. The maximum projection is constructed by stacking images from all z-sections together. Scale bar is 10 μm.

Conclusion

S. pyogenes causes a broad spectrum of disease ranging from mild infections to life-threatening complications when colonizing the skin or mucosal membranes. As an exclusive human pathogen, it is associated with extensive morbidity and mortality worldwide. Although traditional antibiotics (e.g. penicillin, the major choice when treating group A streptococcal infections) are still effective, GAS can circumvent

antibiotics by adhering to and internalizing into host epithelial cells, and subsequently residing as intracellular pathogens. This internalization makes the streptococci refractory to antibiotic treatment and allows them to repopulate the mucosal surface after antibiotic prophylaxis has ended. Thus, there is a need to develop a novel antimicrobials that can penetrate the lipid membrane and eliminate the internalized GAS.

In order to achieve this goal, we first applied a protein engineering approach to geneticially modify streptoccal endolysins that have successfully demonstrated their bacteriolytic activity against GAS *in vitro*. This enzyme-based engineering strategy is carried out by fusing a cell penetrating peptide, termed 'TAT', which has a demonstrated ability to drive large molecules such as globular proteins or nanoparticles across the plasma membrane (Torchilin 2008), to several streptococcal-specific endolysins (including B30, Ply700, and PlyC). To assay the efficacy of TAT-labeled endolysins against internalized GAS, a streptococci/human epithelial cell co-culture model was established. In this assay, we were able to differentiate the non-adherent, adherent (i.e. extracellular), and internalized GAS, which was also validated by confocal microscopy. Surprisingly, none of the TAT-labeled endolysins showed better intracellular bacteriolytic activity than wild-type endolysins, although they depicted comparable extracellular bacteriolytic activity. However, wild-type PlyC possessed the best intracelluar killing efficacy against internalized GAS. Thus, we investigated more formally this unique finding for wild-type PlyC.

First, we established that the intracellular bacteriolytic activity of PlyC is dose-dependent, with 50 μg/ml being sufficient to kill 96% of internalized GAS.

Second, heat-denatured PlyC did not show any intracellular bacteriolytic activity suggesting this unique property is due to enzymatic activity of PlyC. Third, the extracellular repopulation by internalized GAS after antibiotic treatment was confirmed. Although the majority of internalized GAS (95%) were cleared after an additional 24-hour incubation in the presence of antibitoics, an extensive amount (88.5%) of host cell death was also observed. This is because the host cells undergo autolysis induced by internalized bacteria, which were therefore exposed to antibiotics in the supernatant and killed. In contrast, a second dose of PlyC was able to completely sterilize the co-culture and resuce ~ 70% of epithelial host cells. Furthermore, those recovered GAS colonies from either treatment group were grown in liquid culture for MIC (Minimum Inhibitory Concentration) and MBC (Minimum Bactericidal Concentration) testing. These values did not change after intracellular growth, (data not shown) suggesting that surviving GAS did not develop resistance to PlyC or penicillin, which is consistent with previous reports (Fischetti 2005). To the best of our knowlege, this is the first report to show intracellular killing of GAS, or any bacteria, using an endolysin. In addition, our results were extended to primary human tonsilar epithelial cells, which are the major reservoir for streptococcal colonization and invasion. The results look similar to what we observed from a co-culture model with immortalized epithelial cell lines, again supporting the possibility of using the PlyC endolysin therapeutically for recurrent streptococcal infection. Finally, we were able to employ confocal microscopy to obtain direct evidence that PlyC not only internalized, but co-localizes with GAS and remained functionally active in the intracellular niche.

In summary, Chapter 2 describes the identification and characterization of intracellular bacteriolytic activity of PlyC against internalized streptococci. However, these findings only raise additional questions. For example, the domain/motif/residue that mediates internalization of PlyC, and the potential molecules or receptors on the plasma membrane of host cells remains unclear. The above questions will be addressed in Chapter 3.

Chapter 3: Elucidating the interaction between PlyC and the plasma membrane upon internalization

Background

The evidence in the previous chapter has demonstrated that PlyC can enter into the epithelial cell. In a spatial manner, PlyC has to bind and interact with the plasma membrane before it can be internalized. However, the domain/motif/residues of PlyC that mediate this interaction remain unclear.

To answer the above question, we decided to explore the recent crystal structure of the PlyC holoenzyme (McGowan, Buckle et al. 2012). The structural report confirmed that PlyC is assembled from two components: PlyCA and PlyCB with a single PlyCA moiety tethered to a ring-shaped assembly of eight PlyCB molecules (**Figure 3-1a and b**). Interestingly, when we generated a map of the electrostatic surface potential of PlyC based on the crystal structure (**Figure 3-1c and d**), a highly positive-charged surface on PlyCB, composed of a total of 48 surface exposed cationic residues (2 arginines and 4 lysines in each monomer of the PlyCB octamer) was discovered. Appreciably, two recent studies revealed that the cationic cell-penetrating-peptide TAT, interacts with different surface molecules on the plasma membrane upon internalization. In the first study, evidence was provided that a TAT-labeled bacteriophage was internalized utilizing chondroitin sulfate proteoglycans as specific cell surface receptors by biochemical and genetic assays (Kim, Shin et al. 2012). The second study used solid-state NMR to show that the structural interface between TAT and anionic lipid bilayers contained arginine-phosphate salt bridges that interact through hydrogen bonding (Su, Waring et al.

2010). Both studies suggest that the interaction is mediated by anionic lipid phosphates or sulfate proteoglycans via electrostatic interactions to the cationic TAT peptide. The positive-charged surface of PlyC, in particular the bottom face of PlyCB octamer, led us to hypothesize that PlyC mimics the cationic nature of TAT during entry into eukaryotic cells. To test this hypothesis, several biochemical assays, along with site-directed mutagenesis, were conducted. The results are subject of this chapter.

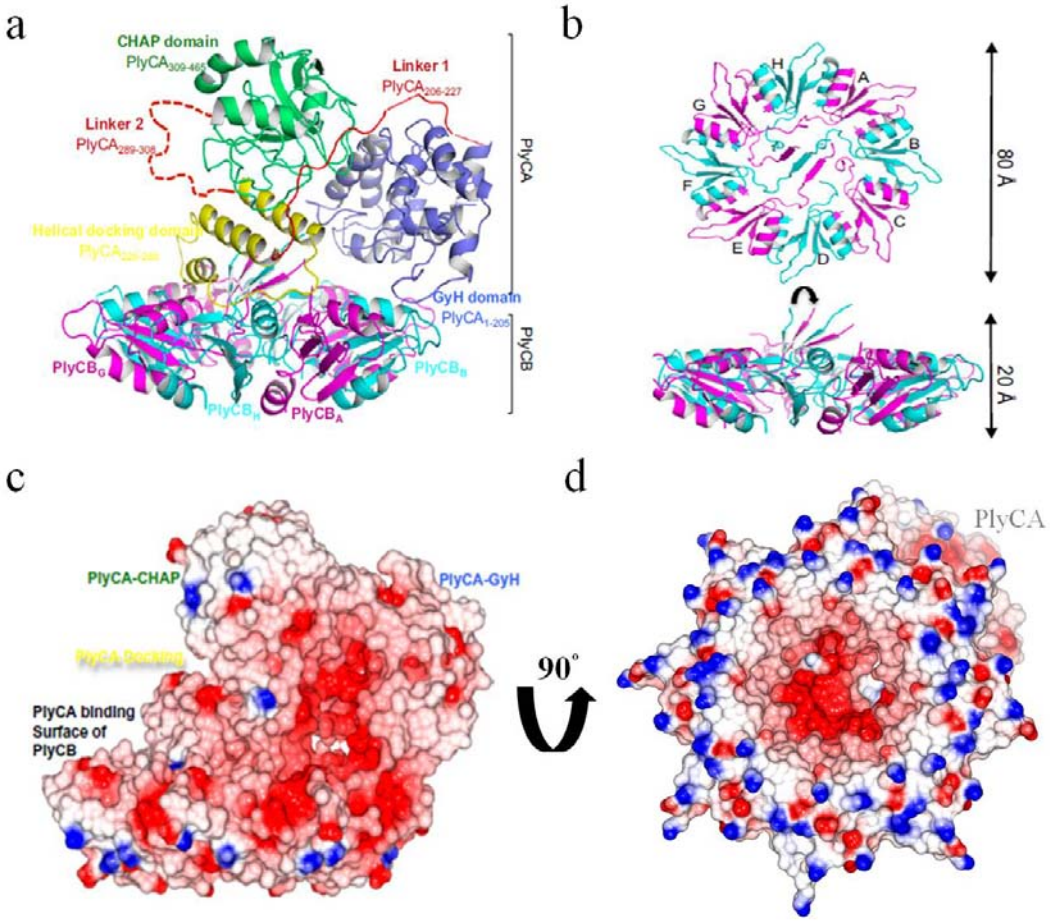

Figure 3-1. Structure and electrostatic surface potential of PlyC

(a) The 3.3-Å X-ray crystal structure of PlyC whereby PlyCB monomers are colored alternately in magenta/cyan and labeled monomers A–H. The PlyCA molecule is colored by domain as indicated. The Cα atoms of the model show the N-terminal residues 1–205 in light

blue (GyH domain, glycosidase activity), the disordered linker 1 (residues 206–227) in red, the helical structure (residues 226–288) that docks PlyCA to PlyCB in yellow, the second disordered linker 2 (residues 289–308) in a dashed red line, and the CHAP domain (amidase activity, residues 309–465) in green. Regions of disordered/absent density are depicted by dashed lines. (b) The PlyCB domain (top and side view) alone colored alternately in magenta/cyan and labeled A–H. (c) Electrostatic surface potential of PlyC as oriented in a. Surfaces are color-coded according to electrostatic potential (calculated by the Poisson–Boltzmann solver within CCP4MG). Lys and Arg residues were assigned a single positive charge, and Asp and Glu residues were assigned a single negative charge; all other residues were considered neutral. The calculation was done assuming a uniform dielectric constant of 80 for the solvent and two for the protein interior. The ionic strength was set to zero. The color of the surface represents the electrostatic potential at the protein surface, going from blue (potential of +10 kT/e) to red (potential of −10 kT/e), where T is temperature, e is the charge of an electron, and k is the Boltzmann constant. The probe radius used was 1.4 Å. (d) The same surface with altered orientation as indicated. Images are adapted from (McGowan, Buckle et al. 2012)

Results

PlyCB domain is responsible for internalization of PlyC

The electrostatic potential map of PlyC suggests that most surface exposed cationic residues are located in the PlyCB domain. To narrow down which domain is responsible for internalization, we were able to clone, express and purify PlyCA and PlyCB respectively, described in (McGowan, Buckle et al. 2012). The purified PlyCA (50 kDa) and PlyCB (octamer is 64 kDa, monomer is ~8 kDa) subunits alone were shown in the SDS-PAGE gel in **Figure 3-1a**. Each subunit was then cross-linked to AlexaFluor555 and confirmed for proper folding of each domain by gel filtration (data not shown). **Figure 3-1b** shows that only fluorescence-labeled PlyCB or PlyC holoenzyme were found to be internalized, whereas PlyCA by itself failed to internalize.

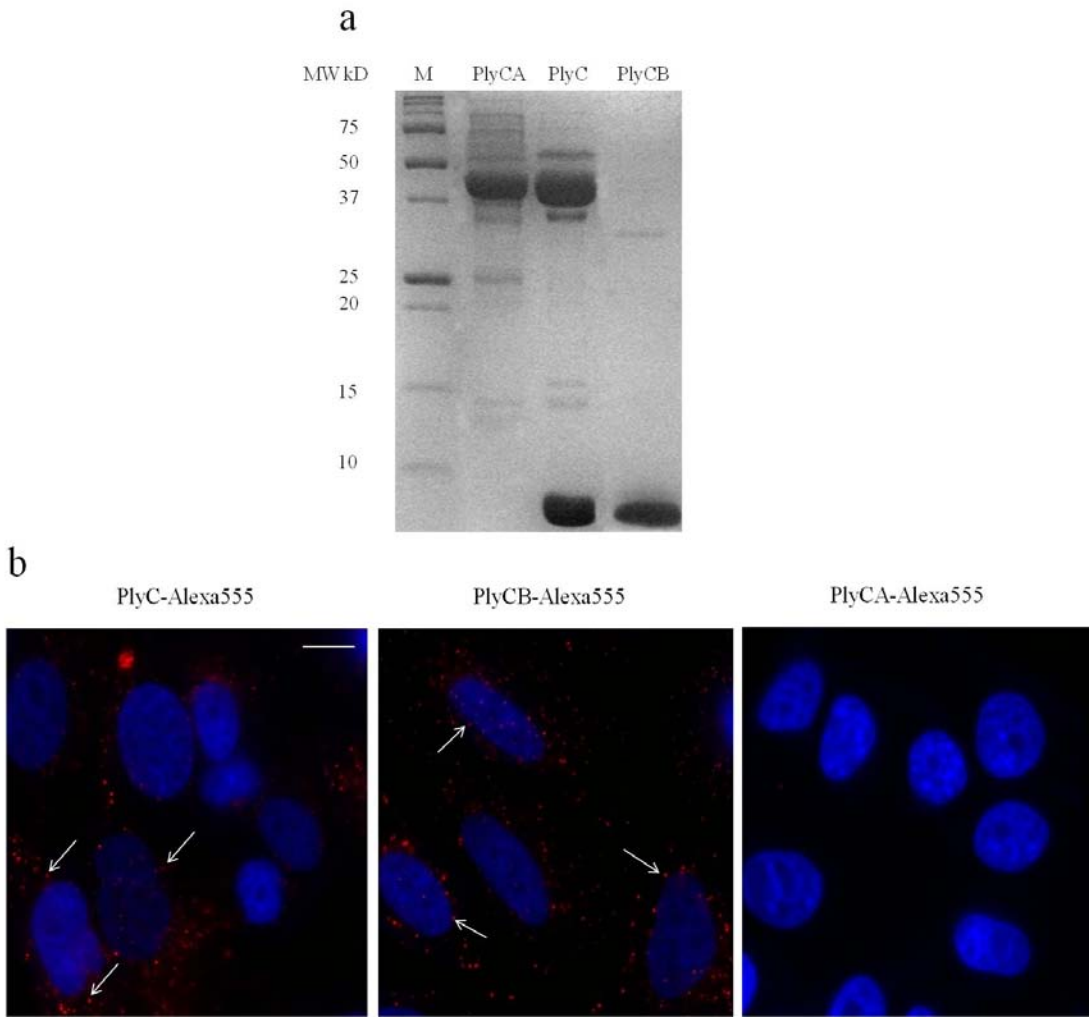

Figure 3-2. Characterization of internalization ability of PlyC, PlyCA and PlyCB

(a) SDS-PAGE gel of PlyC holoenzyme, catalytic PlyCA subunit and cell wall binding subunit PlyCB. (b) A549 cells were incubated with PlyC-Alexa555 (red), PlyCB-Alexa555 or PlyCA-Alexa555 in serum-free F12K medium for 30 min at 37ºC, fixed by 4% PFA in PBS and subsequently stained with and DAPI (nucleus, blue). Arrows indicate the internalized PlyC or PlyCB subunit. Scale bar is 20 μm.

Site-directed mutagenesis and characterization of various PlyCB mutants

Figure 3-1a indicates that the PlyCB octamer possesses a highly positive-charged surface due to multiple lysine (Lys, K) or arginine (Arg, R) residues in each monomer, several of which marked in **Figure 3-3a**. Thus, by site-directed

mutagenesis, single surface exposed positive-charged residues were mutated to glutamic acid (Glu, E), which is a negatively charged amino acid due to an extra carboxyl groups on its side chain. Constructs were then over-expressed and purified by a protocol previously described (Nelson, Schuch et al. 2006). Four out of five constructs, including PlyC(PlyCB$_{K70E,K71E}$), PlyC(PlyCB$_{K23E}$), PlyC(PlyCB$_{K59E}$), and PlyC(PlyCB$_{R66E}$), were soluble and able to be purified as shown by SDS-PAGE (**Figure 3-3b**). However, the PlyC(PlyCB$_{R29E}$) was not used in subsequent studies because of its insolubility. Mutations were confirmed by sequencing (data not shown) as well as analyzing the purified enzymes by mass spectrometry (**Figure 3-3c**). Note, PlyCA does not ionize in mass spectrometry but the PlyCB octamer ionizes as a monomer. As we expected, wild-type PlyCB monomer is 7856.9 daltons, a mutation from Lys to Glu generated a loss of 0.8 daltons, and a mutation from Arg to Glu causes a decrease in molecular weight lower by 27.2 Daltons. These results are consistent with our calculations based on the known molecular mass of Lys (146.2 g/mol), Arg (174.2 g/mol), and Glu (147.1 g/mol). Furthermore, analytical gel filtration showed that all constructs had a retention volume of ~ 12.3 ml, consistent with the 114 kDa wild-type PlyC holoenzyme (**Figure 3-3d**). Finally, we employed infrared spectroscopy, a well-established tool to investigate the structure and dynamics of proteins based on the position of characteristic amide I and amide II vibrational bands (Kupser, Pagel et al. 2010), which provides a direct measure of the underlying secondary structure. The super-imposable spectra of the mutants with wild-type PlyC confirmed that there were no major differences in secondary structure (**Figure 3-3e**). In summary, various analytical methods verify the correct mutations

and proper folding/secondary structure conformation for all constructs except PlyC(PlyCB$_{R29E}$), which presumably misfolds and is insoluble.

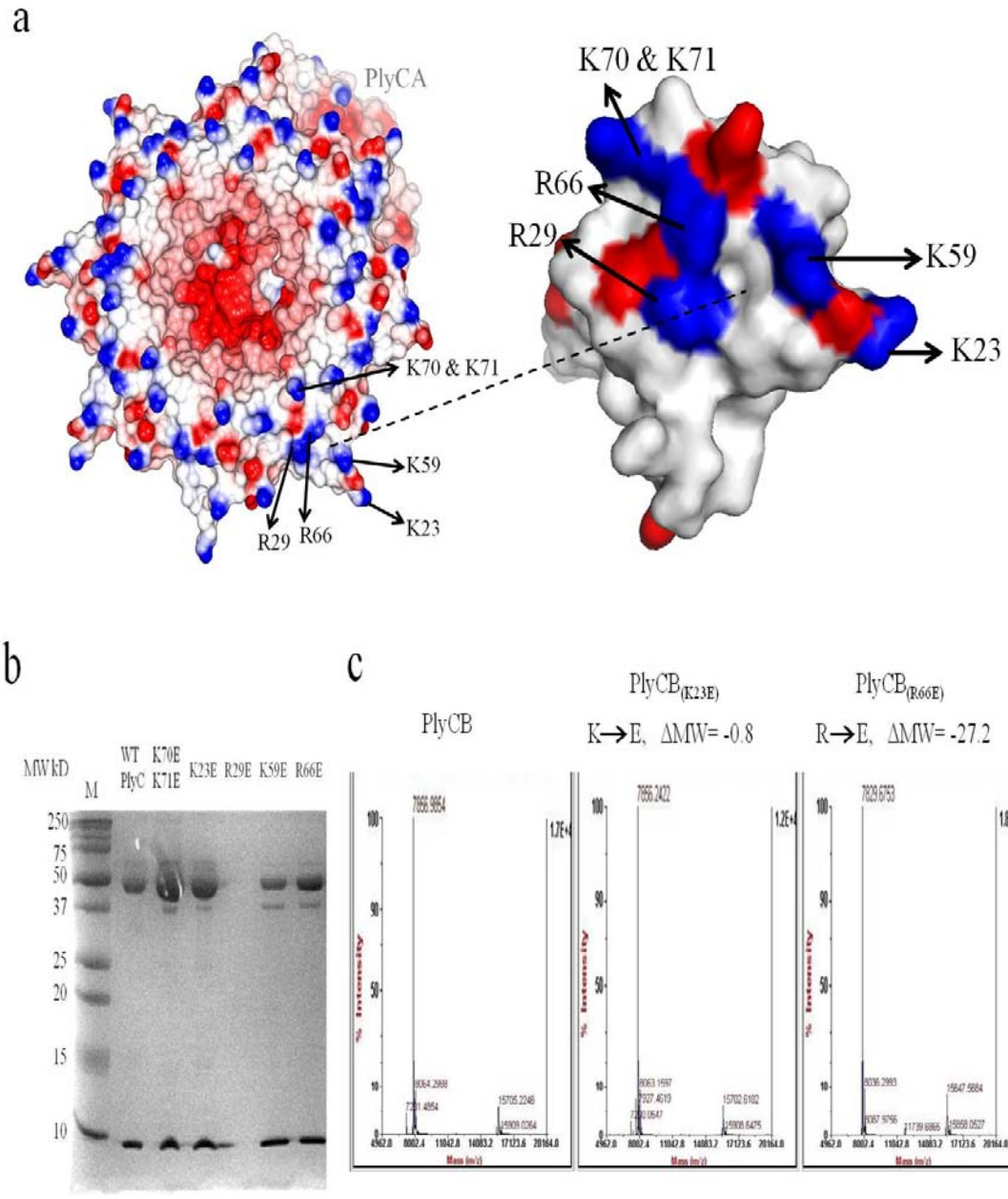

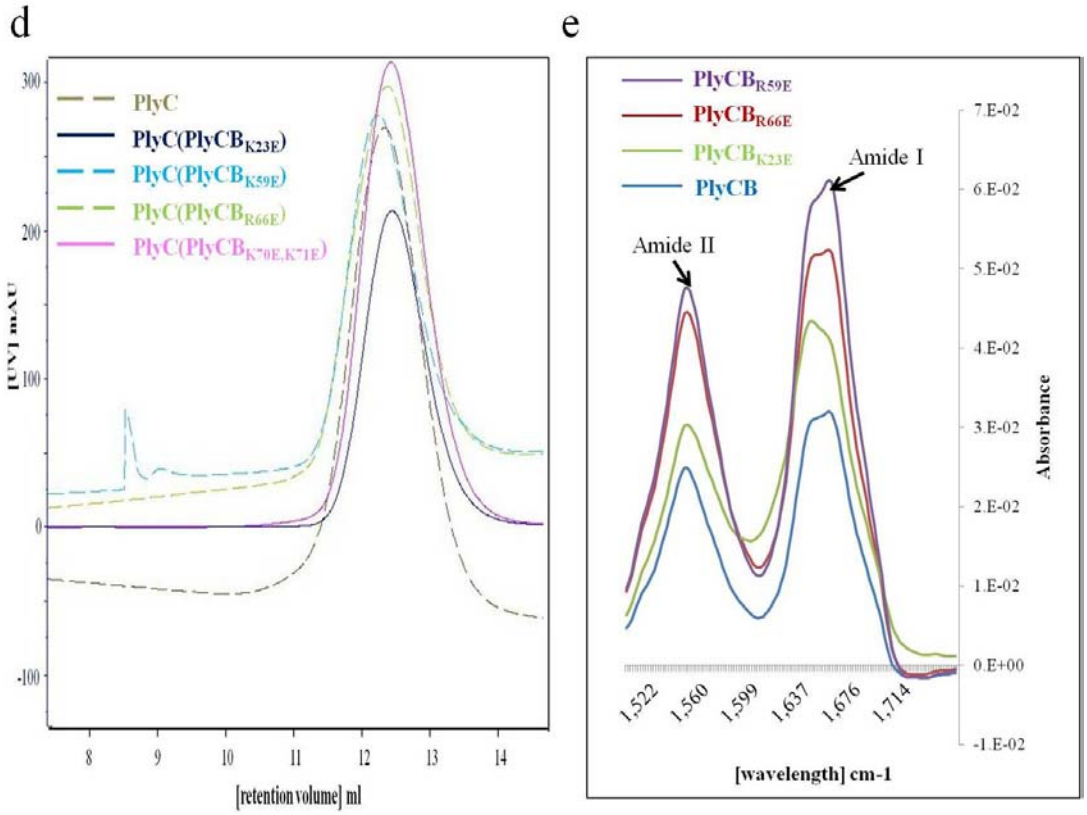

Figure 3-3. Biochemical and biophysical characteristics of PlyC and its mutants

(a) Electrostatic surface potential of PlyC as oriented in **Figure 3-1d**. Lys and Arg residues were assigned a single positive charge, and Asp and Glu residues were assigned a single negative charge; all other residues were considered neutral. The surface exposed Arg, Lys and Glu in one PlyCB monomer were marked. The right panel (backbone of PlyCB colored in Cyan) is the enlarged view of the surface exposed Arg and Lys in one PlyCB monomer. The images were generated and labeled by PyMOL software. (b) SDS-PAGE gel images of purified PlyC and its mutants. Note that PlyC(PlyCB$_{R29E}$) was insoluble, and thus did not show on the gel. (c) Mass spectrometry of PlyC, PlyC(PlyCB$_{K23E}$), and PlyC(PlyCB$_{R66E}$). (d) Analytic gel filtration of PlyC and its mutants. Note, all constructs has a similar retention volumes. (e) Infrared spectroscopy of PlyCB, PlyC(PlyCB$_{K23E}$), PlyC(PlyCB$_{K59E}$), and PlyC(PlyCB$_{R66E}$). Note that all constructs tested has a similar Amide-I and-II peaks.

Benchmark extracellular and intracellular bacteriolytic activity of mutants against wild-type PlyC

The extracellular and intracellular bacteriolytic activities of PlyC mutants were benchmarked against wild-type PlyC (**Figure 3-4**) by turbidity reduction assay and co-culture assay, respectively. Constructs of PlyC(PlyCB$_{K23E}$) and PlyC(PlyCB$_{K70E,K71E}$) showed no effect on extracellular activity, but partially diminished (~ 50%) the intracellular bacteriolytic activity of PlyC against internalized GAS, In addition, constructs of PlyC(PlyCB$_{R66E}$) and PlyC(PlyCB$_{K23E,K59E}$), almost abolished both extracellular and intracellular activity. Furthermore, PlyC(PlyCB$_{K23A}$), which has a change from positive to neutral charge, also showed a moderate decrease in terms of intracellular activity but no change on extracellular activity. Similarly, PlyC(PlyCB$_{D21A}$), a mutation to a non-charged residue did not affect intracellular or extracellular activity at all, suggesting that intracellular bacteriolytic activity of PlyC is truly dependent on surface-exposed positively-charged residues.

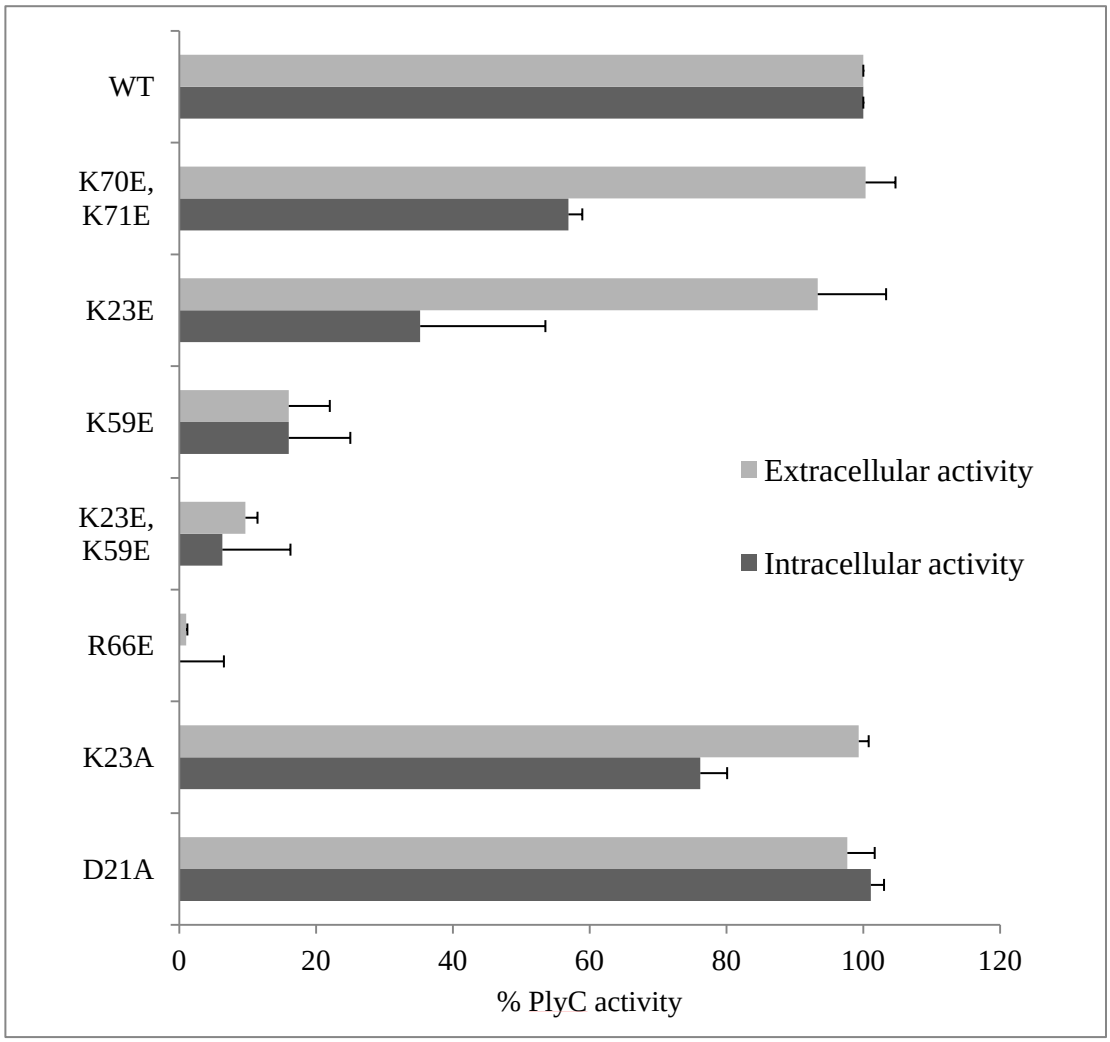

Figure 3-4. Extracellular and intracellular bacteriolytic activity of PlyC

Normalized extracellular and intracellular bacteriolytic activity of PlyC and PlyC mutants (selected residues of PlyCB). Extracellular activity was measured and normalized by turbidity reduction assay, and intracellular activity was obtained and normalized from co-culture assayed as previously described.

Fluorescence microscopic characterization of PlyCB mutants

Next, to determine whether the diminished intracellular activity is truly due to the effect of binding to streptococci or a defect to internalization, both wild-type and mutants of PlyCB were conjugated to AlexaFluor555 and tested for binding to streptococci and uptake by epithelial cells. **Figure 3-5** showed that mutation at Lys-

23 and Lys-59 are involved in internalization but not streptococcal binding, whereas Arg-66 mediates both binding to streptococci and the internalization capacity. Moreover, and a charge-conserved mutation (Arg-66 to Lys-66) was able to retain both phenotypes.

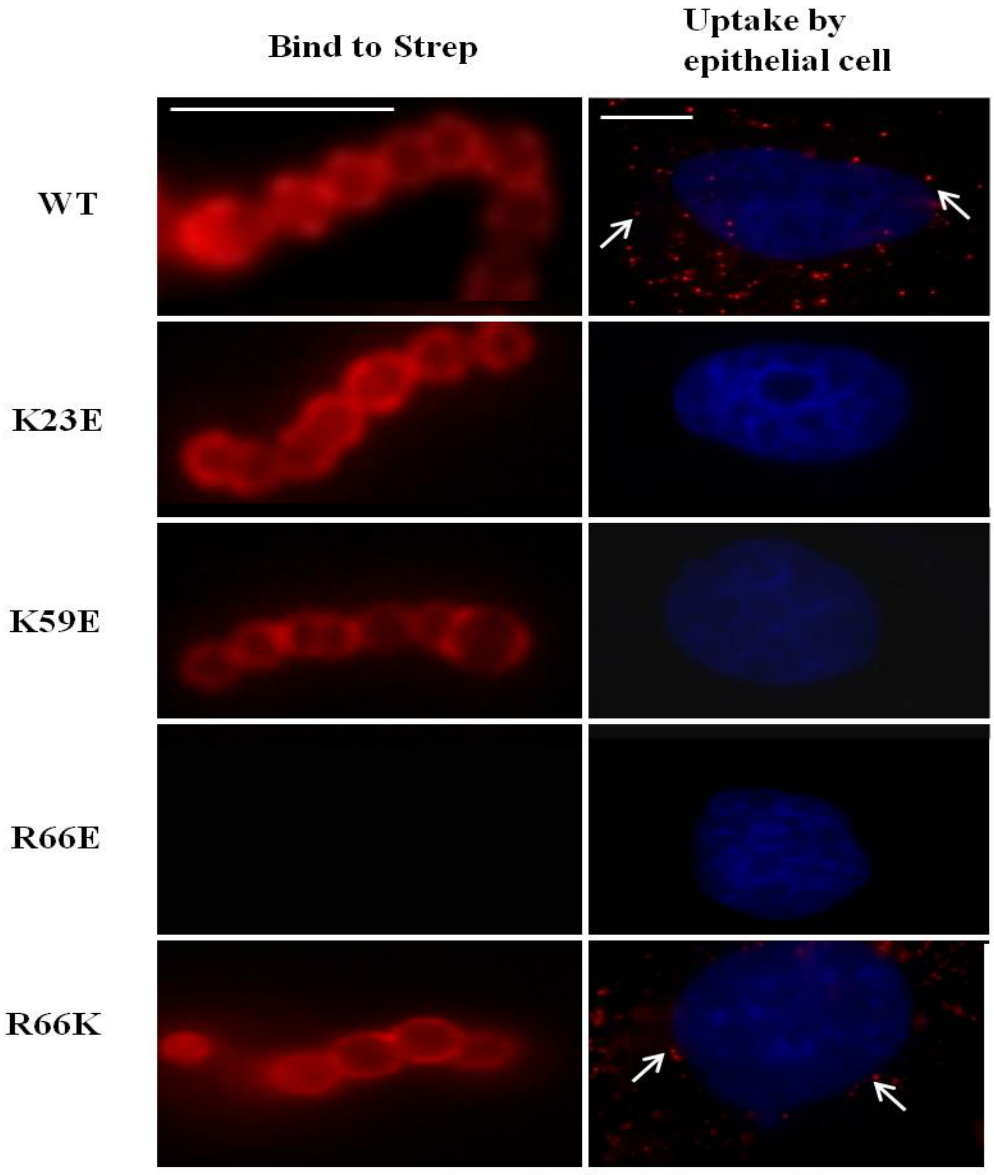

Figure 3-5. Fluorescent microscopic characterization of PlyCB and its mutants

Microscopy of fluorescent-labeled PlyCB on GAS (left column) and internalization into epithelial cell (right column). Arrows point the internalized PlyCB. Scale bar is indicated in each column. The scale bar is 5 μm in left column, and 10 μm in right column.

Neither heparan sulfate nor chondroitin sulfate serve as cell surface receptor that mediates the internalization of PlyCB

Next, we wanted to identify the ligand on the plasma membrane mediate the interaction with PlyCB. Previous studies have shown that uptake of TAT is initiated by non-specific electrostatic interaction with negatively charged glycosaminoglycans (GAGs), such as heparan sulfate (HS) and chondroitin sulfate (CS), linked to cell surface core proteins to form heparan sulfate proteoglycan (HSPG) and chondroitin sulfate proteoglycan (CSPG) (Tyagi, Rusnati et al. 2001; Richard, Melikov et al. 2005). To determine whether PlyCB also utilizes negatively charged GAGs (HS or CS) as cell surface receptors for the cellular uptake, we first examined the effects of soluble GAGs, such as heparin and chondroitin sulfate-B (CS-B), on PlyCB internalization into A549 epithelail cells (**Figure 3-6b and c**). The presence of excess exogenous heparin, a close structural homologue of HS, had no effect on internalization of PlyCB. Similarly, exogenous CS-B did not impede PlyCB entry. Furthermore, the effects of enzymatic removal of cell surface GAGs was examined by treating A549 cells with specific GAG lyases, such as heparinase III to remove endogenous HS and chondroitinase ABC to remove endogenous CS-B (Tyagi, Rusnati et al. 2001) prior to PlyCB incubation. Again, no significant inhibitory effects were observed upon PlyCB internalization when using those two enzymes respectively (**Figure 3-6d and e**). Overall, these results provide evidence that, unlike TAT, cell surface HSPGs are not the cellular receptors responsible for internalization of PlyCB endolysin.

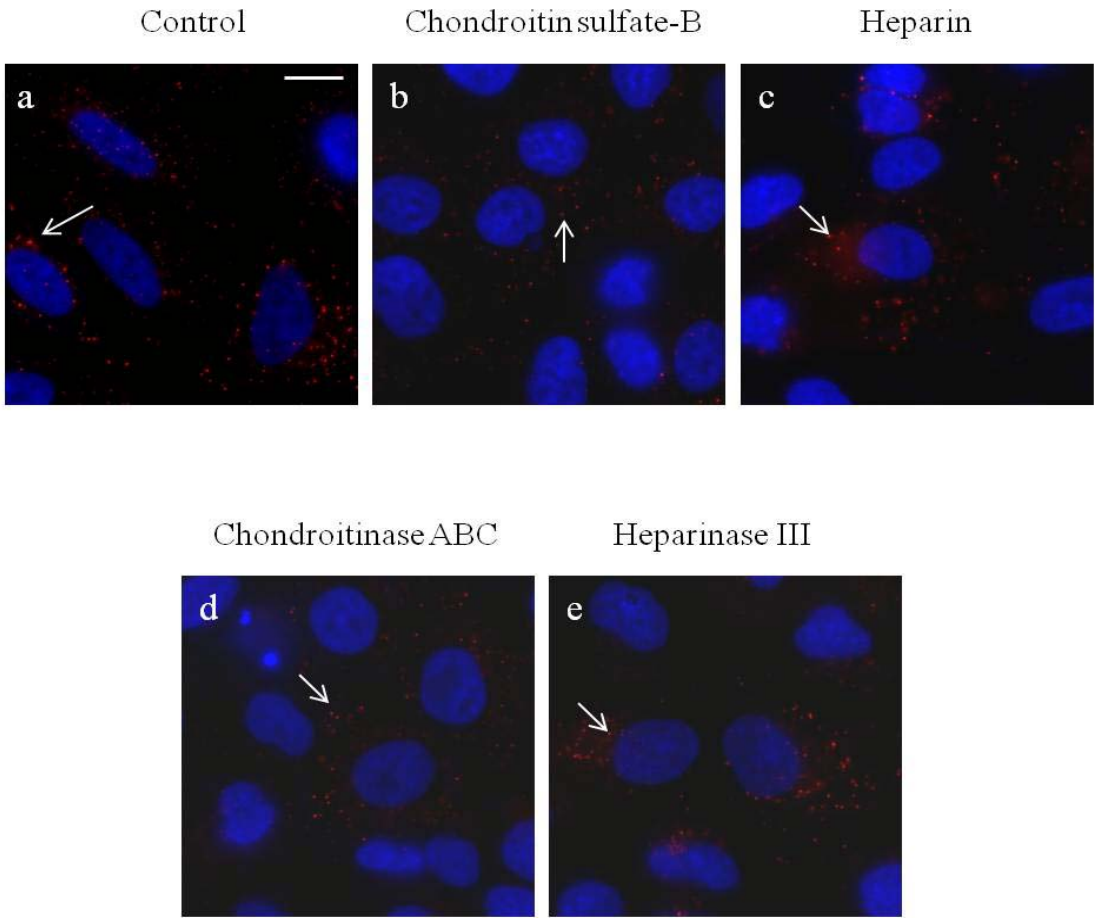

Figure 3-6. Effects of the presence of soluble GAGs or GAG lyase on internalization of PlyCB

(a) A549 cells were incubated with PlyCB-Alexa555 (red) in serum-free medium F12K for 30 min at 37ºC, fixed by 4% PFA in PBS and stained with and DAPI (nucleus, blue). (b) Cells were pre-treated with 50 μg/ml of chondroitin sulfate-B for 30 min then incubated with PlyCB-Alexa555 before being fixed and stained with DAPI. (c) Cells were pre-treated with 100 IU/ml of heparin for 30 min then incubated with PlyCB-Alexa555 before being fixed and stained with DAPI. (d) Cells were pre-treated with 20 mIU/ml of chondroitinase ABC for 1 hour then incubated with PlyCB-Alexa555 before being fixed and stained with DAPI. (e) Cells were pre-treated with 5 mIU/ml of Heparinase III for 1 hour then incubated with PlyCB-Alexa555 before being fixed and stained with DAPI. Arrows indicate the internalized PlyCB. Scale bar is 20 μm.

Phospholipid-PlyCB interaction screening assay

Structural studies on membrane-bound TAT revealed that TAT binding to the membrane-water interface is stabilized not only by electrostatic attraction to the anionic lipids (Arg-phosphate salt bridge), but also by intermolecular hydrogen bonding with the lipid phosphates and water (Su, Waring et al. 2010). This finding led us to hypothesize that the phosphate moiety on the lipid membrane is responsible for interacting with cationic surface of PlyCB for internalization. To further elucidate the phospholipid molecules involved in this uptake event, we performed a phospholipid (PIP) screening assay, which is a protein-lipid overlay technique combined with Western blot that is designed specifically for identification of phosphoinositide-protein interactions. **Figure 3-7** shows that PlyCB specifically and directly interacts with phosphatidylinositol (PtdIn), phosphatidic acid (PA) and phosphatidylserine (PtdSer), but not phosphatidylethanolamine (PtdEtn) or phosphatidylcholine (PtdCho). In addition, phosphorylated PtdIns, such as PtdIns(3)P, PtdIns(3,4)P_2, and PtdIns(3,4,5)P_3 did not bind to PlyCB, suggesting that the binding motif requires some restricted confirmation or local structure. Further comparison to wild-type PlyCB revealed that $PlyCB_{K59E}$ and $PlyCB_{R66E}$ only bind to PA and PtdSer, but not PtdIns, suggesting that PtdIns might be a key molecule on the membrane that secures this interaction with positively-charge residues on PlyCB. If so, this might explain the previous observations that fluorescent labeled mutants K59E and R66E failed to internalize.

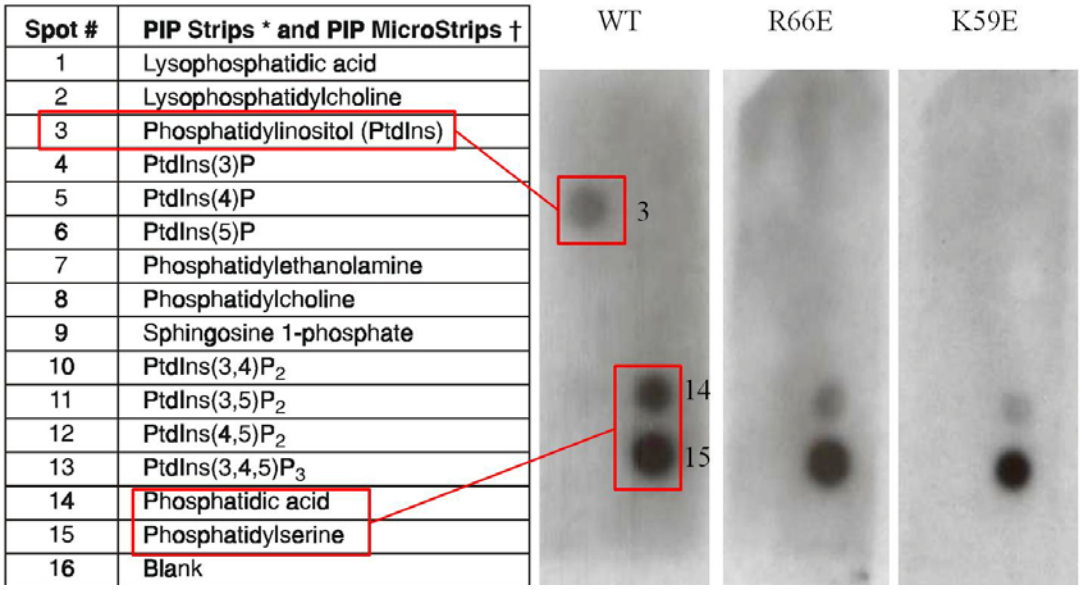

Figure 3-7. Biochemical characterization of PlyCB and PlyCB mutants by phospholipids screening assay

Layout of phospholipids screening assay (left panel) and result (right panel) of lipid binding test of His-tagged PlyCB, $PlyCB_{K59E}$, $PlyCB_{R66E}$. Note that the His tagged $PlyCB_{K23E}$ was insoluble when over expressed (data not shown).

Predicted molecular docking of PlyCB with specific phospholipids

PtdSer and PtdIns are the major anionic glycerophospholipids in eukaryotic plasma membranes (Fadeel and Xue 2009). In quiescent cells, PtdSer is exclusively located at the inner (cytoplasmic) leaflet of the plasma membrane under normal circumstances, but becomes exposed on the surface of the cell undergoing apoptosis (Calderon and Kim 2008), phagocytosis (Dias-Baruffi, Zhu et al. 2003) or cellular uptake (Hirose, Takeuchi et al. 2012). In addition, PtdIns is a component normally found in the cytosolic side of eukaryotic cell membranes and play important roles in lipid raft signaling and membrane trafficking (Bevers, Comfurius et al. 1999; Pike 2003).

Obtaining a co-crystal of PlyCB and phospholipids is failed due to the long fatty acid chains. However, to elucidate the structural insights of interaction between PlyCB and specific phospholipids, we examined a molecular docking model (**Figure 3-8a and b**) suggesting that PlyCB monomer contains a binding pocket, the 'mouth' of which includes the cationic residues such as Lys-59 and Arg-66. The interface contains multiple hydrogen bonds, which help secure the protein-phospholipids interaction. Moreover, attempts to dock $PlyCB_{R66E}$ and PtdIns were unsuccessful, presumably due to the reduced volume of the pocket in the $PlyCB_{R66E}$ mutant that was unable to accommodate the inositol ring of PtdIns, which is consistent with the observation from phospholipids screening assay in **Figure 3-7**.

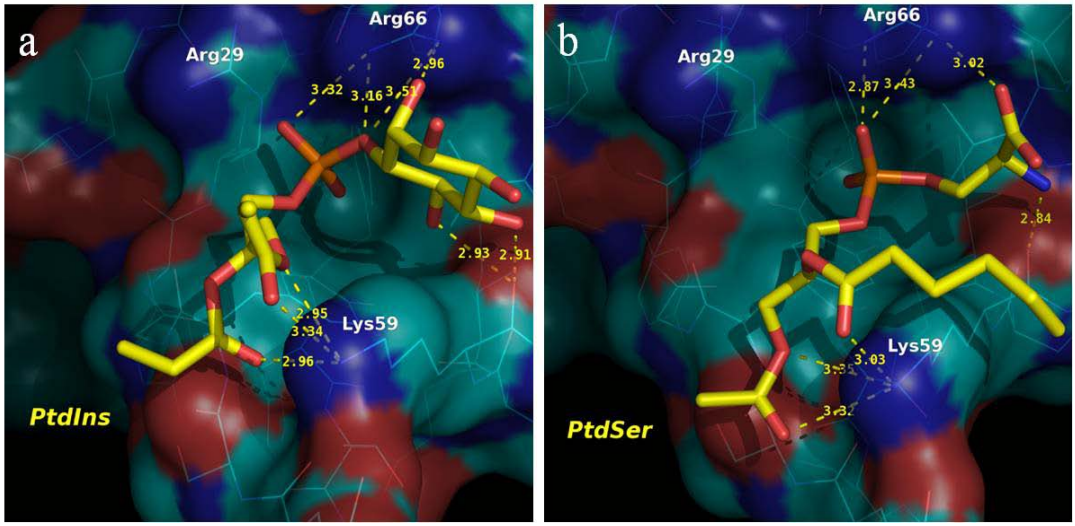

Figure 3-8. Molecular docking of specific phospholipids with PlyCB

Inter-molecule docking of PlyCB monomer and PtdIns (a) and PtdSer (b) by using DOCK6.6 suite software (Lang, Brozell et al. 2009). Note that the fatty acid chains of two phospholipids were trimmed off to avoid unnecessary complication during modeling. Yellow dashed line represent the hydrogen bonding between specific phospholipids and a pocket-like structure formed by Arg-29, Lys-59, Arg-66 on the surface of PlyCB monomer.

Structural effects of the PlyCB$_{R66E}$

Figure 3-3a suggests PlyCB possesses a pocket-like structure that contains the cationic residues such as Arg-29, Lys-59 and Arg-66. To further study the structure-function relationship of PlyCB binding to the plasma membrane, the 1.8-Å X-ray crystal structure of PlyCB$_{R66E}$ was obtained. Superimposing the structure of the PlyCB$_{R66E}$ mutation on wild-type PlyCB (**Figure 3-9**) reveals that the Glu-66 (mutation) side chain maintains the same location as Arg-66 (wild-type), and a hydrogen bond to Glu-36 is preserved. However, Arg-29 of PlyCB$_{R66E}$ adopts a new conformation that enables it to hydrogen bond with both Glu-66 and Glu-36. The implication of the R66E structure is that, since the local structure appears well-ordered, the movement of Arg-29 and subsequent ability to hydrogen bond Glu-66 and/or Glu-36 preclude binding of phosphate moieties in the crucial pocket. Thus the effects of R66E shown in the phospholipids binding or cellular uptake are probably due to the observed changes at the R66E and R29 sites, and not due to general disruption of local secondary structure.

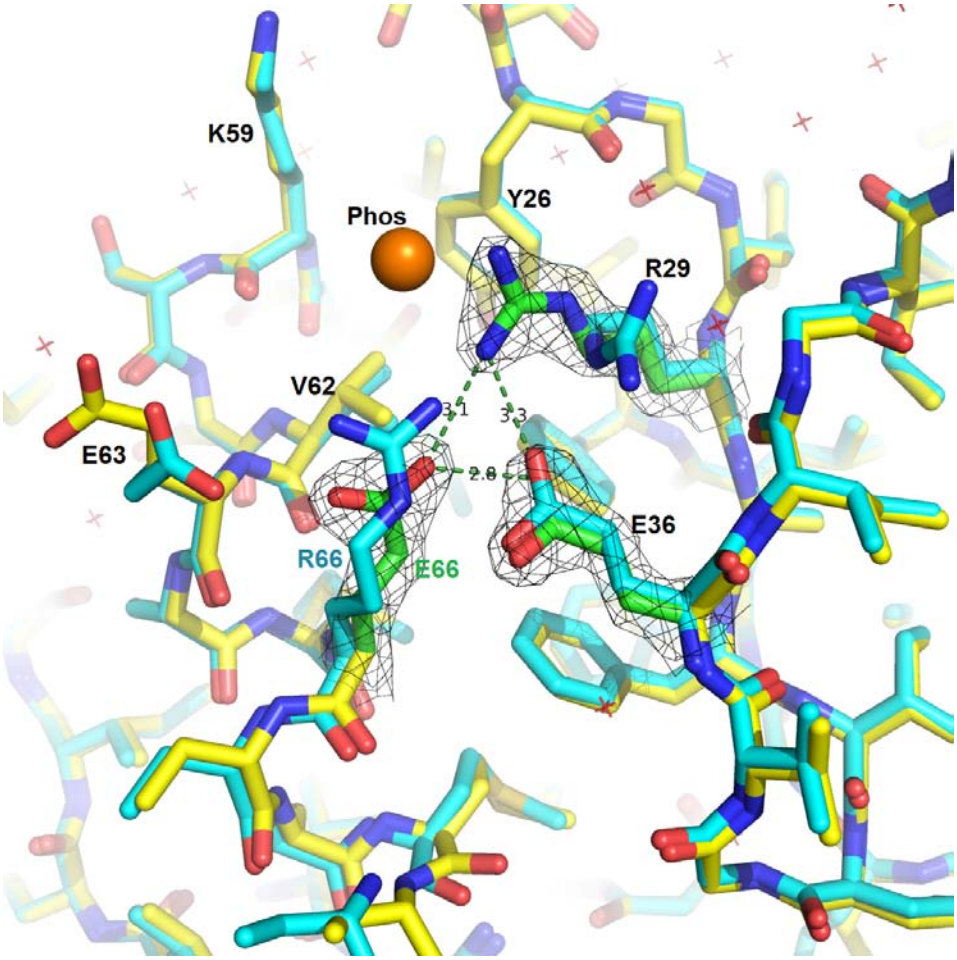

Figure 3-9 Structural effects of the R66E mutation in PlyCB

Crystal structures of the wild-type (blue carbons) and mutant (yellow, with green to emphasize the 3 key residues Arg-29, Glu-36, and Arg/Glu-66; electron density shown. Both structures are at 1.8-Å resolution. The orange sphere shows the location of a putative phosphate site observed to be strongly occupied in the presence of phosphate-bearing ligands. Note that this site holds a water molecule in the native structure, but the site is empty in the mutant, apparently disrupted by the mutation of Arg-66.

Conclusion

This chapter aims to provide insight into the interactions between the plasma membrane and PlyC upon internalization. First, we found a highly positive-charged

surface exposed on the PlyCB octamer based on the crystal structure of PlyC. A total of 16 arginine and 32 lysine residues are identified to be exposed on the surface PlyCB. This finding led us hypothesize that internalization of PlyC mimics cell-penetrating peptides, which are also a group of peptides enriched for cationic residues such as lysine and arginine. However, it should be noted that cell-penetrating peptide are typically 10 amino acids in length whereas PlyC is a holoenzyme composed nine subunits (1 PlyCA: 8 PlyCB) with the cationic face of the PlyCB octamer spread over a diameter of 80 angstroms. Nonetheless, we sought to investigate the role of internalization, if any, of these cationic residues on the PlyCB surface. Fluorescent-labeling of the subunits and holoenzyme revealed that the PlyCB octamer alone or in context of the holoenzyme, but not PlyCA, is sufficient for translocation into epithelial cells. As such, further studies were focused on PlyCB.

Next, we sought to determine whether the internalization of PlyC was mediated or initiated by electrostatic interactions with the cationic residues on PlyCB. There are two existing membrane-associated negative-charged species, glycosaminoglycans (sulfate group) and phospholipid (phosphate group), both of which have been implied to interact with catioinic cell-penetrating peptides upon internalization in the literature. Therefore, to test glycosaminoglycan theory, we conducted internalization assay in competition with chondroitin suflate-B and heparin. Additionally, we treated cells with chondrotinase and heparinase to remove native glycosaminoglycans. However, none of these conditions inhibited or affected the internalization of PlyCB.

After ruling out a glycosaminoglycans candidate, we turned our attention to phospholipid screening assay (i.e.'PIP strips'), which allowed us to identify whether any of the specific phospholipid species interacted with PlyCB. We found that PlyCB specifically and directly interacts with PtdIn, PA and PtdSer, but not PtdEtn or PtdCho, all of which are the common species on the plasma membrane (van Meer, Voelker et al. 2008). The structural differences between different phospholipids species also tells us that all three species have a backbone of phosphatidic acid, which contains two long hydrophobic chain, one glycerol and phosphate group, with a side chain that differs from various species. The fact that PlyCB does not interact with PtdEtn or PtdCho, which has the same PA backbone suggests that side chain must have a carboxyl group (like PtdSer) or hydroxyl group (like PtdIns) to form either hydrogen bonding or salt bridge interaction with cationic residues on the PlyCB.

Site-directed mutagenesis was used to create a series of single mutation to determine whether the cationic residue(s) play a role mediating the internalization of PlyC into epithelial cell. Given the fact that PlyCB forms a homo octameric ring structure, any single point mutant potentiates a change of eight residues on the PlyCB surface. We biochemically and biophysically characterized each mutant, including SDS-PAGE for purity, mass spectrometry for purity and verification of mutation, analytic gel filtration for confirmation of holoenzyme formation, and infrared spectroscopy for detecting secondary structure change and proper folding. All results suggest that the mutants were properly expressed and folded. Next, these mutants were benchmarked for their extracellular and intracellular bacteriolytic activity, streptococcal surface binding, and intracellular localization. The results suggest that

reversing the charge of residues Lys-23, Lys-59 and Arg-66 impairs the internalization ability of PlyCB. Furthermore, PIP screening assay provided more details elucidating the insights into how PlyCB interacts with the specific phospholipids species on the membrane that could potentially mediate the binding and entry into epithelial cells. Finally, two molecular docking models predict that there is a binding pocket formed by Lys-59, Arg-66 that interacts with PtdIns and PtdSer via multiple hydrogen bonds and electrostatic interactions, suggesting that unlike cationic cell-penetrating peptides, PlyC, utilizes a novel binding pocket or motif to interact with specific phospholipid hydroxyl moieties in the membrane, ultimately resulting in internalization of the PlyC endolysin.

Chapter 4: Probing the uptake and trafficking mechanisms of PlyC

Background

The obseravation that PlyC co-localized with internalized GAS in the intracellular environment by confocal microsocopy, led us to hypothesize that internalization of PlyC and GAS might share a similar route when entering the host cells. To illustrate which particular pathway PlyC ultilizes when entering epithelial cells, inhibitors that block specific endocytic pathways, including macropinocytosis, clathrin-mediated endocytosis, caveolae-mediated endocytosis, etc. were screened. Therefore, this chapter is focused on identifying the exact process of PlyC uptake and transport within epithelial cells. Since the previous chapter has demonstrated that PlyCB subunit and PlyC possess equivalent capacity when internalized, fluorescently-labeled PlyCB subunit and confocal microscopy were used to study the internalization and trafficking mechanism.

Results

Internalization of PlyC does not compromise membrane integrity

The first question to be addressed is whether cell membranes still maintain integrity while PlyC is internalized. Propidium iodide (PI), a fluorescent molecule that is membrane impermeable and excluded from viable cells, was employed to assay the effect of PlyC internalization on membrane integrity (**Figure 4-1a**). As an alternative, trypan blue is a vital stain used to selectively dye dead tissues or cells.

This dye exclusion method was used to detect membrane disruption upon PlyC uptake. **Figure 4-1b** showed that there was no statistical difference between the growth media control (no PlyC) and growth media with PlyC (2 or 100 μg/ml) after 1 hour incubation. Both assays suggested that internalization of PlyC does not compromise the membrane integrity of epithelial cells.

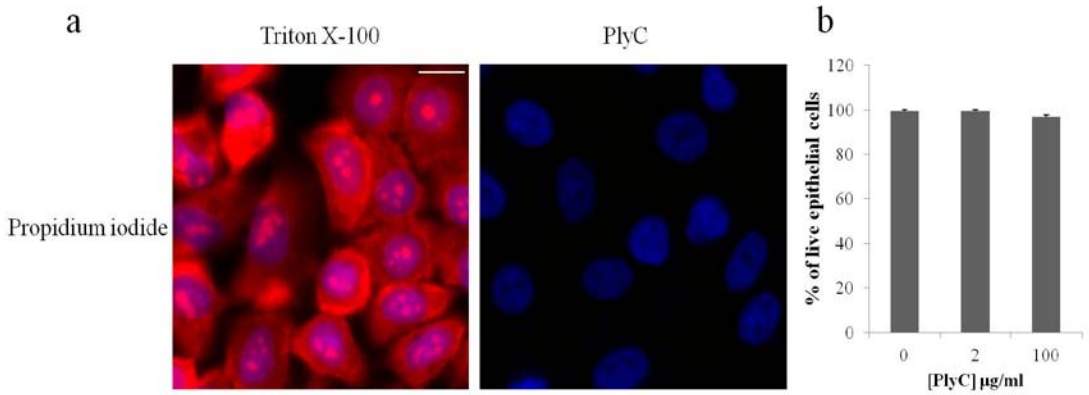

Figure 4-1. Membrane integrity test after incubation with PlyC

(a) Propidium iodide staining by fluorescence microscopy. The left panel showed that epithelial A549 cells (nucleus was stained by DAPI, blue) were pre-permeablized with Triton X-100, and then stained with propidium iodide (red). The right panel showed A549 cells that were pre-incubated with 100 μg/ml of PlyC for 1 hour and then stained with propidium iodide. Scale bar is 20 μm. (b) Trypan blue assay on A549 cells or A549 cells incubated with 2 or 100 μg/ml for 1 hour.

Internalization of PlyCB is dependent on temperature and interaction with lipid raft domains

At 37ºC, internalized PlyCB forms a vesicle-like structure, that has a diameter of ~ 0.5 μm (**Figure 4-2a)**. To elucidate the internalization mechanism of PlyC, low temperature (4ºC) and specific endocytic inhibitors were employed. First, we found that shifting the temperature to 4°C impaired the internalization of PlyCB (**Figure 4-2b**), suggesting this process is energy-dependent and thus probably requires active

transport machinery (Fretz, Penning et al. 2007). Next, internalized PlyCB was shown to co-localize with AlexaFluor555-labeled cholera toxin subunit B (CTxB-Alexa555), a known lipid raft marker which binds to GM1 gangliosides (Latif, Ando et al. 2003), suggesting a possible interaction with lipid raft microdomains upon PlyCB entry (**Figure 4-2c**). Furthermore, PlyCB internalization was partially inhibited and not co-localized with CTxB by chelation of cellular cholesterol when pre-treating with filipin III (**Figure 4-2d**), suggesting that PlyCB entry is mediated by a lipid-raft dependent process such as caveolae-mediated endocytosis (Lee, Lin et al. 2008). In contrast, cytochalasin D (CytD), a representative macropinocytosis inhibitor that induces depolymerization of actin filaments (Wakatsuki, Schwab et al. 2001), did not affect the internalization of PlyCB (**Figure 4-2e and f**). Next, fluorescence-labeled transferrin, a ubiquitous marker of clathrin-mediated endocytosis, was not observed to co-localize with internalized PlyCB in either the absence (**Figure 4-2g**) or presence (**Figure 4-2h**) of monodansylcadaverine (MDC), which has been demonstrated to specifically inhibit clathrin-dependent endocytosis (Wang, Rothberg et al. 1993), suggesting that PlyCB entry is not associated with clathrin-mediated endocytosis.

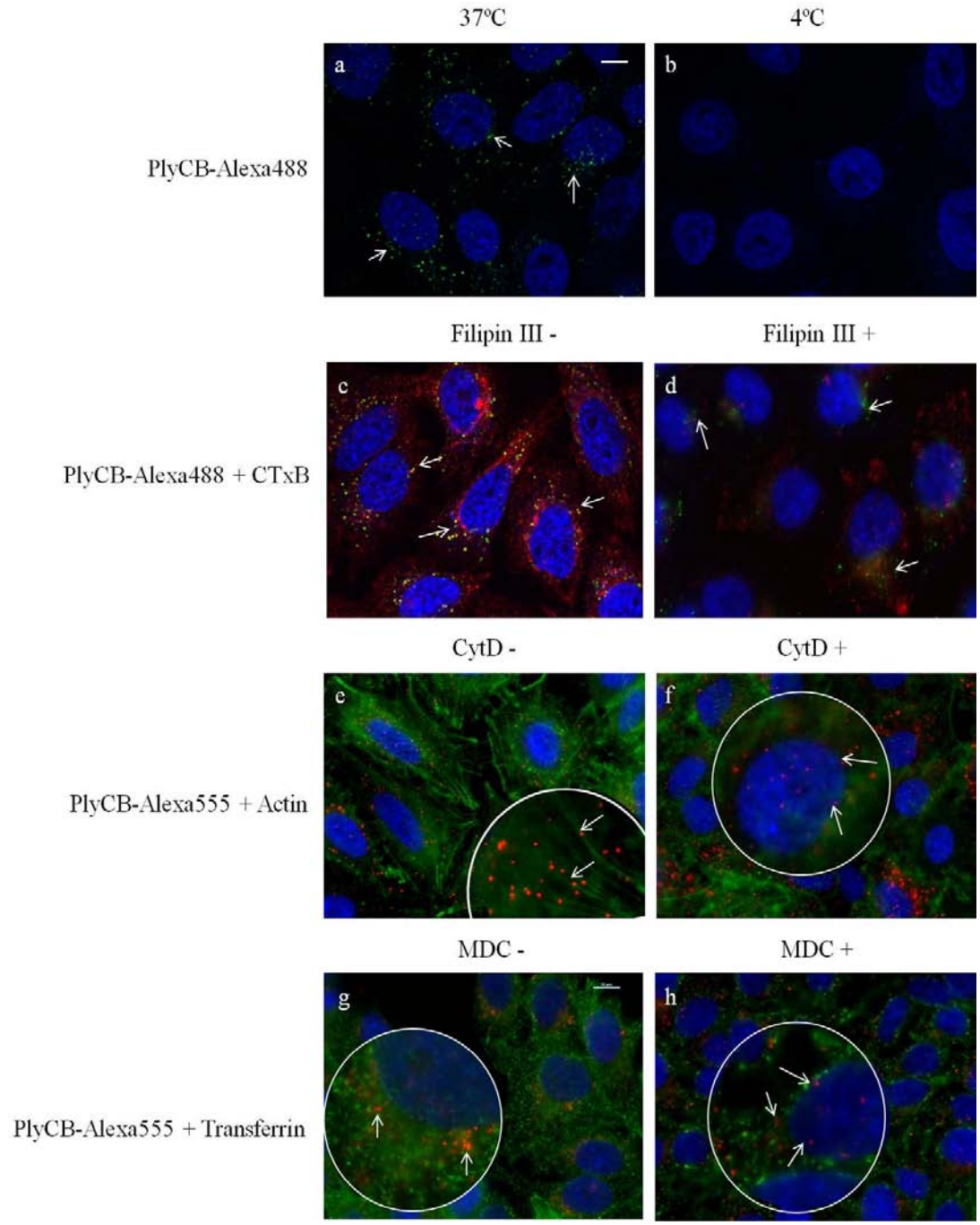

Figure 4-2. Internalization of PlyCB is dependent on temperature and interaction with lipid raft domains

(a) A549 cells were incubated with PlyCB-Alexa488 (green) in serum-free medium F12K for 30 mins at 37 ºC, then were fixed by 4% PFA in PBS and stained with and DAPI (nucleus, blue). (b) No PlyCB internalization was observed when incubating PlyCB-Alexa488 with cells at 4ºC. (c) Cells were incubated with PlyCB-Alexa488 (green) and CTxB-Alexa555

(red) in serum-free medium F12K for 30 min at 37 ºC, fixed and subsequently stained with DAPI (blue). (d) Cells were pre-treated with Filipin III for 30 min, then incubated with PlyC-Alexa488 and CTxB-Alexa555 before being fixed and stained with DAPI. (e) cells were pre-treated with serum-free F12K media or in the presence of CytD (d) for 30 min, then incubated with PlyCB-Alexa555 (red) in serum-free media for an additional 30 min before being fixed and stained with AlexaFluor488 Phalloidin (actin filaments of cytoskeleton, green) and DAPI. Note that actin filaments were depolymerized due to the treatment with CytD. (g) Cells were incubated with PlyCB-Alexa555, then fixed and stained with FITC-conjugated antibodies against human transferrin receptor (FITC-transferrin, green) and DAPI. (h) Cells were pre-treated with MDC then incubated with PlyCB-Alexa555 before being fixed and stained with FITC-transferrin and DAPI. White circle represents the magnifier view. Arrows indicate the internalized PlyCB. Scale bar is 10 μm.

Internalized PlyCB is associated with endocytic pathway

Next, we sought to determine whether internalization of PlyC utilizes a natural endocytic pathways (actin, early endosomes, late endosomes and lysosomes) when transported inside the epithelial cells. Therefore, the internalization of fluorescently labeled PlyCB, and subsequent distribution to different subcellular localizations, was analyzed by confocal microscopy. Z-stack analysis (**Figure 4-3a**) reveals internalized PlyCB (red) co-localized with actin filaments (green) as arrows pointed at Z1 to Z3 section, suggesting the intracellular trafficking of PlyC might be carried by structural elements of the cytoskeleton. In addition, Z-stack analysis and time course experiments were employed to determine whether internalized PlyC co-localized with two subcellular markers, early endosome and lysosome, in a time-lapse manner. **Figure 4-3b** demonstrated that the fluorescent signal for PlyCB-Alex555 was detected in the vesicular compartments found in peripheral region of the cytosol as early as 5 minutes after incubation, and was also observed to co-localize with early endosome in more than 90% of cells within 15 minutes (data not shown). Intracellular

trafficking of the PlyCB was spread throughout the cytosol, which seems to be a different pattern from other reports on the cellular uptake of the cell-penetrating peptides, which are initiated at specific sites (Duchardt, Fotin-Mleczek et al. 2007; Hirose, Takeuchi et al. 2012). Over time (30 to 60 min), more internalized PlyCB was transported from early endosomes to the perinuclear region. In contrast, internalized PlyCB did not fuse to lysosome compartments after 90 minutes of incubation, although a fraction of internalized PlyCB was also found in peripheral region (**Figure 4-3c**). Taken together, the PlyC endolysin, once internalized, is transported from early endosomes to lysosomes, which is consistent with normal intracellular trafficking.

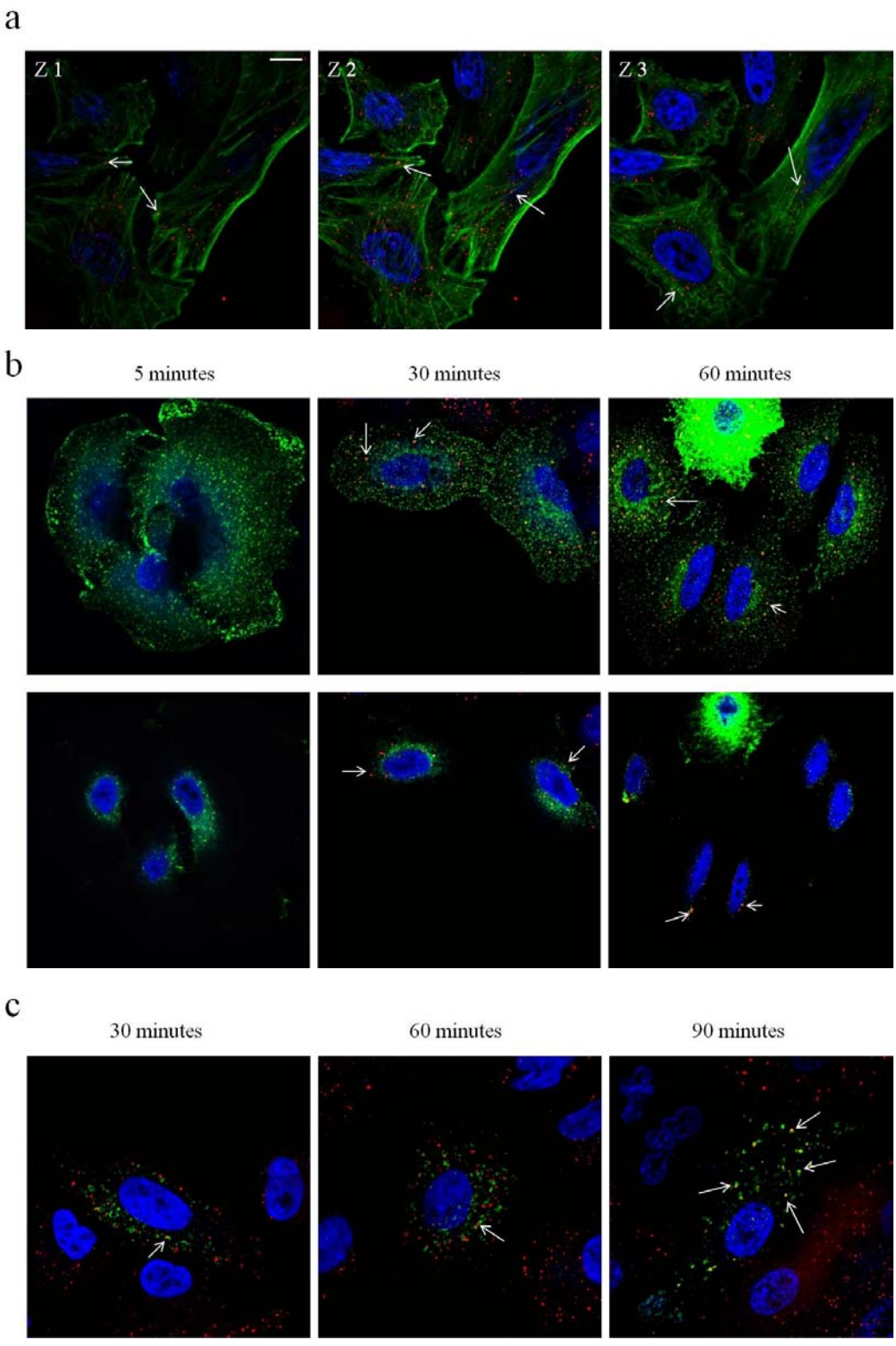
a
Z 1
Z 2
Z 3
b
5 minutes
30 minutes
60 minutes
c
30 minutes
60 minutes
90 minutes

Figure 4-3. Internalized PlyCB is associated with endocytic pathway

(a) A549 cells were incubated with PlyCB-Alexa555 in serum-free medium F12K for 30 min at 37ºC, fixed and stained with Alexa Fluor488 phalloidin (actin filaments of cytoskeleton) and DAPI. The first three sections (Z1 to Z3) from the Z-stack images (8 slices in total 6 μm) are shown. Note the internalized PlyCB (pointed by arrows) is co-localized (shown in yellow) with actin filaments. (b) Cells were transfected with CellLight early endsome-GFP (green) 24 hours prior to treatment of with PlyC-Alexa555. Z-stack fluorescent images of cells incubated with PlyCB-Alexa555 were acquired at various time points (6 slices within a total of 6 μm). Upper panel shows the focal plane where PlyC-Alexa555 co-localizes with early endosome compartments as indicated by the arrow. The lower panel represented the section where internalized PlyC resides at a perinuclear location as indicated by the arrow. (c) Cells were transfected with CellLight lysosome-GFP (green) 24 hours prior to treatment with PlyCB-Alexa555 (red). Cells are fixed with 4% PFA after 30, 60, and 90 min incubations with PlyC. One representative image from each time point was shown. The arrows pointed to the co-localization of PlyCB and lysosomal compartment. Scale bar is 20 μm.

Intracellular trafficking of PlyCB is regulated by PI3K pathway.

When treated with wortmannin, a phosphatidylinositol 3-kinase (PI3K) inhibitor that inhibits fluid-phase macropinocytosis but not receptor-mediated endocytosis (Yao, Li et al. 2009), the internalized PlyCB was found to co-localize with the swollen vacuole-like structure (or vesicle) induced by wortmannin (**Figure 4-4a, b c and d**), suggesting that intracellular trafficking of PlyC is regulated by PI3K pathway. Furthermore, treatment of wortamannin significantly reduce the cellular uptake of the 70 kD FITC-labeled dextran **Figure 4-4e and f**), a known marker for macropinocytosis/fluid-phase uptake (Falcone, Cocucci et al. 2006), confirming the inhibitory effect of wortmannin.

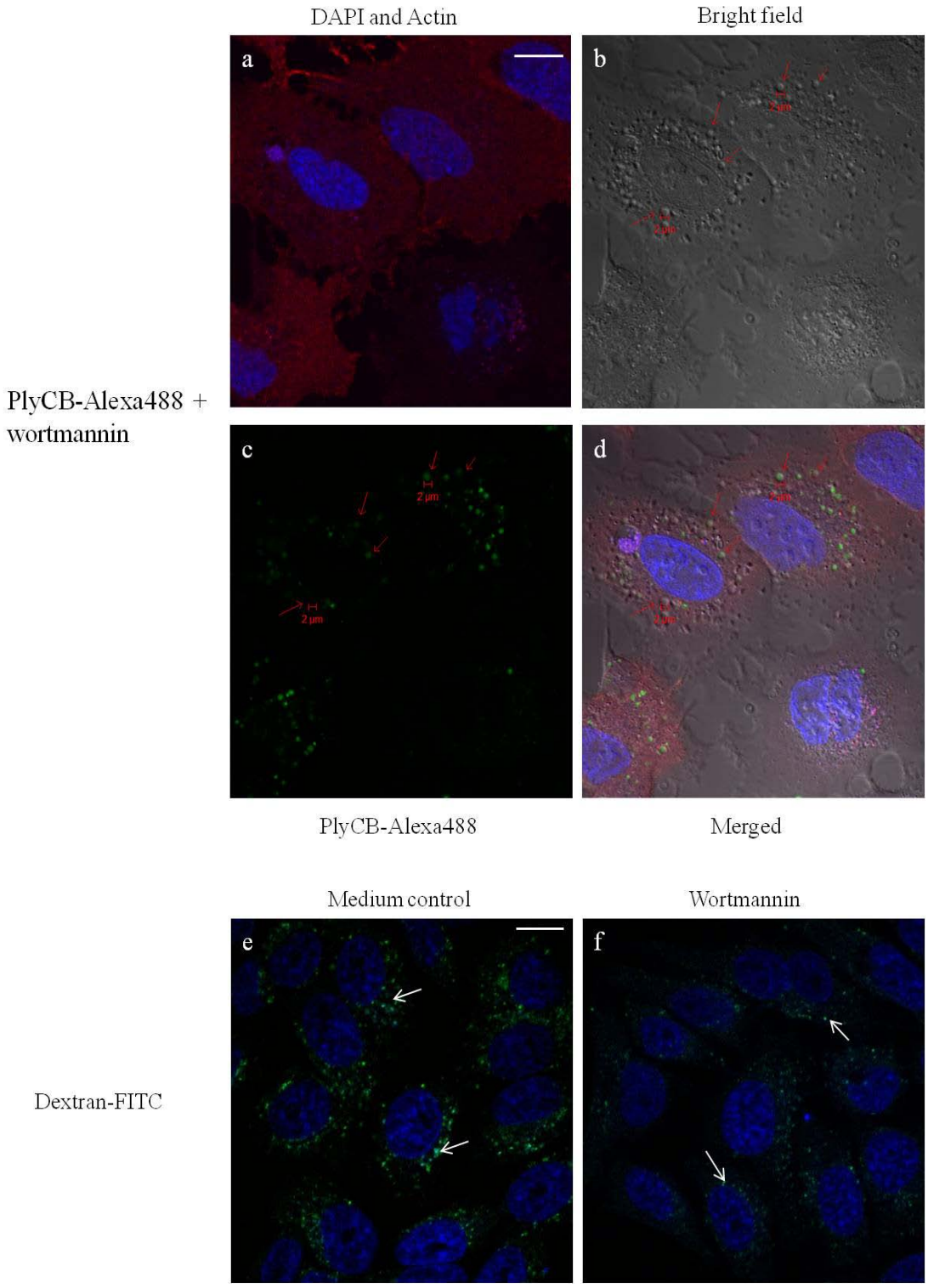

Figure 4-4. Intracellular trafficking of PlyCB is regulated by PI3K pathway

(a, b, c, d) A549 Cells were first transfected with CellLight Actin-RFP (red) at 24 hour prior to incubation with PlyCB-Alexa488 (green) in the presence of wortmannin, cells were then

fixed and stained with DAPI. Note that internalized PlyC is co-localized with swollen vacuole structure (~ 2 μm) induced by wortmannin in the merged image. (e) Fluid-phase uptake of dextran-FITC by macropinocytosis. (f) Wortmannin inhibits the uptake of dextran. Arrows indicate the internalized PlyC-Alexa488 or dextran-FTIC. Scale bar is 20 μm.

Conclusion

The confocal microscopy performed in this chapter clearly revealed that internalization of PlyCB is accompanied by several events. During entry, PlyCB first interacts with lipid raft microdomains (**Figure 4-2c and d**), yet the internalization process does not compromise the membrane integrity (**Figure 4-1a and b**). Second, we show through Z-stack analysis that internalized PlyC, once inside the cells, resides within ~0.5 μm vesicle-like structures in the cytosol and peri-nuclear location (**Figure 4-2a**). Furthermore, the internalized PlyCB is partially associated with actin filaments (**Figure 4-3a**), early endosomes (**Figure 4-3b**) and lysosomes (**Figure 4-3c**) in a spatial and temporal and manner, suggesting that PlyCB entry utilized a traditional endocytic pathway. However, internalized PlyC was not completely degraded by fusion with early endosomal and lysosomal compartments, and eventually reached a perinuclear destination. Given the fact that PlyC has a broad pH spectrum (4 to 11) in terms of lytic activity against GAS (Nelson, Schuch et al. 2006), this is might be a potential benefit for PlyC to retain its functional activity in low pH environments, such as early endosome (pH ~6.5) and lysosome (pH ~5.5). Our observation from our co-culture assay (in Chapter 2) has also confirmed PlyC's intracellular bacteriolytic efficacy, since internalized GAS also share certain characteristics (endosome/lysosome pathway) upon trafficking through host cells. On the other hand, changing the temperature to 4°C completely blocks the internalization of PlyCB

(**Figure 4-2b**), suggesting the uptake process probably requires some active transport machinery, instead of a direct diffusion process. Toward this end, several specific endocytic inhibitors and their corresponding control markers were employed to elucidate the pathway that mediates the uptake of PlyCB. Filipin III, a specific inhibitor can partially inhibit internalization of PlyCB, suggesting that PlyCB entry is mediated by a lipid-raft dependent process such as caveolae-mediated endocytosis. Moreover, wortmannin, which is considered a macropinocytosis inhibitor, appeared to inhibit intracellular trafficking of internalized PlyCB by forming the swollen vacuole like structure (~2 μm) in diameter (**Figure 4-4a, b, c, and d**), although they do not block the uptake of PlyCB, suggesting that intracellular trafficking is dependent on the signaling that is possibly associated with PI3K. Notably, entry of GAS into epithelial cells is also dependent on s PI3K- associated pathway (Wang, Yurecko et al. 2006), suggesting that uptake of GAS or PlyC endolysin shares similar characteristics.

In summary, internalization of PlyC is mediated by interacting with the plasma membrane, and the fate of internalized PlyC is regulated by a traditional endocytic pathway. It should also be acknowledged that intracellular enzyme delivery might take advantage of more than one pathway, depending on various factors such as enzyme concentration, cell line utilized, and cell density (Fonseca, Pereira et al. 2009). Taken together, our results provide a better understanding of the mechanisms involved in internalization and transport of PlyC in an intracellular environment.

Chapter 5: Thesis discussion and future perspectives

Comparison of the internalization mechanism of GAS and other bacteria

Although GAS is traditionally considered an extracellular pathogen, internalization of GAS has recently been reported (LaPenta, Rubens et al. 1994; Greco, De Martino et al. 1995). The proposed mechanisim invovles the fibronectin-binding protein on the GAS surface, which promotes streptococcal adherence to the amino terminus of fibronectin and acts as a bridging molecule between streptococci and the $\alpha_5\beta_1$ integrin on the eukaryotic cells. The cellular receptors responsible for internalization of GAS are integrins capable of fibronectin binding (Molinari, Talay et al. 1997; Ozeri, Rosenshine et al. 1998). Following integrin receptor mediated endocytosis, this process leads to a sequential event involving fusion with endocytic compartments (endosomes and lysosomes). In the lysosomes, the ingested GAS can be degraded within nonphagocytic cells (Nakagawa, Amano et al. 2004). However, a subpopulation, GAS can circuvent host defence by escaping from fusion with the lysosomes, externalize by inducing apoptosis of host cell and sebsequently repopulate the mucosal surface after antibiotic prophylaxis (Marouni and Sela 2004; Kwinn and Nizet 2007).

Likewise, other intracellular Gram-positive bacteria, such as *Staphylococcus aureus*, *Listeria monocytogene*s, *Mycobacteria*, also utilize specific cell surface receptor-mediated internalization for their entry (Clemens and Horwitz 1996; Ellington, Reilly et al. 1999; Pentecost, Kumaran et al. 2010). In addition to the comparable uptake mechanism, these bacteria are able to not only escape the

endosomes or prevent fusion with lysosomes, but they are also able replicate within the host cell (Jarry and Cheung 2006; Pentecost, Kumaran et al. 2010; Manzanillo, Shiloh et al. 2012).

Comparing internalization and intracellular trafficking of GAS and PlyC

Eukaryoic cells are able to internalize foreign proteins from the surrounding medium by endocytosis (Doherty and McMahon 2009; Ziello, Huang et al. 2010). In the endocytic pathway, internalized proteins are delivered to early endosomes, followed by recycling part of this network of tubules and cisternae (containing receptors) back to the plasma membrane, while other components of the endosome are transported to late endosomes and lysosomes for degradation. In this disseration, confocal microsocopy demonstrates that PlyC internalizes through lipid raft-dependent macropinocytosis, which is not exact same mechanism of entry for GAS (receptor-mediated). Nontheless, the observation that PlyC co-localizes with early endosomal and lysosomal compartmetns as well as internalized GAS in the intracellular environment, suggests that they share a similar intracellular trafficking routes after entry into the host cells. As such, this evidence supports the potential application of PlyC targeting intracellular GAS.

Comparing internalization mechanisms of TAT (cell-penetrating peptide) and PlyC

Although the ability of cell-penetrating peptides (i.e. TAT) to translocate across the plasma membrane has been documented extensively, the internalization mechanism(s) that underlie this phenomenon still remain unclear. It has been demonstrated that various properties of these peptides, including net charge, molecule

length, associated cargo, as well as temperature, and specific cell lines all play a role on the mechanism of peptide or peptide-associated protein uptake (Mueller, Kretzschmar et al. 2008). To date, cellular entry of these peptides has been categorized into two different modes: energy-dependent endocytosis and energy-independent direct translocation across the plasma membrane (Fonseca, Pereira et al. 2009). Although most studies support the endocytic mechanisms for cellular uptake, one recent report of three cell-penetrating peptides: penetratin, nona-arginine (R9), and TAT suggests that both modes can be observed in a single system depending on the peptide concentration (Duchardt, Fotin-Mleczek et al. 2007).

Recent reports (Wadia, Stan et al. 2004; Kaplan, Wadia et al. 2005) suggest that transduction of TAT occurs by lipid raft-dependent macropinocytosis (a specialized form of fluid-phase endocytosis) in an energy dependent manner. The current model for TAT mediated protein transduction is proposed as 3-step process that involves binding of TAT to the cell surface, stimulation of macropinocytotic uptake of TAT and cargo into macropinosomes and endosomal escape into the cytoplasm (Gump and Dowdy 2007). In the first step, binding to the cell surface is thought to be through electrostatic interaction with acid regions of surface proteins, sulfated glycans, membrane phospholipid head groups or a combination of all might be involved. In the case of PlyC internalization, we are able to demonstrate that substitution of the positive-charged residues dramatically reduces the efficiency of PlyC internalization. Specific phospholipids (not the sulfated proteoglycan) were identified to mediate the interaction with PlyC. In addition, by using various endocytic inhibitors and corresponding cellular markers, we are able to elucidate that

internalization of PlyC is mediated by interacting with lipid raft domains on the plasma membrane in an energy-dependent manner, which also share similar characteristics to the second step of TAT transduction via endocytosis. The final step in TAT transduction is escape from macropinosomes into cytoplasm after fusion with endosomes or lysosomes. Although we do not have the direct evidence that macropinosomes are involved, we find that PlyC co-localizes with early endosomal and lysosomal compartments in a time and spatial manner, as well as associated with the macropinocytosis pathway by screening with specific inhibitors. This evidence suggests that internalization of PlyC is comparable to uptake of TAT. However, there are some differences in terms of cell-entry mechanisms as more structural insights are obtained when probing the internalization mechanism of PlyC. Unlike the short cationic peptides, PlyC utilizes its positive-charged binding pocket to interact with specific phospholipids on the plasma membrane upon internalization. In addition, transduction of TAT is dependent on cytoskeleton rearrangement (Tunnemann, Martin et al. 2006), whereas we show that depolymerization of actin filaments by cytochalasin D does not inhibit cellular uptake of PlyC.

Fusion to cell-penetrating peptide enable endolysin to kill intracellular bacteria

Endolysin are capable of degrading only extracellular bacteria, while their access to intracellular pathogens is restricted by the plasma membrane of the infected host cell. The hypothesis that endolysins can kill intracellular bacteria upon their induction into cytoplasm of human host cells by fusion with cell-penetrating peptides has been developed (Borysowski and Gorski 2010), although to date no such study has been reported yet. In this dissertation, we found that TAT-labeled endolysins did

not show any intracellular bacteriolytic activity compared to the wild-type endolysins or in the case of PlyC, did not show enhanced activity compared to wild-type PlyC. Several possibilities can explain these observations: 1. TAT-labeled endolysins did not enter the cells; 2. They successfully internalized but failed to have direct contact with intracellular bacteria; 3. They lost their active confirmation for enzymatic activity after internalization. To address above questions, techniques or tools such as confocal microscopy, flow cytometry and Western blot can be applied. In addition, it will be worth trying TAT or other cell-penetrating peptides with different endolyins with specificity against *Staphylococcus aureus* or *Listeria monocytogene*s, two pathogens known to internalize in mamalian cells.

Structure-function relationship

In the infection cycle of bacteriophage, lysis is controlled by a holin, which modulates pore formation in the bacterial plasma membrane. This process allows the cytoplasmically accumulated endolysins to access and digest the peptidoglycan (Wang, Smith et al. 2000) in order to release phage progeny. Previous studies have demonstrated that there is a putative holin located upstream of the PlyC endolysin operon in the C1 bacteriophage genome (Nelson, Schuch et al. 2003). The fact that we failed to prove that PlyCB possesses an additional pore formation (i.e. holin-like) function from membrane integrity test, helps us to rule out the hypothesis that PlyCB behaves like a holin upon internalization of PlyC into epithelial cell.

In terms of a structure-function homology relationship, previous work reveals that in the PlyCB octamer, each monomer is comprised of a four-stranded β-sheet capped on each side by a short α-helix. Oligomerization is mediated through

strand/helix hydrogen bonding interactions at each interface (**Figure 3-1a**). Sequence BLAST searches show that PlyCB contains no significant similarity to any other protein in the database. However, structural similarities search using DALI and VAST reveal distant structural similarity between the PlyCB monomer and two type III secretion proteins (PDB 2W0R, and 3BZR), which function to adhere at the surface of a eukaryotic cell to subvert the target cell. Furthermore, we have noted several interesting parallels between PlyC and a family of type III secretion proteins known as the A-B toxins. This family of toxins is so termed because of their two-component protein composition: An A domain comprises the enzymatic "activity" and a ring-shaped homo-oligomers that encompasses the B (binding) domain. A recent crystal structural report on the anthrax toxin, an A-B toxin family member, revealed that an octameric ring-shaped homo-oligomer of the B domain (known as the protective antigen) forms a membrane-spanning channel that allows the A domain (lethal factor and edema factor) to be endocytosed into eukaryotic cell (Kintzer, Thoren et al. 2009). Similarly, PlyC is a multimeric protein consisting of PlyCA, a CHAP/glycosidase activity domain and 8 identical PlyCB subunits which forms an octamer ring that directs binding and is responsible for initial binding to the membrane. It should be noted that PlyC as well as most A-B toxins are phage encoded (Collier 2001; Johnson and Bradshaw 2001; Rossetto, Seveso et al. 2001; Wagner and Waldor 2002; Nelson, Schuch et al. 2006). Therefore, it is rational to consider that PlyC may share some evolutionary relatedness to the A-B toxins, which evolved from ancestral genes common to all phage, such as those in the lytic system.

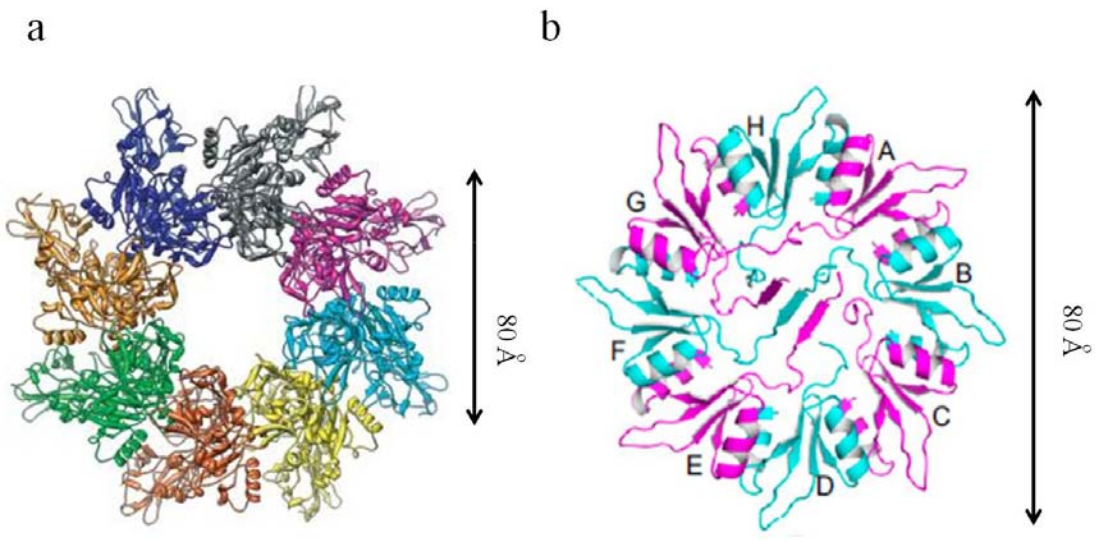

Figure 5-1. Structural view of B domain of the anthrax toxin and PlyCB subunits of the PlyC endolysin

(a) X-ray crystal structure of the B domain of the anthrax toxin in the octameric oligomerization state (PDB 3HVD). Monomer subunit chains are colored uniquely. (b) X-ray crystal structure of PlyCB with monomers colored alternately in magenta/cyan and labeled as A–H (PDB 4F87). Note the similar arrangement between (a) and (b).

Despite the similar structural arrangement and functional patterns we observed between PlyC and members of type III secretion proteins, there are also notable differences between the predicted mechanisms of interaction with the membrane. First, the cell surface receptors for the A-B toxins are either carbohydrates or the carbohydrate portion of gangliosides (Collier 2001; Johnson and Bradshaw 2001; Rossetto, Seveso et al. 2001; Wagner and Waldor 2002), whereas we propose that PlyC specifically and directly interacts with PtdIns and PtdSer on the membrane. Second, in A-B toxins, the A subunit dissociates from the B subunits, translocates through the beta-barrel pore of the B subunits, and enters the cytoplasm while B

subunits remain on the membrane's outer surface. In contrast, the cationic pocket of PlyCB initiates the internalization process, through which both PlyCB and PlyCA (as the PlyC holoenzyme) are internalized via endocytosis. Finally, the fundamental difference in function is that A-B is toxic to eukaryotic cells, however, PlyC is only toxic or lethal to pathogenic group A strepcocci but not eukaryotic cells, which represent a potential therapeutic use.

Future directions

Future work will be focused on biophysically characterizing the interaction between PlyC and the lipid membrane. A collaboration is already in place with Dr. Mathias Lösche at Carnegie Mellon University to study these interactions by surface plasmon resonance to determine the binding affinity, as well as by neutron scattering to probe molecular dynamics of this protein-lipid interaction. In addition, a collaboration is in place with Dr. Travis Gallagher at the National Institute for Standards and Technology to obtain high resolution crystal structure of PlyC in complex with phosphatidylinositol and phosphatidylserine.

Another planned experiment involves demonstration of intracellular killing by PlyC in an *in vivo* model. Our laboratory was recently equipped with a state-of-art *in vivo* imaging system (IVIS), which allows us to follow fluorescent or luminescent labeled streptococci in real time within an animal. Once streptococci colonize and become internalized, treatment with antibiotics will only be able to clear extracellular streptococci due to the inability of antibiotics to internalize into eukaryotic cells. Thus, the intracellular killing efficacy of PlyC against this particular population of

internalized streptococci can be evaluated and monitored in a temporal and spatial manner.

From a translational point of view, the highly efficient trans-membrane action of PlyCB raises the possibility that PlyCB or its derivatives could be developed as a cellular delivery platform. For instance, PlyCA might be replaced by different types of functional enzymatic domains or cargo, such as nanoparticles, radionuclides, quantum dots, or contrast agents. Using PlyCB as a transportation backbone, it will be worthwhile to generate chimerical endolysins that effectively target other traditional intracellular bacterial pathogens, such as *S. aureus* and *Listeria* species. Significantly, another graduate student in the laboratory, Ryan Heselpoth, is currently replacing the PlyC catalytic domains with various orthologous domains. In addition, the fact that internalized PlyCB is primarily associated with the lysosomal compartments can be useful for the delivery of recombinant lysosomal enzymes which are known to be deficient in particular genetic diseases, such as the lysosomal storage disorders.

Therapeutic perspective

The feasibility of using the PlyC endolysin as an effective topical antibacterial agent to eliminate upper respiratory colonization of mice by GAS has been demonstrated (Nelson, Loomis et al. 2001). It has been shown that intracellular bacteria survive not only due to avoiding host cell phagocytosis, but also because the antibiotic concentration in those particular intracellular niches are often too low to be bactericidal. To date, several methods and materials have been developed to enhance the intracellular delivery of antibiotics. In the early stage, several antibiotics were encapsulated into liposomes as drug delivery systems to improve their intracellular

accumulation. Representative studies focused on intracellular *Mycobacterium* (Onyeji, Nightingale et al. 1994), *S. aureus* (Bonventre and Gregoriandis 1978), and *Listeria monocytogenes* (Bakker-Woudenberg, Lokerse et al. 1988). All studies show intracellular efficacy of liposome-entrapped antibiotics was significantly increased and able to reduce the viable colony number compared to free antibiotics. However, drawbacks to liposome-based strategies include stability issues during storage and after administration in biological fluids.

To solve these problems, polymeric nanoparticles were developed as alternative delivery systems to liposomal carriers. With this advanced technique, the stability was improved and a controlled release of the encapsulated antibiotics against intracellular bacteria is achieved. These nanoparticles are primarily designed to transport and release the drugs at lysosomal compartments, where intracellular bacteria primarily reside. Moreover, the polymeric particles were proved to strongly enhance phagocytosis and are suitable for intracellular delivery of antibacterial agents (Lecaroz, Gamazo et al. 2006; Seleem, Munusamy et al. 2009). However, some bacterial pathogens, such as streptococci, have evolved strategies to evade phagolysosomal fusion for degradation, which allows them to survive in the cytosol prior to autophagy and repopulate after inducing apoptosis of the host cell (Kwinn and Nizet 2007). Therefore, target-specific antimicrobials that can go intracellular and possesses intracellular bacteriolytic activity in various compartments such as the cytosol, phagosome, and lysosome will be highly desirable. Our results show that the PlyC endolysin not only meets all of the above requirements, but offers additional advantages including lack of toxicity to host cells, exclusive targeting of pathogenic

GAS, and extreme lytic activity against GAS (10 ng of PlyC is sufficient to sterilize a culture of 10^7 GAS within 5 seconds) (Nelson, Loomis et al. 2001). In addition, our laboratory is currently focused on improving structural stability of PlyC for longer shelf life, since the thermodynamic profile of PlyC is lower than other endolysins (unpublished observation). Previous studies reveal the lack of thermal stability is only observed for the PlyCA domain, whereas the PlyCB octameric ring will not disassemble until temperatures above ~ 90°C (unpublished observation). By directed evolution and rational site-directed mutagenesis, members of the laboratory have already significantly increased the thermostability profile of PlyC for therapeutic use.

Concluding remarks.

It has been suggested that internalization into epithelial cells, along with biofilm formation, are the major mechanisms associated with recurrent streptococcal infection (Ogawa, Terao et al. 2011). Although not part of this dissertation, we recently demonstrated that PlyC retained its bacteriolytic properties against group A streptococcal biofilm bacteria, destroying the biofilm in a layer by layer process (Shen, Koller et al. 2013). In this dissertation, we report for the first time that a bacteriophage-encoded endolysin can effectively eradicate intracellular streptococci and we further elucidate the mechanism of its uptake. Taken together, these data reinforce the potential development of the PlyC endolysin as a topical application to combat refractory streptococcal infection that occurs on the skin or mucous membranes. Additionally, this dissertation provides a rationale to further investigate the intracellular potential of other bacteriophage endolysins for therapeutic application.

Appendices

Materials, methods , and protocols

Contents

A. List of constructs and *E.coli* stocks

B. Molecular cloning

C. Bacterial storage and growth

D. Growth of *E.coli* for expression and purification of PlyC or PlyCB constructs

E. Protein Analysis.

E1 SDS-PAGE for purity analysis

E2 Bradford assay to determine protein concentration

E3 Mass spectrometry to confirm correct mutation

E4 Analytic gel filtration analysis

E5 Infrared spectroscopy

F. Fluorescent-labeling PlyC and mutants

G. Lytic activity of PlyC and its mutants by spectrophotometric lysis assay

H. Immortal epithelial cell culture

I. Primary epithelial cell culture

J. GAS/epithelial cell co-culture assay

K. Confocal microscopy

K1 Low temperature experiments (4°C)

K2 Subcellular localization of internalized PlyCB

K3 Treatment of clathrin-mediated endocytosis inhibitor

K4 Treatment of macropinocytosis inhibitor

K5 Treatment of caveolae-mediated endocytosis inhibitor

K6 Competition assay by glycosaminoglycans

K7 Membrane permeability assay

L. Trypan blue assay

M. Phospholipids screening assay

N. Computational docking

A. List of constructs and *E.coli* stocks

Name	PlyC
Description	Wild-type endolysin encoded by C1 bacteriophage
Plasmid	pBAD 24
Restriction site used	SmaI and HindIII
Expression strain	BL21(DE3)
Antibiotics	Amp^+
Protein sequence	**PlyCA:** SKKYTQQQYEKYLAQPANNTFGLSP QQVADWFMGQAGARPVINSYGVNA SNLVSTYIPKMQEYGVSYTLFLMYT VFEGGGAGNWINHYMYDTGSNGLE CLEHDLQYIHGVWETYFPPALSAPEC YPATEDNAGALDRFYQSLPGRTWGD VMIPSTMAGNAWVWAYNYCVNNQ GAAPLVYFGNPYDSQIDSLLAMGAD PFTGGSITGDGKNPSVGTGNATVSAS SEANREKLKKALTDLFNNNLEHLSG EFYGNQVLNAMKYGTILKCDLTDDG LNAILQLIADVNLQTNPNPDKPTVKS PGQNDLGSGSDRVAANLANAQAQV GKYIGDGQCYAWVGWWSARVCGY SISYSTGDPMLPLIGDGMNAHSIHLG WDWSIANTGIVNYPVGTVGRKEDLR VGAIWCATAFSGAPFYTGQYGHTGII ESWSDTTVTVLEQNILGSPVIRSTYDL NTFLSTLTGLITFK **PlyCB monomer:** SKINVNVENVSGVQGFLFHTDGKES YGYRAFINGVEIGIKDIETVQGFQQIIP SINISKSDVEAIRKAMKK
Protein M.W. (kDa)	114
Protein concentration (mg/ml)	6

Name	PlyCA
Description	Catalytic domain of PlyC
Plasmid	pBAD 24
Restriction site used	SmaI and HindIII
Antibiotics	Amp^+

Protein sequence	SKKYTQQQYEKYLAQPANNTFGLSP QQVADWFMGQAGARPVINSYGVNA SNLVSTYIPKMQEYGVSYTLFLMYT VFEGGGAGNWINHYMYDTGSNGLE CLEHDLQYIHGVWETYFPPALSAPEC YPATEDNAGALDRFYQSLPGRTWGD VMIPSTMAGNAWVWAYNYCVNNQ GAAPLVYFGNPYDSQIDSLLAMGAD PFTGGSITGDGKNPSVGTGNATVSAS SEANREKLKKALTDLFNNNLEHLSG EFYGNQVLNAMKYGTILKCDLTDDG LNAILQLIADVNLQTNPNPDKPTVKS PGQNDLGSGSDRVAANLANAQAQV GKYIGDGQCYAWVGWWSARVCGY SISYSTGDPMLPLIGDGMNAHSIHLG WDWSIANTGIVNYPVGTVGRKEDLR VGAIWCATAFSGAPFYTGQYGHTGII ESWSDTTVTVLEQNILGSPVIRSTYDL NTFLSTLTGLITFK
Protein M.W. (kDa)	50
Protein concentration (mg/ml)	1.7

Name	PlyCB
Description	Octameric cell wall binding subunit of PlyC
Plasmid	pBAD 24
Restriction site used	SmaI and HindIII
Expression strain	BL21(DE3)
Antibiotics	Amp^+
Protein sequence (monomer)	SKINVNVENVSGVQGFLFHTDGKES YGYRAFINGVEIGIKDIETVQGFQQIIP SINISKSDVEAIRKAMKK
Protein M.W. (kDa)	64
Protein concentration (mg/ml)	11.8

Name	$PlyCB_{K23E}$
Description	PlyCB mutant
Plasmid	pBAD 24
Restriction site used	SmaI and HindIII
Expression strain	BL21(DE3)
Antibiotics	Amp^+
Protein sequence (monomer)	SKINVNVENVSGVQGFLFHTDGEESY GYRAFINGVEIGIKDIETVQGFQQIIPS

	INISKSDVEAIRKAMKK
Protein M.W. (kDa)	64
Protein concentration (mg/ml)	15.6

Name	$PlyCB_{R29E}$
Description	PlyCB mutant
Plasmid	pBAD 24
Restriction site used	SmaI and HindIII
Expression strain	BL21(DE3)
Antibiotics	Amp^{+}
Protein sequence (monomer)	SKINVNVENVSGVQGFLFHTDGEESY GYEAFINGVEIGIKDIETVQGFQQIIPS INISKSDVEAIRKAMKK
Protein M.W. (kDa)	64
Protein concentration (mg/ml)	insoluble

Name	$PlyCB_{K59E}$
Description	PlyCB mutant
Plasmid	pBAD 24
Restriction site used	SmaI and HindIII
Expression strain	BL21(DE3)
Antibiotics	Amp^{+}
Protein sequence (monomer)	SKINVNVENVSGVQGFLFHTDGEESY GYRAFINGVEIGIKDIETVQGFQQIIPS INISESDVEAIRKAMKK
Protein M.W. (kDa)	64
Protein concentration (mg/ml)	14.2

Name	$PlyCB_{R66E}$
Description	PlyCB mutant
Plasmid	pBAD 24
Restriction site used	SmaI and HindIII
Expression strain	BL21(DE3)
Antibiotics	Amp^{+}
Protein sequence (monomer)	SKINVNVENVSGVQGFLFHTDGEESY GYRAFINGVEIGIKDIETVQGFQQIIPS INISKSDVEAIEKAMKK
Protein M.W. (kDa)	64
Protein concentration (mg/ml)	14

Name	$PlyCB_{R66K}$
Description	PlyCB mutant
Plasmid	pBAD 24
Restriction site used	SmaI and HindIII
Expression strain	BL21(DE3)
Antibiotics	Amp^{+}
Protein sequence (monomer)	SKINVNVENVSGVQGFLFHTDGEESY GYRAFINGVEIGIKDIETVQGFQQIIPS INISKSDVEAIKKAMKK
Protein M.W. (kDa)	64
Protein concentration (mg/ml)	9.1

Name	$PlyCB_{R66A}$
Description	PlyCB mutant
Plasmid	pBAD 24
Restriction site used	SmaI and HindIII
Expression strain	BL21(DE3)
Antibiotics	Amp^{+}
Protein sequence (monomer)	SKINVNVENVSGVQGFLFHTDGEESY GYRAFINGVEIGIKDIETVQGFQQIIPS INISKSDVEAIAKAMKK
Protein M.W. (kDa)	64
Protein concentration (mg/ml)	22

Name	$PlyCB_{K67E}$
Description	PlyCB mutant
Plasmid	pBAD 24
Restriction site used	SmaI and HindIII
Expression strain	BL21(DE3)
Antibiotics	Amp^{+}
Protein sequence (monomer)	SKINVNVENVSGVQGFLFHTDGEESY GYRAFINGVEIGIKDIETVQGFQQIIPS INISKSDVEAIREAMKK
Protein M.W. (kDa)	64
Protein concentration (mg/ml)	insoluble

Name	$PlyCB_{K70E,K71E}$
Description	PlyCB mutant
Plasmid	pBAD 24
Restriction site used	SmaI and HindIII
Expression strain	BL21(DE3)

Antibiotics	Amp^+
Protein sequence (monomer)	SKINVNVENVSGVQGFLFHTDGEESY GYRAFINGVEIGIKDIETVQGFQQIIPS INISKSDVEAIRKAMEE
Protein M.W. (kDa)	64
Protein concentration (mg/ml)	insoluble

Name	PlyC($PlyCB_{K23E}$)
Description	PlyC mutant
Plasmid	pBAD 24
Restriction site used	SmaI and HindIII
Expression strain	BL21(DE3)
Antibiotics	Amp^+
Protein sequence	**PlyCA:** SKKYTQQQYEKYLAQPANNTFGLSP QQVADWFMGQAGARPVINSYGVNA SNLVSTYIPKMQEYGVSYTLFLMYT VFEGGGAGNWINHYMYDTGSNGLE CLEHDLQYIHGVWETYFPPALSAPEC YPATEDNAGALDRFYQSLPGRTWGD VMIPSTMAGNAWVWAYNYCVNNQ GAAPLVYFGNPYDSQIDSLLAMGAD PFTGGSITGDGKNPSVGTGNATVSAS SEANREKLKKALTDLFNNNLEHLSG EFYGNQVLNAMKYGTILKCDLTDDG LNAILQLIADVNLQTNPNPDKPTVKS PGQNDLGSGSDRVAANLANAQAQV GKYIGDGQCYAWVGWWSARVCGY SISYSTGDPMLPLIGDGMNAHSIHLG WDWSIANTGIVNYPVGTVGRKEDLR VGAIWCATAFSGAPFYTGQYGHTGII ESWSDTTVTVLEQNILGSPVIRSTYDL NTFLSTLTGLITFK **PlyCB monomer:** SKINVNVENVSGVQGFLFHTDGEESY GYRAFINGVEIGIKDIETVQGFQQIIPS INISKSDVEAIRKAMKK
Protein M.W. (kDa)	114
Protein concentration (mg/ml)	6.1

Name	PlyC($PlyCB_{R29E}$)
Description	PlyC mutant

Plasmid	pBAD 24
Restriction site used	SmaI and HindIII
Expression strain	BL21(DE3)
Antibiotics	Amp^+
Protein sequence	**PlyCA:** SKKYTQQQYEKYLAQPANNTFGLSP QQVADWFMGQAGARPVINSYGVNA SNLVSTYIPKMQEYGVSYTLFLMYT VFEGGGAGNWINHYMYDTGSNGLE CLEHDLQYIHGVWETYFPPALSAPEC YPATEDNAGALDRFYQSLPGRTWGD VMIPSTMAGNAWVWAYNYCVNNQ GAAPLVYFGNPYDSQIDSLLAMGAD PFTGGSITGDGKNPSVGTGNATVSAS SEANREKLKKALTDLFNNNLEHLSG EFYGNQVLNAMKYGTILKCDLTDDG LNAILQLIADVNLQTNPNPDKPTVKS PGQNDLGSGSDRVAANLANAQAQV GKYIGDGQCYAWVGWWSARVCGY SISYSTGDPMLPLIGDGMNAHSIHLG WDWSIANTGIVNYPVGTVGRKEDLR VGAIWCATAFSGAPFYTGQYGHTGII ESWSDTTVTVLEQNILGSPVIRSTYDL NTFLSTLTGLITFK **PlyCB monomer:** SKINVNVENVSGVQGFLFHTDGKES YGYEAFINGVEIGIKDIETVQGFQQIIP SINISKSDVEAIRKAMKK
Protein M.W. (kDa)	114
Protein concentration (mg/ml)	insoluble

Name	PlyC($PlyCB_{K59E}$)
Description	PlyC mutant
Plasmid	pBAD 24
Restriction site used	SmaI and HindIII
Expression strain	BL21(DE3)
Antibiotics	Amp^+
Protein sequence	**PlyCA:** SKKYTQQQYEKYLAQPANNTFGLSP QQVADWFMGQAGARPVINSYGVNA SNLVSTYIPKMQEYGVSYTLFLMYT VFEGGGAGNWINHYMYDTGSNGLE CLEHDLQYIHGVWETYFPPALSAPEC YPATEDNAGALDRFYQSLPGRTWGD

	VMIPSTMAGNAWVWAYNYCVNNQ GAAPLVYFGNPYDSQIDSLLAMGAD PFTGGSITGDGKNPSVGTGNATVSAS SEANREKLKKALTDLFNNNLEHLSG EFYGNQVLNAMKYGTILKCDLTDDG LNAILQLIADVNLQTNPNPDKPTVKS PGQNDLGSGSDRVAANLANAQAQV GKYIGDGQCYAWVGWWSARVCGY SISYSTGDPMLPLIGDGMNAHSIHLG WDWSIANTGIVNYPVGTVGRKEDLR VGAIWCATAFSGAPFYTGQYGHTGII ESWSDTTVTVLEQNILGSPVIRSTYDL NTFLSTLTGLITFK **PlyCB monomer:** SKINVNVENVSGVQGFLFHTDGKES YGYRAFINGVEIGIKDIETVQGFQQIIP SINISESDVEAIRKAMKK
Protein M.W. (kDa)	114
Protein concentration (mg/ml)	12

Name	PlyC(PlyCB$_{R66E}$)
Description	PlyC mutant
Plasmid	pBAD 24
Restriction site used	SmaI and HindIII
Expression strain	BL21(DE3)
Antibiotics	Amp^{+}
Protein sequence	**PlyCA:** SKKYTQQQYEKYLAQPANNTFGLSP QQVADWFMGQAGARPVINSYGVNA SNLVSTYIPKMQEYGVSYTLFLMYT VFEGGGAGNWINHYMYDTGSNGLE CLEHDLQYIHGVWETYFPPALSAPEC YPATEDNAGALDRFYQSLPGRTWGD VMIPSTMAGNAWVWAYNYCVNNQ GAAPLVYFGNPYDSQIDSLLAMGAD PFTGGSITGDGKNPSVGTGNATVSAS SEANREKLKKALTDLFNNNLEHLSG EFYGNQVLNAMKYGTILKCDLTDDG LNAILQLIADVNLQTNPNPDKPTVKS PGQNDLGSGSDRVAANLANAQAQV GKYIGDGQCYAWVGWWSARVCGY SISYSTGDPMLPLIGDGMNAHSIHLG WDWSIANTGIVNYPVGTVGRKEDLR VGAIWCATAFSGAPFYTGQYGHTGII

	ESWSDTTVTVLEQNILGSPVIRSTYDL NTFLSTLTGLITFK **PlyCB monomer:** SKINVNVENVSGVQGFLFHTDGKES YGYRAFINGVEIGIKDIETVQGFQQIIP SINISKSDVEAIEKAMKK
Protein M.W. (kDa)	114
Protein concentration (mg/ml)	10

Name	PlyC(PlyCB$_{K70E, K71E}$)
Description	PlyC mutant
Plasmid	pBAD 24
Restriction site used	SmaI and HindIII
Expression strain	BL21(DE3)
Antibiotics	Amp^{+}
Protein sequence	**PlyCA:** SKKYTQQQYEKYLAQPANNTFGLSP QQVADWFMGQAGARPVINSYGVNA SNLVSTYIPKMQEYGVSYTLFLMYT VFEGGGAGNWINHYMYDTGSNGLE CLEHDLQYIHGVWETYFPPALSAPEC YPATEDNAGALDRFYQSLPGRTWGD VMIPSTMAGNAWVWAYNYCVNNQ GAAPLVYFGNPYDSQIDSLLAMGAD PFTGGSITGDGKNPSVGTGNATVSAS SEANREKLKKALTDLFNNNLEHLSG EFYGNQVLNAMKYGTILKCDLTDDG LNAILQLIADVNLQTNPNPDKPTVKS PGQNDLGSGSDRVAANLANAQAQV GKYIGDGQCYAWVGWWSARVCGY SISYSTGDPMLPLIGDGMNAHSIHLG WDWSIANTGIVNYPVGTVGRKEDLR VGAIWCATAFSGAPFYTGQYGHTGII ESWSDTTVTVLEQNILGSPVIRSTYDL NTFLSTLTGLITFK **PlyCB monomer:** SKINVNVENVSGVQGFLFHTDGKES YGYRAFINGVEIGIKDIETVQGFQQIIP SINISKSDVEAIRKAMEE
Protein M.W. (kDa)	114
Protein concentration (mg/ml)	14.5

Name	PlyC(PlyCB$_{K23A}$)
Description	PlyC mutant
Plasmid	pBAD 24
Restriction site used	SmaI and HindIII
Expression strain	BL21(DE3)
Antibiotics	Amp^{+}
Protein sequence	**PlyCA:** SKKYTQQQYEKYLAQPANNTFGLSP QQVADWFMGQAGARPVINSYGVNA SNLVSTYIPKMQEYGVSYTLFLMYT VFEGGGAGNWINHYMYDTGSNGLE CLEHDLQYIHGVWETYFPPALSAPEC YPATEDNAGALDRFYQSLPGRTWGD VMIPSTMAGNAWVWAYNYCVNNQ GAAPLVYFGNPYDSQIDSLLAMGAD PFTGGSITGDGKNPSVGTGNATVSAS SEANREKLKKALTDLFNNNLEHLSG EFYGNQVLNAMKYGTILKCDLTDDG LNAILQLIADVNLQTNPNPDKPTVKS PGQNDLGSGSDRVAANLANAQAQV GKYIGDGQCYAWVGWWSARVCGY SISYSTGDPMLPLIGDGMNAHSIHLG WDWSIANTGIVNYPVGTVGRKEDLR VGAIWCATAFSGAPFYTGQYGHTGII ESWSDTTVTVLEQNILGSPVIRSTYDL NTFLSTLTGLITFK **PlyCB monomer:** SKINVNVENVSGVQGFLFHTDGAES YGYRAFINGVEIGIKDIETVQGFQQIIP SINISKSDVEAIRKAMKK
Protein M.W. (kDa)	114
Protein concentration (mg/ml)	9.2

Name	PlyC(PlyCB$_{K23E, K59E}$)
Description	PlyC mutants
Plasmid	pBAD 24
Restriction site used	SmaI and HindIII
Expression strain	BL21(DE3)
Antibiotics	Amp^{+}
Protein sequence	**PlyCA:** SKKYTQQQYEKYLAQPANNTFGLSP QQVADWFMGQAGARPVINSYGVNA SNLVSTYIPKMQEYGVSYTLFLMYT VFEGGGAGNWINHYMYDTGSNGLE

	CLEHDLQYIHGVWETYFPPALSAPEC YPATEDNAGALDRFYQSLPGRTWGD VMIPSTMAGNAWVWAYNYCVNNQ GAAPLVYFGNPYDSQIDSLLAMGAD PFTGGSITGDGKNPSVGTGNATVSAS SEANREKLKKALTDLFNNNLEHLSG EFYGNQVLNAMKYGTILKCDLTDDG LNAILQLIADVNLQTNPNPDKPTVKS PGQNDLGSGSDRVAANLANAQAQV GKYIGDGQCYAWVGWWSARVCGY SISYSTGDPMLPLIGDGMNAHSIHLG WDWSIANTGIVNYPVGTVGRKEDLR VGAIWCATAFSGAPFYTGQYGHTGII ESWSDTTVTVLEQNILGSPVIRSTYDL NTFLSTLTGLITFK **PlyCB monomer:** SKINVNVENVSGVQGFLFHTDGEESY GYRAFINGVEIGIKDIETVQGFQQIIPS INISESDVEAIRKAMKK
Protein M.W. (kDa)	114
Protein concentration (mg/ml)	4.8

Name	PlyC(PlyCB$_{D21A}$)
Description	PlyC mutant
Plasmid	pBAD 24
Restriction site used	SmaI and HindIII
Expression strain	BL21(DE3)
Antibiotics	Amp^{+}
Protein sequence	**PlyCA:** SKKYTQQQYEKYLAQPANNTFGLSP QQVADWFMGQAGARPVINSYGVNA SNLVSTYIPKMQEYGVSYTLFLMYT VFEGGGAGNWINHYMYDTGSNGLE CLEHDLQYIHGVWETYFPPALSAPEC YPATEDNAGALDRFYQSLPGRTWGD VMIPSTMAGNAWVWAYNYCVNNQ GAAPLVYFGNPYDSQIDSLLAMGAD PFTGGSITGDGKNPSVGTGNATVSAS SEANREKLKKALTDLFNNNLEHLSG EFYGNQVLNAMKYGTILKCDLTDDG LNAILQLIADVNLQTNPNPDKPTVKS PGQNDLGSGSDRVAANLANAQAQV GKYIGDGQCYAWVGWWSARVCGY SISYSTGDPMLPLIGDGMNAHSIHLG

	WDWSIANTGIVNYPVGTVGRKEDLR VGAIWCATAFSGAPFYTGQYGHTGII ESWSDTTVTVLEQNILGSPVIRSTYDL NTFLSTLTGLITFK **PlyCB monomer:** SKINVNVENVSGVQGFLFHTAGKES YGYRAFINGVEIGIKDIETVQGFQQIIP SINISKSDVEAIRKAMKK
Protein M.W. (kDa)	114
Protein concentration (mg/ml)	9.2

Name	PlyCB-His_6
Description	N-term His tag of PlyCB
Plasmid	pBAD 24
Restriction site used	EcoRI and XbaI
Expression strain	BL21(DE3)
Antibiotics	Amp^+
Protein sequence (monomer)	HHHHHHSKINVNVENVSGVQGFLFH TDGKESYGYRAFINGVEIGIKDIETVQ GFQQIIPSINISKSDVEAIRKAMKK
Protein M.W. (kDa)	64
Protein concentration (mg/ml)	0.7

Name	$PlyCB_{K23E}$-His_6
Description	N-term His tag of $PlyCB_{K23E}$
Plasmid	pBAD 24
Restriction site used	EcoRI and XbaI
Expression strain	BL21(DE3)
Antibiotics	Amp^+
Protein sequence (monomer)	HHHHHHSKINVNVENVSGVQGFLFH TDGEESYGYRAFINGVEIGIKDIETVQ GFQQIIPSINISKSDVEAIRKAMKK
Protein M.W. (kDa)	72
Protein concentration (mg/ml)	insoluble

Name	$PlyCB_{K59E}$-His_6
Description	N-term His tag of $PlyCB_{K59E}$
Plasmid	pBAD 24
Restriction site used	EcoRI and XbaI
Expression strain	BL21(DE3)
Antibiotics	Amp^+

Protein sequence (monomer)	HHHHHHSKINVNVENVSGVQGFLFH TDGKESYGYRAFINGVEIGIKDIETVQ GFQQIIPSINISESDVEAIRKAMKK
Protein M.W. (kDa)	72
Protein concentration (mg/ml)	1.1

Name	$PlyCB_{R66E}$-His_6
Description	N-term His tag of $PlyCB_{R66E}$
Plasmid	pBAD 24
Restriction site used	EcoRI and XbaI
Expression strain	BL21(DE3)
Antibiotics	Amp^+
Protein sequence (monomer)	HHHHHHSKINVNVENVSGVQGFLFH TDGKESYGYRAFINGVEIGIKDIETVQ GFQQIIPSINISKSDVEAIEKAMKK
Protein M.W. (kDa)	72
Protein concentration (mg/ml)	1.8

Site directed single mutation are highlighted as yellow.

B. Molecular cloning

PCR and subcloning were performed according to Molecular Cloning (MacCallum 2000). Site directed mutagenesis was conducted per manufacturer (Affymetrix, Santa Clara, CA) protocols. All constructs were verified by DNA sequencing before being transformed into expression strains BL21(DE3).

C. Bacterial storage and growth

Streptococci were routinely grown in THY medium (Todd-Hewitt broth supplemented with 1% [wt/vol] yeast extract.

A single colony of DH5α or BL21(DE3) strain containing the correct construct was inoculated and grown in LB-Miller (Luria broth containing 10 g/L NaCl) medium with 100 μg/ml ampicillin. The overnight bacteria was pelleted and

resuspended in fresh LB with 1/3 volume of 80% glycerol before being stored in a -80°C freezer.

D. Growth of *E.coli* for expression and purification of PlyC or PlyCB constructs

- Grow pre-culture by inoculating 10 μl frozen BL21(DE3) bacteria stock into 100mL overnight into LB media with ampicillin (100 μg/ml). Shake at 250 rpm, 37ºC for overnight.
- Dilute the pre-culture into 2 flasks of 1.5L LB-medium at 1: 30 ratio. Shake at 250 rpm, 37ºC overnight.
- When OD_{600nm} (the cell density) reaches 1.2, supplements with a final concentration of 0.25% arabinose to induce protein expression at 37ºC (26ºC for His-tag PlyCB constructs) overnight.
- Harvest the cells by centrifugation at 6,000 rpm for 20 min at 4ºC
- Resuspend the pellets in PBS (50ml per 1.5L culture) and add a final concentration of 1mM phenylmethanesulfonylfluoride (PMSF), a protease inhibitor.
- Pre-chill the cell suspension on ice water for 10min, then sonicate at 30% duty cycle, power level 7,10 min.
- Centrifuge at 17,000 rpm for 1h at 4ºC to separate the supernatant from pellet.
- Load supernatant through ceramic hydroxyapatite (CHA) column
- Run 1 column volume (CV) of 250mM phosphate buffer (pH 7.2) to wash off non-specific binding proteins to CHA.

- Elute PlyC or PlyCB with 1.5 CV of 1M phosphate buffer (pH 7.2).
- Dialyze the PlyC or PlyCB sample against 20mM phosphate and 100mM NaCl buffer at 4ºC overnight.
- Inject the dialyzed PlyC sample through a 26/60 S200 gel filtration column controlled by an AKTA FPLC and collect the fractions corresponding to the dominant peak for further SDS-PAGE analysis.
- Purified enzymes were routinely stored in PBS at 4°C and were stable for several months.

E. Protein Analysis

E1 SDS-PAGE for purity analysis

- Prepare loading samples by mixing 5 µl protein and 5 µl 2x Laemmli sample buffer, with 0.5 µM β-mercaptoethanol.
- Heat samples at 100 ºC for 5 min.
- Load 10 µl sample as well as marker into each well of a 12.5% mini gel for protein electrophoresis at 250 volts for 35 min.
- Stain the gel with Coomassie blue solution and destain with the destain solution.

Coomassie blue stain

50% ethanol	50 mL
0.25% Coomassie R250	0.31 g
40% H_2O	40 mL
10% Acetic acid	10 mL

Total	100 mL

Destain solution

5% ethanol	25 mL
7.5% acetic acid	37.5 mL
87.5% H_2O	447.5 mL
Total	500 mL

E2 Bradford assay to determine protein concentration

- Prepare a series of diluted bovine serum albumin (BSA) with 0.15 M NaCl buffer to final concentrations of 0 (blank = NaCl buffer only), 250, 500, 750 and 1000 µg/ml.
- Add 20 µL of each of the above to 1mL Bradford solution (BIO-RAD Inc. CA, USA)in a cuvette spectrophotometer, wait 5 min and then read at to a wavelength of 595 nm and generate a standard curve based on the absorbance and the known concentration.
- Repeat the step 2 with PlyC samples to obtain the absorbance, which will be simultaneously converted to concentration based on the standard curve created by step 2.

E3 Mass spectrometry to confirm correct mutation

Matrix solution:

20 mg/mL sinapinic acid

50% acetonitrile

0.1% trifluoroacetic acid

Mix well and store in aliquots at -20°C

- Mix 1 μl protein sample and 1 μl matrix solution on a 100-well sample plate. The protein solution should be at least 1 mg/ml and with a very low ionic concentration.
- Put the sample plate at 37°C with circular air to allow the drop to dry faster.
- Insert the plate into the mass spectrophotometer and acquire data.
- Compare the mass spec peak position of mutants with the wild-type PlyCB (note that only PlyCB can be detected with mass spec).

E4 Analytic gel filtration analysis

Purified PlyC or mutants were injected into Superose 12 (GE Healthcare), a prepacked gel filtration column with high resolution on FPLC system. Run with PBS at a flow rate of 0.5 mL/min. Collect the fraction that corresponding to the dominant peak for SDS-PAGE analysis.

E5 Infrared spectroscopy

Samples of PlyCB or mutants were placed in a 7 μm Biotools Biocell and transmission infrared spectra were collected with an MCT detector in a Nikon Hyperion microscope with a Bruker Vertex 80 FTIR spectrometer. 480 scans were taken for both background and sample spectra. Contributions from water vapor were subtracted and secondary structure was evaluated using Bruker's OPUS 6.5 software.

F. Fluorescent-labeling PlyC and mutants

5 mg of each of purified PlyC, PlyCA, PlyCB or indicated mutants was reacted with the carboxylic acid, succinimidyl ester of Alexa Fluor 555, or Alexa Fluor 488 (Molecular Probes) according to the manufacturer's instructions. Unreacted dye was removed from the labeled protein by application to a 5-ml HiTrap desalting column (GE Healthcare) equilibrated with PBS. Cross-linked protein samples were subjected to analytical gel filtration on a Superose 12 column (GE Healthcare) calibrated with gel-filtration standards (BIO-RAD Inc. CA, USA).

G. Lytic activity of PlyC and PlyC mutants by spectrophotometric lysis assay

S. pyogenes (strain D471) was grown overnight at 37°C, washed in PBS, and resuspended to the desired concentration with the optical density OD_{600nm} of 1.0 determined by spectrophotometer. 100 µl containing D471 was mixed with 100 µL of purified PlyC or mutants (1 µg) in a 96 well plate. The OD_{600} was measured on a SpectraMax 190 (Molecular Devices) every 15 sec over a 20 min time period to monitor OD changes that correlate to lysis of the bacteria. PlyC mutants' activity was normalized against wild-type PlyC endolysin which represented 100% activity in the 20 min assay.

H. Immortal epithelial cell culture

Hep-2 (Human Larynx Carcinoma cell line, CCL-23) cells were obtained from ATCC and cells were routinely grown in Eagle's Minimum Essential Medium supplemented with 10% (v/v) fetal bovine serum (FBS). A549 (Human Lung Carcinoma cell line, CCL-185) were cultured in F-12K medium supplemented with 10% FBS at 37ºC , 5% CO_2 and 95% relative humidity.

I. Primary epithelial cell culture

The experimental protocol received Institutional Review Board approvals from both the Rockefeller University (VAF-0621-1207) and the Weill Cornell Medical College (nos. 0803009695 and 0806009857) and individual patient consent for the use of tissue in research applications was obtained prior to the surgical procedure. Human primary tonsil epithelial cells were isolated and grown in Dulbecco's modified Eagles medium (DMEM) (Gibco BRL, Grand Island, NY, USA) supplemented with 10% FBS and antibiotic / anti-mycotic cocktail (penicillin [100 µg/ml], streptomycin [100 µg/ml], amphotericin B [2.5 µg/ml].

J. Streptococci/epithelial cell co-culture assay

In order to evaluate the intracellular bacteriolytic efficacy of TAT-labeled endolysins against internalized GAS, we first established a co-culture assay to evaluate the rate of GAS adherence and invasion. In this model, epithelial cells were grown to 80% confluent monolayers in 24-well tissue culture plates (approximately 2 x 10^5 cells/well). Overnight pathogenic GAS strain D471 was washed in sterile phosphate-buffered saline (PBS), resuspended in serum-free media, and the concentration was adjusted to ~2 x 10^7 colony forming units (CFU) and incubated with epithelial cells at a multiplicity of infection (MOI) = 100 bacterial cells/ one epithelial cell for 1 hour. Next, each well was washed 3x in PBS and 100 µl of a 0.25% trypsin-0.02% EDTA solution was added to each well to detach cells from the bottom of wells. Then, 400 µl of a 0.025% Triton X-100 solution in PBS was added to lyse the epithelial cells. Ruptured cells were visible within 5-10 minutes. Finally, the lysis solution was serially diluted and plated on THY agar plates for enumeration

of viable CFUs, which represent both adhered and internalized streptococci. For determination of internalized cell counts, 10 μg/ml penicillin and 200 μg/ml gentamicin was added to the co-culture for 1 hour prior to lysis to kill non-adherent and adherent but not internalized bacterial cells. These antibiotics are not taken up by the epithelial cells so internalized bacteria can be serially diluted and plated on blood agar plates for enumeration after epithelial cell lysis. Thus, we can truly differentiate non adherent vs. adherent vs. internalized GAS. To determine the efficacy of endolysins for eliminating internalized GAS, post-antibiotic treated co-cultures were washed 3x in PBS and incubated with endolysin for one hour before lysis and further enumeration of recovered GAS colonies.

K. Confocal microscopy

Epithelial cells were seeded onto 12-mm^2 cover slips in 24-well tissue culture plates. When reaching 80% confluence, cells were washed twice with PBS prior to incubation with 20 μg/ml AlexaFluor labeled PlyC, PlyCB or mutants in serum-free medium for 30 min. The cells were again washed three times with PBS, fixed by 4% paraformaldehyde (PFA), and mounted with ProLong® Gold Antifade Reagent with 4',6-diamidino-2-phenylindole (DAPI) on glass slide for microscopic examination using a Carl Zeiss 710 inverted microscope in combination with the Zeiss Argon laser scanning confocal imaging system. Images and z-stack analysis were obtained with a 100x/1.7 objective lens, analyzed by Zen 2010 digital imaging software (Carl Zeiss).

K1 Low temperature experiments (4°C)

Cells were washed three times with ice cold PBS prior to incubation with 20 μg/ml AlexaFluor labeled PlyCB in a refrigerator (4 °C) for 30 min.

K2 Subcellular localization of internalized PlyCB

For the observation of intracellular distribution of internalized PlyCB, cells were transfected with CellLight® early endsome-GFP (green), CellLight® lysosome-RFP (red), or CellLight® actin-GFP (green) 24 hours prior to counter staining with 20 μg/ml PlyCB-Alexa555, or PlyCB-Alexa488 for 30 min, respectively. The cells were then washed with PBS twice, fixed by 4% PFA, and then mounted with ProLong® Gold Antifade Reagent with DAPI on a glass slide. Finally, the fluorescence distribution was acquired by confocal microscopy.

K3 Treatment of clathrin-mediated endocytosis inhibitor

Cells on the coverslip were washed with PBS and pretreated with 50 μM monodansylcadaverine (MDC) or medium only as a control at 37°C for 30 min, then washed with PBS twice and incubated with 20 μg/ml PlyCB-Alexa555 in the presence MDC for additional 30 min. The cells were then washed with PBS twice and fixed by 4% PFA. Followed by another 2x PBS wash, cells were permeablized with 0.02% Triton x-100 for 15 min, washed with PBS twice and incubated with FITC Mouse Anti-Human CD71 (Transferrin Receptor, 1 μg/mL in 1% BSA-PBS) for 30 min. After another 2X washing with PBS, cells were mounted with ProLong® Gold Antifade Reagent with DAPI on a glass slide for confocal microscopy.

K4 Treatment of macropinocytosis inhibitor

Cells were washed with PBS and pretreated with 0.5 μM CytD or medium only as a control at 37°C for 30 min followed by a 2X PBS wash and incubated with 20 μg/ml PlyCB-Alexa555 in the presence of CytD for additional 30 min. The cells were then washed with PBS twice and fixed by 4% PFA. Following another 2x PBS

wash, cells were incubated with 5 μg/ml AlexaFluor®488 Phalloidin (green) to stain the actin filaments of cytoskeleton, then washed with PBS twice and mounted with ProLong® Gold Antifade Reagent with DAPI on a glass slide for confocal microscopy.

Alternatively, cells were washed with PBS and pretreated with 3 mM amiloride or 0.5 μM wortmannin at 37°C for 30 min then washed with PBS twice and incubated with 20 μg/ml PlyCB-Alexa488 or dextran-FITC (control marker for macropinocytosis) in the presence of amiloride or wortmannin for additional 30 min. The cells were then washed with PBS twice and fixed by 4% PFA and mounted with ProLong® Gold Antifade Reagent with DAPI on a glass slide for confocal microscopy.

K5 Treatment of caveolae-mediated endocytosis inhibitor

Cells were washed with PBS and pretreated with 1 μg/ml Filipin III (which inhibits caveolar endocytosis) at 37°C for 30 min, then washed with PBS twice and incubated with 20 μg/ml PlyCB-Alexa488 in the presence Filipin III for additional 30 min. Followed by another 2x PBS wash, cells were incubated with 5 μg/ml AlexaFluor555 cholera toxin subunit B (red) for 30 min to stain lipid raft domains. Then the cells were washed with PBS twice and fixed by 4% PFA and mounted with ProLong® Gold Antifade Reagent with DAPI on a glass slide for confocal microscopy.

K6 Competition assay by glycosaminoglycans

Cells were pre-treated with 50 μg/ml of Chondroitin sulfate-B, 100 IU/mL of heparin, 20 mIU/mL of chondroitinase ABC or 5 mIU/mL of Heparinase III for one

hour prior to incubation with PlyCB-Alexa555 before fixed and mounted with ProLong® Gold Antifade Reagent with DAPI on a glass slide for confocal microscopy.

K7 Fluorescent membrane permeability assay

Cells were either permeablized with 0.02% Triton X-100 (positive control) or incubated with 100 μg/ml PlyC at 37°C for 30 min, washed with PBS twice and fixed by 4% PFA and mounted with ProLong® Gold Antifade Reagent with DAPI on a glass slide for confocal microscopy.

L. Trypan blue assay

Cells were seeded into 24-well tissue culture plates. When 80% confluent, cells were washed twice with PBS prior to incubation with various concentrations (0, 2, 100 μg/ml) of PlyC at 37°C for 30 min. Next, cells were washed 3x in PBS and 100 μl of a 0.25% trypsin-0.02% EDTA solution was added to each well to detach cells from the bottom of wells. The trypsinized cells were mixed with 1:1 [vol/vol] with a trypan blue solution (Thermo Scientific) at 37°C for 30 min, and then counted in a haemocytometer for total number of cells and viability.

M. Phospholipids screening assay

Phospholipids screening assay is a protein-lipid overlay technique combined with Western blot that is designed specifically for identification of phosphoinositide-protein interactions. The assay (Invitrogen, Carlsbad, CA) is based on a nitrocellulose membrane on which 15 distinct phospholipids pre-spotted. Manufacture's protocol is slightly modified and shown as follows:

- Block the membrane. Use TBS-T + 3% fatty acid–free BSA, and gently agitate for one hour at room temperature.
- Incubate the membrane. Incubate using 1 μg/ml of PlyCB-His_6, $PlyCB_{K59E}$-His_6, or $PlyCB_{R66E}$-His_6 in 25 ml of TBS-T + 3% fatty acid–free BSA for 20 hours at room temperature.
- Wash the membrane. Wash the membrane with TBS-T + 3% fatty acid–free BSA three times using gentle agitation for ten minutes each time.
- Primary antibody. Incubate the membrane with 1:1000 (0.1μg/ml) His Tag monoclonal antibody (GeneScript) for 4 hours at room temperature.
- Wash the membrane. Wash the membrane with TBS-T + 3% fatty acid–free BSA three times using gentle agitation for ten minutes each time.
- Secondary antibody. Incubate the membrane with 1:2000 (0.5μg/ml) goat anti-mouse IgG antibody (H&L) [HRP] (GeneScript) for 4 hours at room temperature.
- Wash the membrane. Wash the membrane with TBS-T + 3% fatty acid–free BSA three times using gentle agitation for ten minutes each time.
- Detection. SuperSignal™ West Pico Chemiluminescent Substrate kit (Thermo Scientific) was used to detect the signal on the PIP membrane accompany with mini-medical series 90 film developer manufactured by AFP IMAGING (Elmsford, NY, USA).

TBS-T: 10 mM Tris–HCl, pH 8.0, 150 mM NaCl, containing 0.1% (v/v) Tween® 20 detergent

TBS-T + 3% BSA: 100 mL of TBS-T plus 3 g of fatty acid–free bovine serum albumin (BSA)

N. Computational docking

The binding of Phosphatidylinositol and Phosphatidylserine to a PlyCB monomer was computationally modeled using the following procedure. The corresponding structures of ligands and protein were obtained from crystal structures (PDB code: 1UW5, 3BIB, and 4F87 respectively), and were prepared using the UCSF Chimera package (Pettersen, Goddard et al. 2004) to add polar hydrogen atoms and partial charges. The long ends of the fatty acid chains were trimmed off to avoid unnecessary complication in the modeling. Then the DOCK6.6 suite of programs (Lang, Brozell et al. 2009) was used for the molecular docking. In brief, the DOCK6.6 suite finds the potential binding sites and represents them as spheres. It then searches reasonable ligand binding poses by matching the ligand atoms with the binding site spheres, evaluated by a set of force-field based scoring functions. The flexibility of ligand is well treated in the fragmentation-fashioned search algorithms. The computationally generated potential candidates were then further scrutinized manually to avoid unreasonable artifacts. The best fit results were demonstrated using the PyMOL 0.99rc6 software (DeLano Scientific LLC, Palo Alto, CA).

Non-Dissertation Publications

1. J. Hsu, D. Serrano, T. Bhowmick, K. Kumar, **Shen Y.,** Y.C. Kuo, C. Garnacho, S. Muro. (2011) Enhanced Endothelial Delivery and Biochemical Effects of α Galactosidase by ICAM-1-Targeted Nanocarriers for Fabry Disease, J. Control Release 149 323–331.
2. **Shen, Y**., Mitchell, M., Donovan, D.M., & Nelson, D.C. (2012) Phage-based Enzybiotics. In S. Abedon & P. Hyman (eds.): Bacteriophages in Health and Disease. CABI Press, pp. 217-239.
3. McGowan, S., Buckle, A.M., Mitchell, M.S., Hoopes, J.T., Gallagher, D.T., Heselpoth, R.D, **Shen, Y.**, Reboul, C.F., Law, R.H.P, Fischetti, V.A., Whisstock, J.C., & Nelson, D.C. (2012) X-ray Crystal Structure of the Streptococcal Specific Phage Lysin PlyC. Proc. Natl. Acad. Sci. U.S.A 109: 12752-12757.
4. Zhang, J., **Shen, Y.,** May, S.L., Nelson, D.C., & Li, S. (2012) Ratiometric Fluorescence Detection of Pathogenic Bacteria Resistant to Broad-Spectrum β-Lactam Antibiotics. Angew. Chem. Int. Ed. Engl. 124:1901-1904.
5. **Shen, Y.**, T. Köller, K. Bernd., Nelson, D.C. (2013) Rapid Degradation of *Streptococcus pyogenes* Biofilms by PlyC, a Bacteriophage-encoded Endolysin. J.Antimicrob Chemother. 1.doi:10.1093/jac/dkt104, first published online: April 4, 2013
6. Bales PM, Renke EM, May SL, **Shen Y**, Nelson DC (2013) Purification and Characterization of Biofilm-Associated EPS Exopolysaccharides from ESKAPE Organisms and Other Pathogens. PLoS ONE 8(6): e67950. doi:10.1371/journal.pone.0067950
7. Shen, Y., Chandrakanth, R.K., Donovan, D.M., Nelson, D.C. Comparing Therapeutic Efficacy of Bacteriophage GRCS, LysK, and Lysostaphin in a Model of Systematic Methicillin-resistant *Staphylococcus aureus* Infection. [submitted]

Bibliography

Abedon, S. T. (2011). "Lysis from without." Bacteriophage **1**(1): 46-49.

Alisky, J., K. Iczkowski, et al. (1998). "Bacteriophages show promise as antimicrobial agents." J Infect **36**(1): 5-15.

Arnoldi, M., M. Fritz, et al. (2000). "Bacterial turgor pressure can be measured by atomic force microscopy." Phys Rev E Stat Phys Plasmas Fluids Relat Interdiscip Topics **62**(1 Pt B): 1034-1044.

Bakker-Woudenberg, I. A., A. F. Lokerse, et al. (1988). "Effect of lipid composition on activity of liposome-entrapped ampicillin against intracellular *Listeria monocytogenes*." Antimicrob Agents Chemother **32**(10): 1560-1564.

Baldassarri, L., R. Creti, et al. (2006). "Therapeutic failures of antibiotics used to treat macrolide-susceptible *Streptococcus pyogenes* infections may be due to biofilm formation." J Clin Microbiol **44**(8): 2721-2727.

Bateman, A. and N. D. Rawlings (2003). "The CHAP domain: a large family of amidases including GSP amidase and peptidoglycan hydrolases." Trends Biochem. Sci. **28**: 234-237.

Beachey, E. H. and W. A. Simpson (1982). "The adherence of group A streptococci to oropharyngeal cells: the lipoteichoic acid adhesin and fibronectin receptor." Infection **10**(2): 107-111.

Becker, S. C., J. Foster-Frey, et al. (2008). "The phage K lytic enzyme LysK and lysostaphin act synergistically to kill MRSA." FEMS Microbiol Lett **287**(2): 185-191.

Bevers, E. M., P. Comfurius, et al. (1999). "Lipid translocation across the plasma membrane of mammalian cells." Biochim Biophys Acta **1439**(3): 317-330.

Bonventre, P. F. and G. Gregoriandis (1978). "Killing of intraphagocytic *Staphylococcus aureus* by dihydrostreptomycin entrapped within liposomes." Antimicrob Agents Chemother **13**(6): 1049-1051.

Borysowski, J. and A. Gorski (2010). "Fusion to cell-penetrating peptides will enable lytic enzymes to kill intracellular bacteria." Med Hypotheses **74**(1): 164-166.

Borysowski, J., B. Weber-Dabrowska, et al. (2006). "Bacteriophage endolysins as a novel class of antibacterial agents." Exp Biol Med (Maywood) **231**(4): 366-377.

Briers, Y., M. Schmelcher, et al. (2009). "The high-affinity peptidoglycan binding domain of *Pseudomonas* phage endolysin KZ144." Biochem Biophys Res Commun **383**(2): 187-191.

Briers, Y., G. Volckaert, et al. (2007). "Muralytic activity and modular structure of the endolysins of *Pseudomonas aeruginosa* bacteriophages phiKZ and EL." Mol Microbiol **65**(5): 1334-1344.

Calderon, F. and H. Y. Kim (2008). "Detection of intracellular phosphatidylserine in living cells." J Neurochem **104**(5): 1271-1279.

Carapetis, J. R., A. C. Steer, et al. (2005). "The global burden of group A streptococcal diseases." Lancet Infect Dis **5**(11): 685-694.

CDC. (2008). "Group A Streptococcal (GAS) Disease."

Celia, L. K., D. Nelson, et al. (2008). "Characterization of a bacteriophage lysin (Ply700) from *Streptococcus uberis*." Vet Microbiol **130**(1-2): 107-117.

Cheng, Q. and V. A. Fischetti (2007). "Mutagenesis of a bacteriophage lytic enzyme PlyGBS significantly increases its antibacterial activity against group B streptococci." Appl Microbiol Biotechnol **74**(6): 1284-1291.

Cheng, Q., D. Nelson, et al. (2005). "Removal of group B streptococci colonizing the vagina and oropharynx of mice with a bacteriophage lytic enzyme." Antimicrob. Agents Chemother. **49**: 111-117.

Clemens, D. L. and M. A. Horwitz (1996). "The *Mycobacterium tuberculosis* phagosome interacts with early endosomes and is accessible to exogenously administered transferrin." J Exp Med **184**(4): 1349-1355.

Clokie, M. R., A. D. Millard, et al. (2011). "Phages in nature." Bacteriophage **1**(1): 31-45.

Collier, R. J. (2001). "Understanding the mode of action of diphtheria toxin: a perspective on progress during the 20th century." Toxicon **39**: 1793-1803.

Conley, J., M. E. Olson, et al. (2003). "Biofilm formation by group a streptococci: is there a relationship with treatment failure?" J Clin Microbiol **41**(9): 4043-4048.

Croux, C., C. Ronda, et al. (1993). "Interchange of functional domains switches enzyme specificity: construction of a chimeric pneumococcal-clostridial cell wall lytic enzyme." Molec. Microbiol. **9**: 1019-1025.

Cunningham, M. W. (2000). "Pathogenesis of group A streptococcal infections." Clin Microbiol Rev **13**(3): 470-511.

d'Herelle, F. H. (1917). "Sur un microbe invisible antagoniste des bacilles dysenteriques." Comptes Rendu. Acad. Sci. **165**: 373-375.

Dale, J. B., T. A. Penfound, et al. (2011). "New 30-valent M protein-based vaccine evokes cross-opsonic antibodies against non-vaccine serotypes of group A streptococci." Vaccine **29**(46): 8175-8178.

Daniel, A., C. Euler, et al. (2010). "Synergism Between a Novel Chimeric Lysin and Oxacillin Protects Against Infection by Methicillin-Resistant *Staphylococcus aureus*." Antimicrob Agents Chemother.

Daniel, A., C. Euler, et al. (2010). "Synergism between a novel chimeric lysin and oxacillin protects against infection by methicillin-resistant *Staphylococcus aureus*." Antimicrob Agents Chemother **54**(4): 1603-1612.

Darouiche, R. O. and R. J. Hamill (1994). "Antibiotic penetration of and bactericidal activity within endothelial cells." Antimicrob Agents Chemother **38**(5): 1059-1064.

Dias-Baruffi, M., H. Zhu, et al. (2003). "Dimeric galectin-1 induces surface exposure of phosphatidylserine and phagocytic recognition of leukocytes without inducing apoptosis." J Biol Chem **278**(42): 41282-41293.

Diaz, E., R. Lopez, et al. (1990). "Chimeric phage-bacterial enzymes: A clue to the modular evolution of genes." Proc. Natl. Acad. Sci. USA **87**: 8125-8129.

Diaz, E., R. Lopez, et al. (1991). "Chimeric pneumococcal cell wall lytic enzymes reveal important physiological and evolutionary traits." J Biol Chem **266**(9): 5464-5471.

Djurkovic, S., J. M. Loeffler, et al. (2005). "Synergistic killing of *Streptococcus pneumoniae* with the bacteriophage lytic enzyme Cpl-1 and penicillin or gentamicin depends on the level of penicillin resistance." Antimicrob Agents Chemother **49**(3): 1225-1228.

Doherty, G. J. and H. T. McMahon (2009). "Mechanisms of endocytosis." Annu Rev Biochem **78**: 857-902.

Donovan, D. M. (2007). "Bacteriophage and peptidoglycan degrading enzymes with antimicrobial applications." Recent Pat Biotechnol **1**(2): 113-122.

Donovan, D. M., J. Foster-Frey, et al. (2006). "The cell lysis activity of the *Streptococcus agalactiae* bacteriophage B30 endolysin relies on the cysteine, histidine-dependent amidohydrolase/peptidase domain." Appl Environ Microbiol **72**(7): 5108-5112.

Duchardt, F., M. Fotin-Mleczek, et al. (2007). "A comprehensive model for the cellular uptake of cationic cell-penetrating peptides." Traffic **8**(7): 848-866.

Ellen, R. P. and R. J. Gibbons (1972). "M protein-associated adherence of Streptococcus pyogenes to epithelial surfaces: prerequisite for virulence." Infect Immun **5**(5): 826-830.

Ellington, J. K., S. S. Reilly, et al. (1999). "Mechanisms of *Staphylococcus aureus* invasion of cultured osteoblasts." Microb Pathog **26**(6): 317-323.

Entenza, J. M., J. M. Loeffler, et al. (2005). "Therapeutic effects of bacteriophage Cpl-1 lysin against *Streptococcus pneumoniae* endocarditis in rats." Antimicrob Agents Chemother **49**(11): 4789-4792.

Facklam, R. (2002). "What happened to the streptococci: overview of taxonomic and nomenclature changes." Clin Microbiol Rev **15**(4): 613-630.

Fadeel, B. and D. Xue (2009). "The ins and outs of phospholipid asymmetry in the plasma membrane: roles in health and disease." Crit Rev Biochem Mol Biol **44**(5): 264-277.

Falcone, S., E. Cocucci, et al. (2006). "Macropinocytosis: regulated coordination of endocytic and exocytic membrane traffic events." J Cell Sci **119**(Pt 22): 4758-4769.

Fenton, M., P. G. Casey, et al. (2010). "The truncated phage lysin CHAP(k) eliminates *Staphylococcus aureus* in the nares of mice." Bioeng Bugs **1**(6): 404-407.

Fischetti, V. A. (2005). "Bacteriophage lytic enzymes: novel anti-infectives." Trends Microbiol **13**(10): 491-496.

Fischetti, V. A. (2008). "Bacteriophage lysins as effective antibacterials." Curr Opin Microbiol **11**(5): 393-400.

Fischetti, V. A. (2010). "Bacteriophage endolysins: a novel anti-infective to control Gram-positive pathogens." Int J Med Microbiol **300**(6): 357-362.

Fischetti, V. A., E. C. Gotschlich, et al. (1971). "Purification and physical properties of group C streptococcal phage-associated lysin." J. Exp. Med. **133**(5): 1105-1117.

Fluckiger, U., K. F. Jones, et al. (1998). "Immunoglobulins to group A streptococcal surface molecules decrease adherence to and invasion of human pharyngeal cells." Infect Immun **66**(3): 974-979.

Fonseca, S. B., M. P. Pereira, et al. (2009). "Recent advances in the use of cell-penetrating peptides for medical and biological applications." Adv Drug Deliv Rev **61**(11): 953-964.

Fretz, M. M., N. A. Penning, et al. (2007). "Temperature-, concentration- and cholesterol-dependent translocation of L- and D-octa-arginine across the plasma and nuclear membrane of CD34+ leukaemia cells." Biochem J **403**(2): 335-342.

Gaeng, S., S. Scherer, et al. (2000). "Gene cloning and expression and secretion of *Listeria monocytogenes* bacteriophage-lytic enzymes in *Lactococcus lactis*." Appl Environ Microbiol **66**(7): 2951-2958.

Garcia, E., J. L. Garcia, et al. (1988). "Molecular evolution of lytic enzymes of *Streptococcus pneumoniae* and its bacteriophages." Proc. Natl. Acad. Sci. USA **85**: 914-918.

Garcia, J. L., E. Garcia, et al. (1987). "Cloning, purification, and biochemical characterization of the pneumococcal bacteriophage Cp-1 lysin." J Virol **61**(8): 2573-2580.

Garcia, P., J. L. Garcia, et al. (1990). "Modular organization of the lytic enzymes of *Streptococcus pneumoniae* and its bacteriophages." Gene **86**: 81-88.

Garcia, P., B. Martinez, et al. (2010). "Synergy between the phage endolysin LysH5 and nisin to kill *Staphylococcus aureus* in pasteurized milk." Int J Food Microbiol **141**(3): 151-155.

Gerova, M., N. Halgasova, et al. (2011). "Endolysin of bacteriophage BFK20: evidence of a catalytic and a cell wall binding domain." FEMS Microbiol Lett **321**(2): 83-91.

Gilmer, D. B., J. E. Schmitz, et al. (2013). "Novel Bacteriophage Lysin with Broad Lytic Activity Protects Against Mixed Infection by *Streptococcus pyogenes* and Methicillin-Resistant *Staphylococcus aureus*." Antimicrob Agents Chemother.

Goodfellow, A. M., M. Hibble, et al. (2000). "Distribution and antigenicity of fibronectin binding proteins (SfbI and SfbII) of *Streptococcus pyogenes* clinical isolates from the northern territory, Australia." J Clin Microbiol **38**(1): 389-392.

Grandgirard, D., J. M. Loeffler, et al. (2008). "Phage lytic enzyme Cpl-1 for antibacterial therapy in experimental pneumococcal meningitis." J Infect Dis **197**(11): 1519-1522.

Greco, R., L. De Martino, et al. (1995). "Invasion of cultured human cells by *Streptococcus pyogenes*." Res Microbiol **146**(7): 551-560.

Gu, J., W. Xu, et al. (2011). "LysGH15, a novel bacteriophage lysin, protects a murine bacteremia model efficiently against lethal methicillin-resistant *Staphylococcus aureus* infection." J Clin Microbiol **49**(1): 111-117.

Gump, J. M. and S. F. Dowdy (2007). "TAT transduction: the molecular mechanism and therapeutic prospects." Trends Mol Med **13**(10): 443-448.

Gupta, R. and Y. Prasad (2011). "P-27/HP endolysin as antibacterial agent for antibiotic resistant *Staphylococcus aureus* of human infections." Curr Microbiol **63**(1): 39-45.

Hanski, E., P. A. Horwitz, et al. (1992). "Expression of protein F, the fibronectin-binding protein of Streptococcus pyogenes JRS4, in heterologous streptococcal and enterococcal strains promotes their adherence to respiratory epithelial cells." Infect Immun **60**(12): 5119-5125.

Hermoso, J. A., J. L. Garcia, et al. (2007). "Taking aim on bacterial pathogens: from phage therapy to enzybiotics." Curr Opin Microbiol **10**(5): 461-472.

Hermoso, J. A., B. Monterroso, et al. (2003). "Structural basis for selective recognition of pneumococcal cell wall by modular endolysin from phage Cp-1." Structure **11**(10): 1239-1249.

Hing, E., M. J. Hall, et al. (2008). "National Hospital Ambulatory Medical Care Survey: 2006 outpatient department summary." Natl Health Stat Report(4): 1-31.

Hirose, H., T. Takeuchi, et al. (2012). "Transient focal membrane deformation induced by arginine-rich peptides leads to their direct penetration into cells." Mol Ther **20**(5): 984-993.

Horgan, M., G. O'Flynn, et al. (2009). "Phage lysin LysK can be truncated to its CHAP domain and retain lytic activity against live antibiotic-resistant staphylococci." Appl Environ Microbiol **75**(3): 872-874.

Jado, I., R. Lopez, et al. (2003). "Phage lytic enzymes as therapy for antibiotic-resistant *Streptococcus pneumoniae* infection in a murine sepsis model." J Antimicrob Chemother **52**(6): 967-973.

Jadoun, J., V. Ozeri, et al. (1998). "Protein F1 is required for efficient entry of *Streptococcus pyogenes* into epithelial cells." J Infect Dis **178**(1): 147-158.

Jarry, T. M. and A. L. Cheung (2006). "*Staphylococcus aureus* escapes more efficiently from the phagosome of a cystic fibrosis bronchial epithelial cell line than from its normal counterpart." Infect Immun **74**(5): 2568-2577.

Johnson, E. A. and M. Bradshaw (2001). "*Clostridium botulinum* and its neurotoxins: a metabolic and cellular perspective." Toxicon **39**: 1703-1722.

Kaplan, I. M., J. S. Wadia, et al. (2005). "Cationic TAT peptide transduction domain enters cells by macropinocytosis." J Control Release **102**(1): 247-253.

Kim, A., T. H. Shin, et al. (2012). "Cellular internalization mechanism and intracellular trafficking of filamentous M13 phages displaying a cell-penetrating transbody and TAT peptide." PLoS One **7**(12): e51813.

Kintzer, A. F., K. L. Thoren, et al. (2009). "The protective antigen component of anthrax toxin forms functional octameric complexes." J Mol Biol **392**(3): 614-629.

Korndorfer, I. P., J. Danzer, et al. (2006). "The crystal structure of the bacteriophage PSA endolysin reveals a unique fold responsible for specific recognition of *Listeria* cell walls." J Mol Biol **364**(4): 678-689.

Kupser, P., K. Pagel, et al. (2010). "Amide-I and -II vibrations of the cyclic beta-sheet model peptide gramicidin S in the gas phase." J Am Chem Soc **132**(6): 2085-2093.

Kutter, E., D. De Vos, et al. (2010). "Phage therapy in clinical practice: treatment of human infections." Curr Pharm Biotechnol **11**(1): 69-86.

Kwinn, L. A. and V. Nizet (2007). "How group A *Streptococcus* circumvents host phagocyte defenses." Future Microbiol **2**(1): 75-84.

Lang, P. T., S. R. Brozell, et al. (2009). "DOCK 6: combining techniques to model RNA-small molecule complexes." RNA **15**(6): 1219-1230.

LaPenta, D., C. Rubens, et al. (1994). "Group A streptococci efficiently invade human respiratory epithelial cells." Proc Natl Acad Sci U S A **91**(25): 12115-12119.

Larckum, N. (1932). "Bacteriophage in clinical medicine." J.Lab.Clin.Med **17**(675).

Latif, R., T. Ando, et al. (2003). "Localization and regulation of thyrotropin receptors within lipid rafts." Endocrinology **144**(11): 4725-4728.

Lecaroz, C., C. Gamazo, et al. (2006). "Nanocarriers with gentamicin to treat intracellular pathogens." J Nanosci Nanotechnol **6**(9-10): 3296-3302.

Lee, C. J., H. R. Lin, et al. (2008). "Cholesterol effectively blocks entry of flavivirus." J Virol **82**(13): 6470-6480.

Lembke, C., A. Podbielski, et al. (2006). "Characterization of biofilm formation by clinically relevant serotypes of group A streptococci." Appl Environ Microbiol **72**(4): 2864-2875.

Loeffler, J. M., S. Djurkovic, et al. (2003). "Phage lytic enzyme Cpl-1 as a novel antimicrobial for pneumococcal bacteremia." Infect Immun **71**(11): 6199-6204.

Loeffler, J. M. and V. A. Fischetti (2003). "Synergistic lethal effect of a combination of phage lytic enzymes with different activities on penicillin-sensitive and -resistant *Streptococcus pneumoniae* strains." Antimicrob Agents Chemother **47**(1): 375-377.

Loeffler, J. M., D. Nelson, et al. (2001). "Rapid killing of *Streptococcus pneumoniae* with a bacteriophage cell wall hydrolase." Science **294**: 2170-2172.

Loessner, M. J. (2005). "Bacteriophage endolysins--current state of research and applications." Curr Opin Microbiol **8**(4): 480-487.

Loessner, M. J., S. Gaeng, et al. (1998). "The two-component lysis system of *Staphylococcus aureus* bacteriophage Twort: a large TTG-start holin and an associated amidase endolysin." FEMS Microbiol Lett **162**(2): 265-274.

Low, L. Y., C. Yang, et al. (2005). "Structure and lytic activity of a *Bacillus anthracis* prophage endolysin." J Biol Chem **280**(42): 35433-35439.

MacCallum, J. S. a. P., Ed. (2000). Molecular Cloning: A Laboratory Manual. Cold Spring Harbor, New York, Cold Spring Harbor Laboratory Press.

Manzanillo, P. S., M. U. Shiloh, et al. (2012). "*Mycobacterium tuberculosis* activates the DNA-dependent cytosolic surveillance pathway within macrophages." Cell Host Microbe **11**(5): 469-480.

Marouni, M. J. and S. Sela (2004). "Fate of *Streptococcus pyogenes* and epithelial cells following internalization." J Med Microbiol **53**(Pt 1): 1-7.

McCullers, J. A., A. Karlstrom, et al. (2007). "Novel strategy to prevent otitis media caused by colonizing *Streptococcus pneumoniae*." PLoS Pathog **3**(3): e28.

McGowan, S., A. M. Buckle, et al. (2012). "X-ray crystal structure of the streptococcal specific phage lysin PlyC." Proc Natl Acad Sci U S A **109**(31): 12752-12757.

McIver, K. S. (2009). "Stand-alone response regulators controlling global virulence networks in streptococcus pyogenes." Contrib Microbiol **16**: 103-119.

McNeil, S. A., S. A. Halperin, et al. (2005). "Safety and immunogenicity of 26-valent group a *streptococcus* vaccine in healthy adult volunteers." Clin Infect Dis **41**(8): 1114-1122.

Merabishvili, M., J. P. Pirnay, et al. (2009). "Quality-controlled small-scale production of a well-defined bacteriophage cocktail for use in human clinical trials." PLoS One **4**(3): e4944.

Merril, C. R., D. Scholl, et al. (2003). "The prospect for bacteriophage therapy in Western medicine." Nat Rev Drug Discov **2**(6): 489-497.

Mitchell, G. J., D. C. Nelson, et al. (2010). "Quantifying enzymatic lysis: estimating the combined effects of chemistry, physiology and physics." Phys Biol **7**(4): 046002.

Molinari, G., S. R. Talay, et al. (1997). "The fibronectin-binding protein of *Streptococcus pyogenes*, SfbI, is involved in the internalization of group A streptococci by epithelial cells." Infect Immun **65**(4): 1357-1363.

Mueller, J., I. Kretzschmar, et al. (2008). "Comparison of cellular uptake using 22 CPPs in 4 different cell lines." Bioconjug Chem **19**(12): 2363-2374.

Nakagawa, I., A. Amano, et al. (2004). "Autophagy defends cells against invading group A Streptococcus." Science **306**(5698): 1037-1040.

Navarre, W. W., H. Ton-That, et al. (1999). "Multiple enzymatic activities of the murein hydrolase from staphylococcal phage phi11. Identification of a D-alanyl-glycine endopeptidase activity." J Biol Chem **274**(22): 15847-15856.

Neeman, R., N. Keller, et al. (1998). "Prevalence of internalisation-associated gene, prtF1, among persisting group-A *streptococcus* strains isolated from asymptomatic carriers." Lancet **352**(9145): 1974-1977.

Nelson, D., L. Loomis, et al. (2001). "Prevention and elimination of upper respiratory colonization of mice by group A streptococci by using a bacteriophage lytic enzyme." Proc Natl Acad Sci U S A **98**(7): 4107-4112.

Nelson, D., R. Schuch, et al. (2006). "PlyC: a multimeric bacteriophage lysin." Proc Natl Acad Sci U S A **103**(28): 10765-10770.

Nelson, D., R. Schuch, et al. (2003). "Genomic sequence of C1, the first streptococcal phage." J Bacteriol **185**(11): 3325-3332.

Nelson, D. C., L. Rodriguez, et al. (2012). Endolysins as Antimicrobials. Advances in Virus Research. M. Lobocka and W. Szybalski, Elsevier Press.

Nitsche-Schmitz, D. P., M. Rohde, et al. (2007). "Invasion mechanisms of Gram-positive pathogenic cocci." Thromb Haemost **98**(3): 488-496.

Nobbs, A. H., R. J. Lamont, et al. (2009). "*Streptococcus* adherence and colonization." Microbiol Mol Biol Rev **73**(3): 407-450, Table of Contents.

O'Flaherty, S., A. Coffey, et al. (2005). "The recombinant phage lysin LysK has a broad spectrum of lytic activity against clinically relevant staphylococci, including methicillin-resistant *Staphylococcus aureus*." J Bacteriol **187**(20): 7161-7164.

O'Flaherty, S., R. P. Ross, et al. (2009). "Bacteriophage and their lysins for elimination of infectious bacteria." FEMS Microbiol Rev **33**(4): 801-819.

Ogawa, T., Y. Terao, et al. (2011). "Biofilm formation or internalization into epithelial cells enable *Streptococcus pyogenes* to evade antibiotic eradication in patients with pharyngitis." Microb Pathog **51**(1-2): 58-68.

Onyeji, C. O., C. H. Nightingale, et al. (1994). "Efficacies of liposome-encapsulated clarithromycin and ofloxacin against Mycobacterium avium-M. intracellulare complex in human macrophages." Antimicrob Agents Chemother **38**(3): 523-527.

Osterlund, A. and L. Engstrand (1997). "An intracellular sanctuary for *Streptococcus pyogenes* in human tonsillar epithelium--studies of asymptomatic carriers and in vitro cultured biopsies." Acta Otolaryngol **117**(6): 883-888.

Osterlund, A., R. Popa, et al. (1997). "Intracellular reservoir of *Streptococcus pyogenes* in vivo: a possible explanation for recurrent pharyngotonsillitis." Laryngoscope **107**(5): 640-647.

Ozeri, V., I. Rosenshine, et al. (1998). "Roles of integrins and fibronectin in the entry of *Streptococcus pyogenes* into cells via protein F1." Mol Microbiol **30**(3): 625-637.

Passali, D., M. Lauriello, et al. (2007). "Group A *streptococcus* and its antibiotic resistance." Acta Otorhinolaryngol Ital **27**(1): 27-32.

Pastagia, M., C. Euler, et al. (2011). "A novel chimeric lysin shows superiority to mupirocin for skin decolonization of methicillin-resistant and -sensitive *Staphylococcus aureus* strains." Antimicrob Agents Chemother **55**(2): 738-744.

Pentecost, M., J. Kumaran, et al. (2010). "*Listeria monocytogenes* internalin B activates junctional endocytosis to accelerate intestinal invasion." PLoS Pathog **6**(5): e1000900.

Pettersen, E. F., T. D. Goddard, et al. (2004). "UCSF Chimera--a visualization system for exploratory research and analysis." J Comput Chem **25**(13): 1605-1612.

Pfoh, E., M. R. Wessels, et al. (2008). "Burden and economic cost of group A streptococcal pharyngitis." Pediatrics **121**(2): 229-234.

Pike, L. J. (2003). "Lipid rafts: bringing order to chaos." J Lipid Res **44**(4): 655-667.

Porter, C. J., R. Schuch, et al. (2007). "The 1.6 A crystal structure of the catalytic domain of PlyB, a bacteriophage lysin active against *Bacillus anthracis*." J Mol Biol **366**(2): 540-550.

Pritchard, D. G., S. Dong, et al. (2004). "The bifunctional peptidoglycan lysin of *Streptococcus agalactiae* bacteriophage B30." Microbiol. **150**: 2079-2087.

Pritchard, D. G., S. Dong, et al. (2007). "LambdaSa1 and LambdaSa2 prophage lysins of *Streptococcus agalactiae*." Appl Environ Microbiol **73**(22): 7150-7154.

Rashel, M., J. Uchiyama, et al. (2007). "Efficient elimination of multidrug-resistant *Staphylococcus aureus* by cloned lysin derived from bacteriophage phi MR11." J Infect Dis **196**(8): 1237-1247.

Richard, J. P., K. Melikov, et al. (2005). "Cellular uptake of unconjugated TAT peptide involves clathrin-dependent endocytosis and heparan sulfate receptors." J Biol Chem **280**(15): 15300-15306.

Rigden, D. J., M. J. Jedrzejas, et al. (2003). "Amidase domains from bacterial and phage autolysins define a family of gamma-D,L-glutamate-specific amidohydrolases." Trends Biochem.Sci. **28**(5): 230-234.

Rossetto, O., M. Seveso, et al. (2001). "Tetanus and botulinum neurotoxins: turning bad guys into good by research." Toxicon **39**: 27-41.

Rothbard, J. B., T. C. Jessop, et al. (2004). "Role of membrane potential and hydrogen bonding in the mechanism of translocation of guanidinium-rich peptides into cells." J Am Chem Soc **126**(31): 9506-9507.

Ryan, P. A., V. Pancholi, et al. (2001). "Group A streptococci bind to mucin and human pharyngeal cells through sialic acid-containing receptors." Infect Immun **69**(12): 7402-7412.

Sabharwal, H., F. Michon, et al. (2006). "Group A *streptococcus* (GAS) carbohydrate as an immunogen for protection against GAS infection." J Infect Dis **193**(1): 129-135.

Schindler, C. A. and V. T. Schuhardt (1964). "Lysostaphin: A New Bacteriolytic Agent for the *Staphylococcus*." Proc Natl Acad Sci U S A **51**: 414-421.

Schmelcher, M., A. M. Powell, et al. (2012). "Chimeric phage lysins act synergistically with lysostaphin to kill mastitis-causing *Staphylococcus aureus* in murine mammary glands." Appl Environ Microbiol **78**(7): 2297-2305.

Schmelcher, M., V. S. Tchang, et al. (2011). "Domain shuffling and module engineering of *Listeria* phage endolysins for enhanced lytic activity and binding affinity." Microb Biotechnol.

Schuch, R., D. Nelson, et al. (2002). "A bacteriolytic agent that detects and kills *Bacillus anthracis*." Nature **418**: 884-889.

Seleem, M. N., P. Munusamy, et al. (2009). "Silica-antibiotic hybrid nanoparticles for targeting intracellular pathogens." Antimicrob Agents Chemother **53**(10): 4270-4274.

Shen, Y., T. Koller, et al. (2013). "Rapid degradation of *Streptococcus pyogenes* biofilms by PlyC, a bacteriophage-encoded endolysin." J Antimicrob Chemother.

Shen, Y. M., M. S.; Donovan, D. M.; Nelson, D. C. (2012). Phage-based enzybiotics, CABI.

Shet, A., E. L. Kaplan, et al. (2003). "Immune response to group A streptococcal C5a peptidase in children: implications for vaccine development." J Infect Dis **188**(6): 809-817.

Steer, A. C., M. R. Batzloff, et al. (2009). "Group A streptococcal vaccines: facts versus fantasy." Curr Opin Infect Dis **22**(6): 544-552.

Steer, A. C., J. B. Dale, et al. (2013). "Progress toward a global group a streptococcal vaccine." Pediatr Infect Dis J **32**(2): 180-182.

Steer, A. C., I. Law, et al. (2009). "Global emm type distribution of group A streptococci: systematic review and implications for vaccine development." Lancet Infect Dis **9**(10): 611-616.

Su, Y., A. J. Waring, et al. (2010). "Membrane-bound dynamic structure of an arginine-rich cell-penetrating peptide, the protein transduction domain of HIV TAT, from solid-state NMR." Biochemistry **49**(29): 6009-6020.

Sulakvelidze, A., Z. Alavidze, et al. (2001). "Bacteriophage therapy." Antimicrob Agents Chemother **45**(3): 649-659.

Tart, A. H., M. J. Walker, et al. (2007). "New understanding of the group A *Streptococcus* pathogenesis cycle." Trends Microbiol **15**(7): 318-325.

Thulin, P., L. Johansson, et al. (2006). "Viable group A streptococci in macrophages during acute soft tissue infection." PLoS Med **3**(3): e53.

Thumm, G. and F. Gotz (1997). "Studies on prolysostaphin processing and characterization of the lysostaphin immunity factor (Lif) of *Staphylococcus simulans* biovar *staphylolyticus*." Mol Microbiol **23**(6): 1251-1265.

Torchilin, V. P. (2008). "Tat peptide-mediated intracellular delivery of pharmaceutical nanocarriers." Adv Drug Deliv Rev **60**(4-5): 548-558.

Tunnemann, G., R. M. Martin, et al. (2006). "Cargo-dependent mode of uptake and bioavailability of TAT-containing proteins and peptides in living cells." FASEB J **20**(11): 1775-1784.

Twort, F. W. (1915). "An investigation on the nature of ultra-microscopic viruses." Lancet **ii**: 1241-1246.

Tyagi, M., M. Rusnati, et al. (2001). "Internalization of HIV-1 tat requires cell surface heparan sulfate proteoglycans." J Biol Chem **276**(5): 3254-3261.

van Meer, G., D. R. Voelker, et al. (2008). "Membrane lipids: where they are and how they behave." Nat Rev Mol Cell Biol **9**(2): 112-124.

Wadia, J. S., R. V. Stan, et al. (2004). "Transducible TAT-HA fusogenic peptide enhances escape of TAT-fusion proteins after lipid raft macropinocytosis." Nat Med **10**(3): 310-315.

Wagner, P. L. and M. K. Waldor (2002). "Bacteriophage control of bacterial virulence." Infect. lmmun. **70**(8): 3985-3993.

Wakatsuki, T., B. Schwab, et al. (2001). "Effects of cytochalasin D and latrunculin B on mechanical properties of cells." J Cell Sci **114**(Pt 5): 1025-1036.

Wang, B., R. S. Yurecko, et al. (2006). "Integrin-linked kinase is an essential link between integrins and uptake of bacterial pathogens by epithelial cells." Cell Microbiol **8**(2): 257-266.

Wang, I. N., D. L. Smith, et al. (2000). "Holins: the protein clocks of bacteriophage infections." Annu Rev Microbiol **54**: 799-825.

Wang, L. H., K. G. Rothberg, et al. (1993). "Mis-assembly of clathrin lattices on endosomes reveals a regulatory switch for coated pit formation." J Cell Biol **123**(5): 1107-1117.

Witzenrath, M., B. Schmeck, et al. (2009). "Systemic use of the endolysin Cpl-1 rescues mice with fatal pneumococcal pneumonia." Crit Care Med **37**(2): 642-649.

Yao, W., K. Li, et al. (2009). "Macropinocytosis contributes to the macrophage foam cell formation in RAW264.7 cells." Acta Biochim Biophys Sin (Shanghai) **41**(9): 773-780.

Yoong, P., R. Schuch, et al. (2006). "PlyPH, A bacteriolytic enzyme with a broad pH range of activity and lytic action against *Bacillus anthracis*." J. Bacteriol. **188**: 2711-2714.

Zaman, M., A. B. Abdel-Aal, et al. (2012). "Immunological evaluation of lipopeptide group A *streptococcus* (GAS) vaccine: structure-activity relationship." PLoS One **7**(1): e30146.

Ziello, J. E., Y. Huang, et al. (2010). "Cellular endocytosis and gene delivery." Mol Med **16**(5-6): 222-229.